THE ACTIVITY OF SODIUM IN CRYOLITE-ALUMINUM MELTS

by

PETER ERIC JOHN AYLEN

A THESIS SUBMITTED IN PARTIAL FULFILMENT OF

THE REQUIREMENTS FOR THE DEGREE OF

MASTER OF APPLIED SCIENCE

in the Department

of

METALLURGY

We accept this thesis as conforming to the

standard required from candidates for the

degree of MASTER OF APPLIED SCIENCE

Members of the Department

of Metallurgy

THE UNIVERSITY OF BRITISH COLUMBIA

August 1962

In presenting this thesis in partial fulfilment of the requirements for an advanced degree at the University of British Columbia, I agree that the Library shall make it freely available for reference and study. I further agree that permission for extensive copying of this thesis for scholarly purposes may be granted by the Head of my Department or by his representatives. It is understood that copying or publication of this thesis for financial gain shall not be allowed without my written permission.

Department of Metallurgy

The University of British Columbia,
Vancouver 8, Canada.

Date September 5, 1962

ABSTRACT

Activities of sodium in alumina-saturated cryolite-aluminum melts have been measured by the equilibration of a three phase system of cryolite, aluminum and lead. An approximate linear increase in the activity of sodium was noted on a log plot of activity as a function of $NaF-AlF_3$ weight ratios over the range pertinent to commercial reduction cell operation.

Activities of sodium in cryolite-aluminum melts have been calculated by employing the equilibrium reaction between cryolite and aluminum metal and the thermodynamic data from an analysis of the $NaF-AlF_3$ phase diagram.

Differences between the reversible deposition potential for aluminum and sodium at one atmosphere partial pressure were calculated from the measured equilibrium sodium activities. The values obtained were of the order of .15 to .40 volts, increasing with decreasing $NaF-AlF_3$ ratio.

ACKNOWLEDGEMENT

The author gratefully acknowledges Dr. C. S. Samis for his supervision and instruction during the course of this work. Thanks are also extended to Mrs. A. M. Armstrong and Dr. E. Peters for their helpful suggestions and to the staff of the computing centre who assisted with the mathematical interpretation and programming for one section of the thesis.

The author wishes to thank the Kaiser Aluminum and Chemical Corporation, the Aluminum Company of Canada, Limited, and Aluminium Laboratories Limited for supplying materials and information and carrying out analyses.

The author is grateful to the National Research Council of Canada for the financial assistance which made this work possible.

TABLE OF CONTENTS

Table of Contents Continued

Table of Contents Continued

LIST OF FIGURES

LIST OF TABLES

List of Tables Continued

THE ACTIVITY OF SODIUM IN CRYOLITE-ALUMINUM MELTS

INTRODUCTION

Aluminum is produced commercially by the electrolytic reduction of aluminum oxide dissolved in molten cryolite (Na_3AlF_6). The technical process is based on the independent discoveries of Hall (U.S.A.) and Heroult (France) in 1886.

Although the process is over 70 years old there is still a great deal of controversy over the mechanisms of the reactions involved. Some of the unsolved problems include the identification of the structural constituents of the melt, the mechanisms of the anode and cathode reactions, the significance of the metal fog formed when metallic aluminum is added to molten fluorides, and the question of which of the metals, sodium or aluminum, is reduced directly in the electrolysis. The various theories which have been proposed to explain the situation are reviewed by Pearson[1], Grjotheim[2] and Foster[3].

One of the major reasons for the scarcity of knowledge in this field is the electrolyte involved. Molten cryolite is one of the most corrosive materials known. It vapourizes with decomposition at the melting point and changes its constitution and freezing point. It oxidizes in air to form alumina which dissolves in the melt and hydrolyses at high temperature in the presence of water vapour.

The corrosive nature of aluminum metal is also a factor in the difficulties inherent in any study of the process. Aluminum alloys with practically all metals. Platinum is one of the few metals which will

withstand the attack of cryolite, but it cannot be used if aluminum is present.

One of the practical problems associated with the electrolytic production of aluminum is the low current efficiency of the cell. This has been attributed by many investigators to the formation of metallic sodium[4,5,6,7,8]. As a result, considerable interest has been shown in the estimation or determination of sodium in aluminum metal in contact with the electrolytic melts. Recently it has been suggested that formation of monovalent aluminum compounds, which are reoxidized at the anode, account for the low current efficiencies[9,10]. Most probably the loss in efficiency is due to a combination of factors involving these processes as well as side reactions.

1. Summary of Previous Work

(a) Activity of Sodium

The equilibrium between sodium and aluminum in contact with fluoride melts has been studied by Jander and Hermann[11]. They investigated the equilibrium reaction

$$(3NaF)_{(l)} + Al_{(l)} \rightleftharpoons [3Na]_{(dil)} + (AlF_3)_{(l)} \quad \ldots\ldots(1)$$

at 1090°C. in alumina crucibles in an atmosphere of dry, oxygen-free nitrogen. The concentration of sodium in liquid aluminum in contact with molten mixtures of sodium fluoride and aluminum fluoride was determined. No attempt was made to measure activities and the equilibrium constant was expressed in concentrations. The results of their investigation are shown in Figure 1.

Pearson and Waddington[12] determined the sodium content of liquid aluminum at 1000°C. in contact with fluoride melts whose composition was close to that of cryolite. Their results are also shown in Figure 1. and show a fair agreement with those of Jander and Hermann.

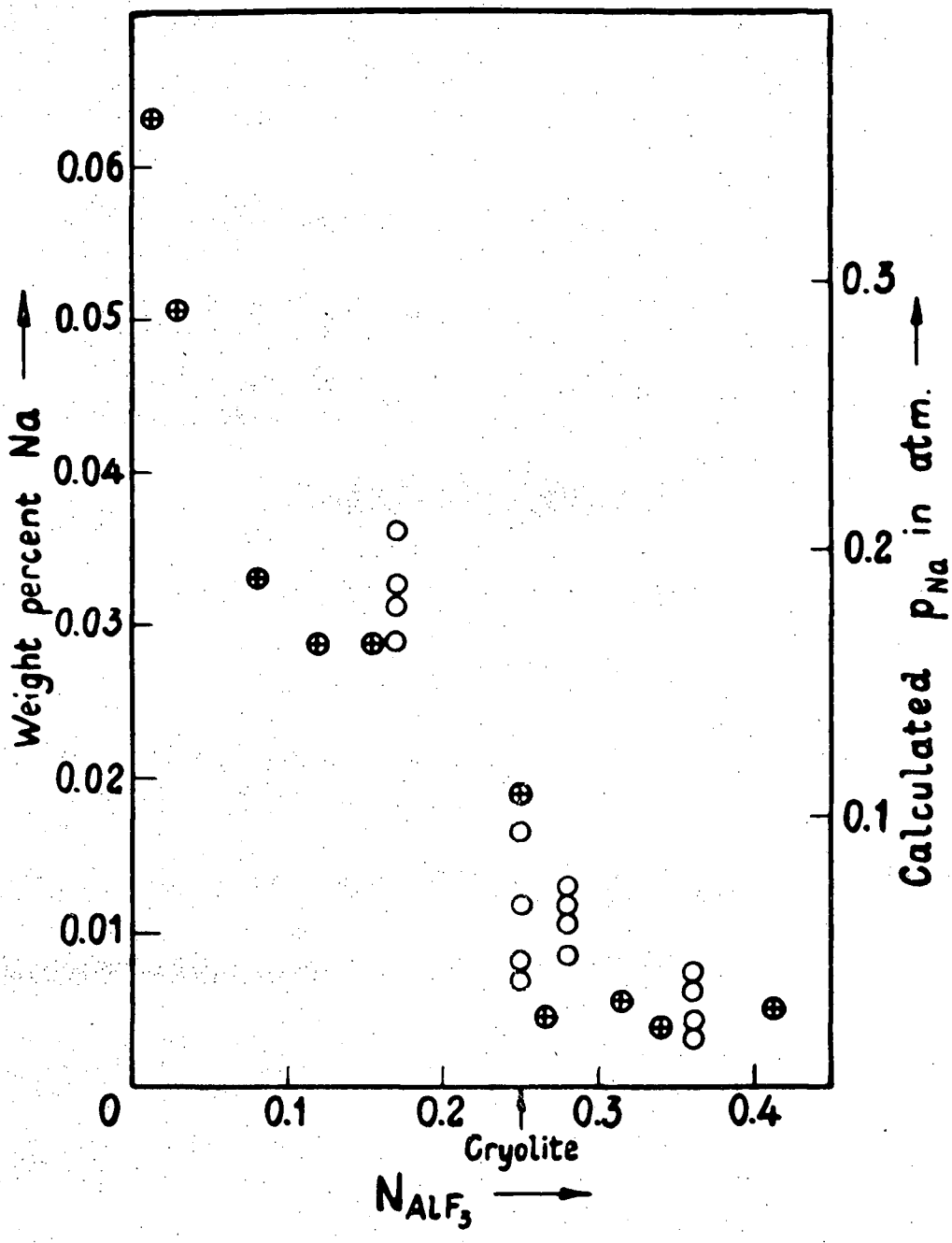

Figure 1. Sodium Content of Liquid Al in Equilibrium with Molten Mixtures of NaF and AlF_3. Crossed circles from Jander and Hermann[11], open circles from Pearson and Waddington[12]. (Diagram from Grjotheim[2]).

Feinleib and Porter[13] measured the activities of sodium in molten aluminum in contact with cryolite saturated with alumina in order to determine the difference in decomposition potential between sodium and aluminum. Their work was carried out in alumina crucibles over a temperature range of 940-1010°C. An attempt was made to obtain final cryolite ratios of 1.50 by adjusting the initial composition of the melts, but a wide variation occurred. Lead was used as an auxiliary phase in the melts for the determination of sodium concentration and activity. An independent study was carried out to determine the activity of sodium in sodium-lead alloys at high temperatures[14].

(b) Dissociation of Cryolite

In order to carry out a thermodynamic analysis of the $NaF-AlF_3$ system, it is necessary to have some idea of the degree and type of dissociation involved when cryolite melts. The effect of alumina and calcium fluoride additions to the dissociation is also of significance. Many hypotheses have been advanced concerning various dissociation schemes. These are discussed in detail by Grjotheim[2].

The most recent dissociation calculations have been carried out by Grjotheim[2] and Frank and Foster[15]. Grjotheim based his calculations on a cryoscopic study of the $NaF-AlF_3$ system, while Foster and Frank developed their scheme on the basis of the density of $NaF-AlF_3$ melts. Both arrived at the same dissociation scheme.

$$Na_3AlF_6 \rightleftharpoons 3Na^+ + AlF_6^{\equiv} \qquad .....(2)$$

$$AlF_6^{\equiv} \rightleftharpoons AlF_4^- + 2F^- \qquad .....(3)$$

The recent review by Foster[3] suggested that 31 per cent of the NaF present in the melt is dimerized. The latter refinement is an attempt

to correct the failure of the previous theory to account for the experimental shape of the NaF side of the eutectic on the NaF-AlF_3 phase diagram and the electrical conductance.

Several reaction schemes for the dissolution of alumina in cryolite have been studied by Foster and Frank[16] and interpreted in terms of their cryolite dissociation scheme[15]. The activities of the solvent were calculated for the proposed equilibria. If the ionic constituents present are representative of the true equilibrium a plot of ln a vs 1/T will result in a straight line the slope of which is the heat of fusion of cryolite. Foster and Frank found the most likely mechanism to be

$$3F^- + Al_2O_3 \rightleftharpoons 3/2AlO_2^- + 1/2AlF_6^{\equiv} \qquad .....(4)$$

The addition of calcium fluoride to cryolite melts would be expected to add calcium and fluoride ions in the following manner

$$CaF_2 \rightleftharpoons Ca^{++} + 2F^- \qquad .....(5)$$

(c) Effect of Additives

Foreign ions of Al_2O_3 and CaF_2 added to cryolite may

(i) act only as diluents in the melt, or

(ii) affect the activity of sodium.

Grube and Hantelmann[31] found in their studies that the presence of Al_2O_3 did not affect the reactions between sodium or aluminum and NaF-AlF_3 melts. From an ionic standpoint (considering equations (1), (2), (3), and (4) it would appear that Al_2O_3 would act primarily as a diluent in the melt. On the other hand the addition of fluorine ions from the dissociation of CaF_2 (see equation (5) might decrease the activity of sodium due to a reversal of the cryolite dissociation (equations (1), (2), and (3).

2. Object and Scope of the Present Investigation

The object of the present investigation was to determine the activities of sodium in aluminum metal in contact with cryolite melts over a range of $NaF-AlF_3$ weight ratios between 1.00 and 2.00.* These sodium activities could then be related to the difference in deposition potential between aluminum and sodium in order to evaluate the likelihood of simultaneous sodium and aluminum deposition in commercial cells.

The activity measurements were carried out using two different grades of cryolite (pure laboratory grade and commercial electrolyte containing 7-8% CaF_2). In addition, 7% CaF_2 was added to both grades of cryolite in order to assess the affect of CaF_2 content on the sodium activity.

Activities were determined experimentally by the equilibration of a three phase system of cryolite, aluminum and lead. Aluminum and sodium are highly immiscible and thermodynamic data for the Al-Na system has not been measured. Therefore, lead was used as a third phase. Sodium concentrations can be measured easily in lead and activities can be calculated from a calibration of the lead-sodium system.

The experiments were restricted to cryolite melts saturated with alumina. Any readily available crucible materials other than alumina would introduce components into the melt which could affect the activities. As

---

* Throughout this paper $NaF-AlF_3$ ratio is used to represent the weight ratios, e.g. the compound cryolite ($3NaF.AlF_3$) has an $NaF-AlF_3$ ratio of

$$\frac{3NaF}{AlF_3} = \frac{126}{84} = 1.50$$

commercial electroytes contain dissolved alumina in varying concentrations, the experimental technique used here can be compared with the commercial operation at one stage.

Activities were also calculated by a thermodynamic analysis of the $NaF-AlF_3$ and the Na-Al phase diagrams. Thermodynamic data for NaF and AlF_3 were calculated from the experimental results. The sodium-lead system was investigated to provide a consistent extrapolation of activity data to high temperatures.

EXPERIMENTAL

The experimental procedure involved the equilibration of cryolite (alumina-saturated) with pure aluminum metal and a sodium-lead alloy. The reaction was carried out in alumina crucibles and the heat supplied by an induction furnace. At the end of each run the crucible was air quenched to preserve the equilibrium conditions, the phases separated and samples taken for analysis.

As a preliminary step, it was necessary to adjust the composition of the starting materials. The cryolite was saturated with Al_2O_3 in order to prevent destructive attack of the crucibles and AlF_3 and CaF_2 were added to synthesize melts of a desired composition. Lead-sodium alloys were prepared and used in the runs.

The use of induction heating made it necessary to make a check of the temperature of the melt. Recorded temperatures were taken outside the reaction crucible and would therefore be slightly in error if the melt were to act as a susceptor.

1. Saturation of Cryolite with Alumina

(a) Materials

Cryolite samples were kindly supplied by the Kaiser Aluminum and Chemical Corporation, Spokane, Washington and by Aluminium Laboratories Limited, Arvida, Quebec. Analyses of the three materials used are shown in Table I.

TABLE I.

Analysis of Cryolite

Material	$NaF-AlF_3$ Ratio	CaF_2	Free Al_2O_3
Pure Cryolite	1.52	-	0.25%
Reduction Cell Electrolyte	1.55	7.6%	4.0 %
Reduction Cell Electrolyte	1.39	8.2%	5.6 %

The alumina used was Alcoa A-10 and the aluminum fluoride was supplied by Aluminium Laboratories. This material was 89.8% grade, with the major impurity alumina. Sodium fluoride and calcium fluoride were Baker and Adamson reagent grade.

(b) Crucible

A standard form 300 cc Engelhard Platinum evaporating dish, No. 202, was used as the container for the preparation of the saturated cryolite.

(c) Furnace

A simple glo-bar furnace was used. Construction details are shown in Figure 2. The source of power was a 4.5 kva transformer.

(d) Temperature Control

Temperature control was maintained by a platinum, platinum 10%-rhodium thermocouple attached to a "Wheelco" mercury switch controller.

(e) Procedure

Saturated cryolite was prepared in batches of 200 to 350 grams. Alumina, AlF_3, NaF and CaF_2 were added in varying proportions in order to produce saturated cryolite of different $NaF-AlF_3$ ratios and CaF_2 contents. The batches were mixed and placed in the furnace. The temperature was raised to 1100°C. and reduced to 1000°C. after the material became molten.

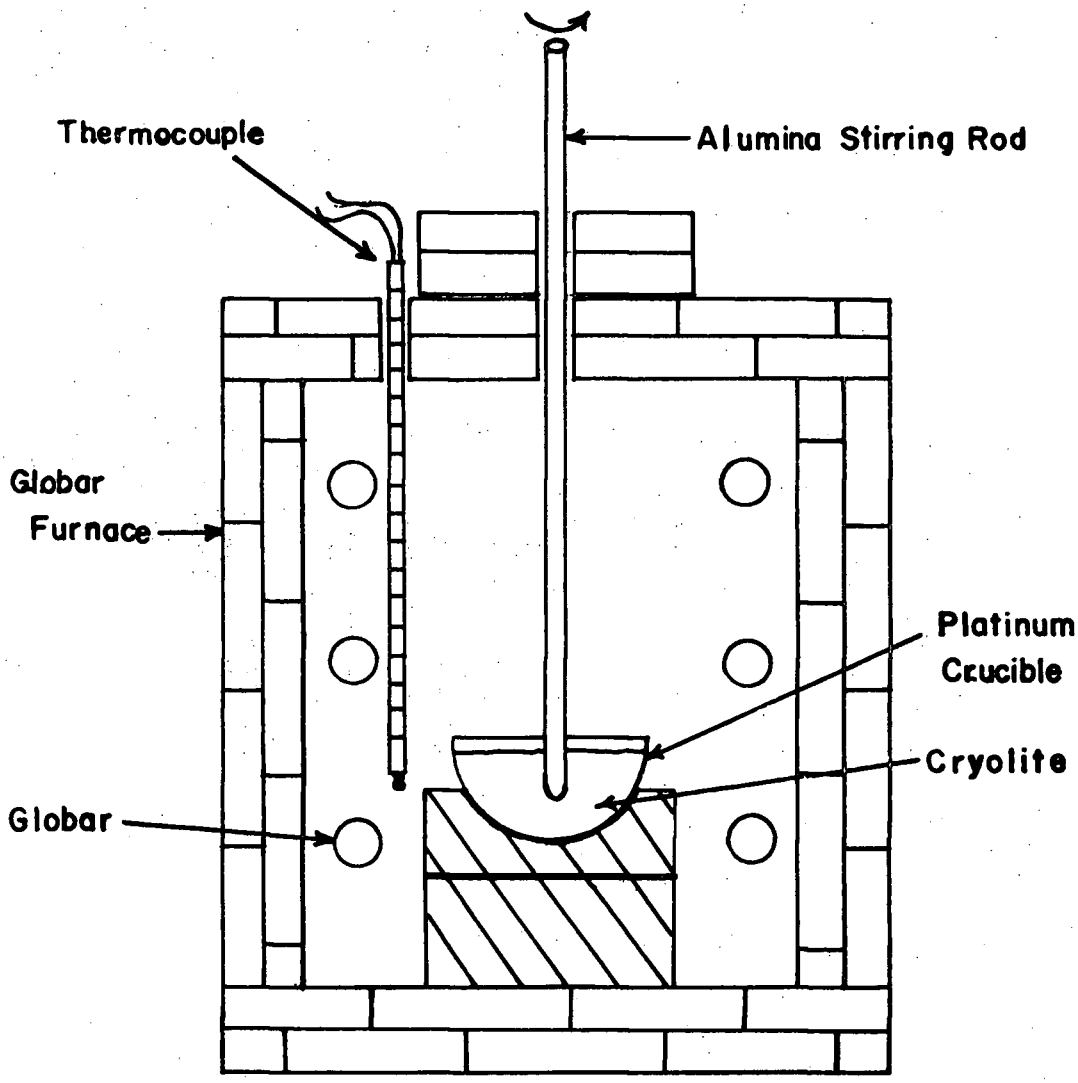

Figure 2. Construction Details of Experimental Furnace for Alumina Saturation.

The mixture was stirred with a Morganite recrystallized alumina rod (see Figure 2) for 30 minutes and then removed from the furnace and air-cooled to prevent segregation of the melt.

2. Preparation of Lead-Sodium Alloy

(a) Materials

American Smelting and Refining Company Test Lead, high purity lead foil and Baker and Adamson reagent grade sodium were used.

(b) Crucible

The materials were melted in a graphite crucible.

(c) Furnace

A small 230 volt, 3600 watt "Multiple Unit" electrical resistance, muffle furnace was used for the melting operation.

(d) Temperature Control

Temperature control was maintained by a chromel-alumel thermocouple attached to a Hoskins hunting device controller.

(e) Procedure

Three batches of Pb-Na alloy were prepared in the following manner. Test lead was melted in the graphite crucible at 600°C. in the muffle furnace. Sodium metal was cleaned of oxide material and wrapped in lead foil. The lead-covered sodium was immersed in the molten lead, using a hollowed graphite rod. When sufficient sodium had been added to the molten lead the slag was skimmed and the metal poured into a stainless steel tray. After cooling, the metal was kept in a vacuum desiccator until used. An analysis of the three batches is shown in Table II.

TABLE II.

Analyses of Lead-Sodium Alloys

No.	Na Content (wt.%)
1	8.6 %
2	6.6 %
3	2.8 %

3. Equilibrium Studies

(a) Materials

The materials used for these studies included those prepared in Parts 1 and 2 of this section. Other materials used included super-purity Alcan aluminum, (99.99%) and the alumina, AlF_3, NaF and Pb which have been discussed in the last two sections.

(b) Crucibles

The experimental equilibration measurements were carried out in McDanel vitrified alumina crucibles. Covers for the crucibles were fabricated from 99% Al_2O_3 brick, made by Harbison Walker. The graphite susceptor crucible and lid were machined out of graphite stock and this was enclosed in a large fireclay crucible (see Figures 3 and 4).

(c) Furnace

A 170/550 v, 3 phase, 12 kw output, Phillips induction furnace was used (see Figure 3) for the experiments.

(d) Temperature Control

Temperature control was accomplished with a chromel-alumel thermocouple attached to an IMRA recorder. The Phillips induction unit had been adapted for automatic temperature control by hooking up a type PH 1653 regulating unit to the recorder and thermocouple, (see Figure 3).

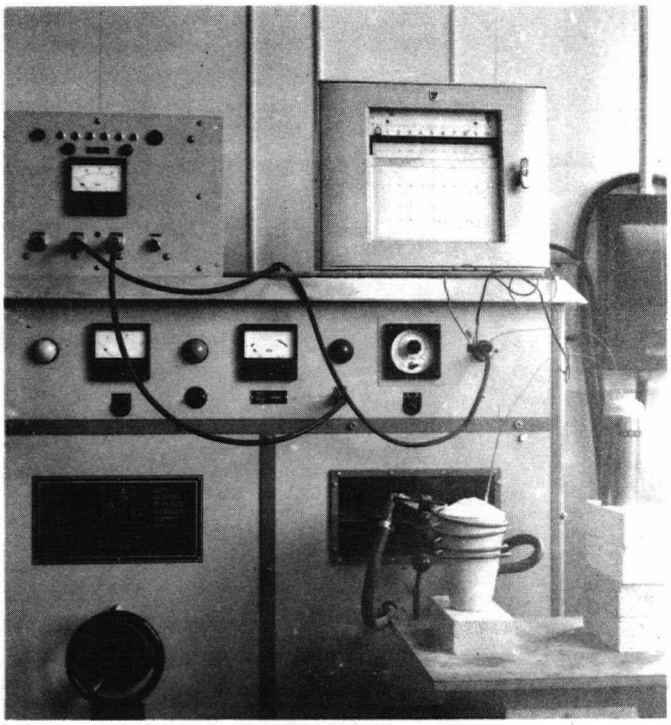

Figure 3. Experimental Setup and Furnace

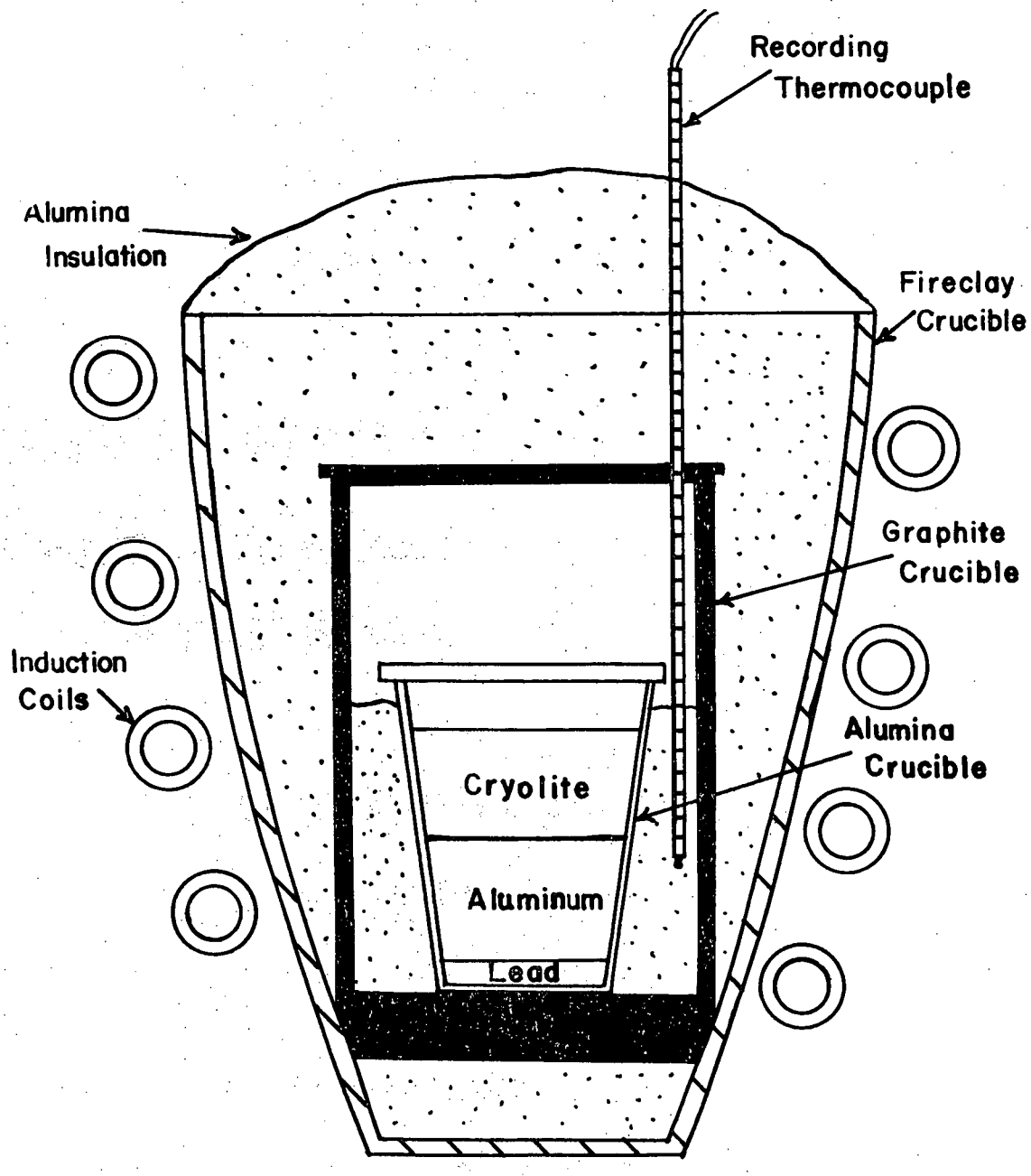

Figure 4. Cross-Section of Experimental Setup

(e) Procedure

The materials were weighed and added to the crucible which was placed inside the graphite susceptor. The experimental apparatus was set up as in Figure 4. The temperature was raised to approximately 1000°C. and the regulator was set to control the temperature at this level. The time of the runs was chosen as two hours, after which the alumina crucible was removed and quenched with a fan in order to retain the equilibrium conditions. The melts were broken out of the crucible and the three phases separated. The lead was analysed for sodium content and the cryolite for $NaF-AlF_3$ ratio, and CaF_2 where necessary.

(f) Chemical Analysis

Analysis of the lead phase for sodium was carried out using a Beckman flame spectrophotometer. Standard solutions of 0.025, 0.05 and 0.1 mg/ml NaCl were used for calibration. Analyses of the cryolite were kindly carried out by the Kaiser Aluminum and Chemical Corporation, Spokane, Washington and by the Aluminum Company of Canada, Kitimat, B.C.

(g) Determination of Activities of Sodium

A summary of the thermodynamic data for the lead-sodium system is presented in Appendix A. An extrapolation of the known data to higher temperature has been carried out and the relationship between activities of sodium in lead and the concentration of sodium in lead is shown in Figure A-7.

As a result of the thermodynamic equilibrium established in the experimental procedure, the measured concentrations of sodium in lead can be converted directly to equivalent activities of sodium in aluminum using Figure A-7.

(h) Equilibration Time

The reaction time of two hours was chosen as a result of previous work. Jander and Hermann[11] stated that a period of one hour was sufficient for the melt to reach equilibrium. However Feinleib and Porter[13] found that it was necessary to react their melts for a period of two hours, and attributed this to the fact that they had lead as an additional phase in the system. They used intermittent stirring in an attempt to reach equilibrium as quickly as possible. In this work it was hoped that susceptance by the melt would cause enough stirring action for equilibrium to be reached within two hours.

As a check on the establishment of equilibrium conditions, two sets of special runs were prepared. One set was made up with an excess of NaF in the bath, and a similar amount of Na was removed from the lead phase. The second set contained an excess of AlF_3 in the bath. Both sets contained exactly the same quantity of the significant materials, but the distribution between the phases of the system was changed. The two sets were subjected to the same test conditions and compared to see if they approached the same equilibrium values as a normal run.

As a further check on the equilibrium, one of the standard test runs was extended to four hours.

The composition and results of the two sets of equilibration check runs are shown in Table III. The analyses are in reasonable agreement and are within experimental error. The results of the four hour run (# 61) show little deviation from comparable two hour runs. Therefore it can be assumed that equilibrium was reached in the period of two hours.

TABLE III.

Equilibrium Time Data

Run No.	Composition	Time	Wt.% Na	ϱ_{Na}	$NaF-AlF_3$ Ratio
41	20.25 gm Al 20.0 gm Pb-Na alloy (3) 19.36 gm Pb (high purity foil) 60.0 gm Na_3AlF_6 (9) 1.17 gm NaF	2 hrs	2.20	.024	1.42 1.41
42	20.0 gm Al 40.0 gm Pb-Na (3) 60.0 gm Na_3AlF_6 (9) 0.78 gm AlF_3	2 hrs	2.40	.027	1.44 1.37
43	20.0 gm Al 40.0 gm Pb-Na (3) 60.0 gm Na_3AlF_6 (9)	2 hrs	2.60	.030	1.45 1.43
59	20.25 gm Al 20.0 gm Pb-Na alloy (3) 19.36 gm Pb (high purity foil) 60.00 gm Na_3AlF_6 (16) 1.17 gm NaF	2 hrs	1.50	.018	1.25 1.27
60	20.0 gm Al 40.0 gm Pb-Na alloy (3) 60.0 gm Na_3AlF_6 (16) 0.78 gm AlF_3	2 hrs	1.70	.019	1.24 1.20
61	20.0 gm Al 40.0 gm Pb-Na alloy (3) 60.0 gm Na_3AlF_6 (16)	4 hrs	1.80	.015	1.26 1.18

(i) Equilibrium Temperature

The experimental setup, shown in Figure 4. was designed to provide equilibrium heating conditions. It was assumed that a constant temperature could be maintained within the graphite crucible due to the four π geometry. However, if the melt were to act as a susceptor as well, there would be a thermal gradient between the alumina crucible and the graphite susceptor and the recorded temperature would be slightly in error.

A check on the accuracy of the recorded temperature readings was made by designing a special experimental setup to obtain an independent temperature measurement within the melt, (see Figure 5). An otherwise normal equilibration run was made and potentiometer readings taken at specific intervals.

The data collected are presented in Table IV. The potentiometer readings taken from the thermocouple immersed in the melt increased slowly for an hour and then remained stable at 41.7 mv (1010°C.) which was 0.4 mv (10°C.) above that of the recording thermocouple. The equilibrium temperature in this study has therefore been taken as 1010°C. ± 5°C.

The results of the temperature study suggest that the melt acts as a susceptor. Therefore considerable stirring action could be expected which would assist in attaining equilibrium.

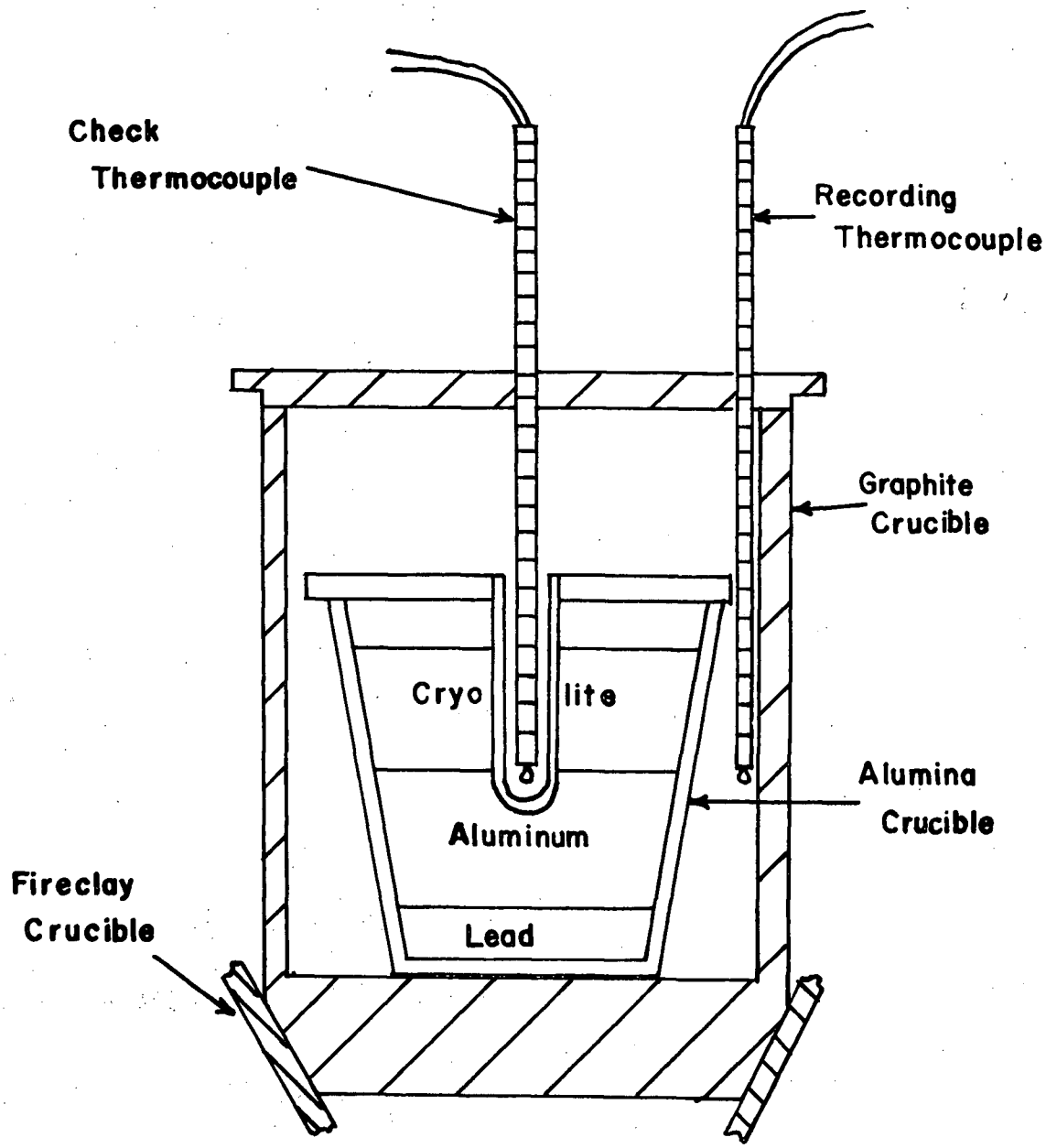

Figure 5. Cross-Section of Experimental Setup for Temperature Check

TABLE IV.

Equilibration Temperature Data

Time (min)	IMRA Recorder mv.	Temperature °C.	Pye Potentiometer mv.	Temperature °C.
10	41.3	1010	41.1	994
20	"	"	41.4	1002
35	"	"	41.6	1007
50	"	"	41.6	1007
65	"	"	41.7	1010
80	"	"	41.7	1010
95	"	"	41.7	1010
110	"	"	41.7	1010

RESULTS

The molten material in an aluminum electrolytic cell consists of two phases, aluminum metal (which acts as the cathode of the cell) and cryolite (which acts as the electrolyte). A thermodynamic equilibrium exists between the two phases, which is expressed by the simplified equation

$$Al_{(l)} + (3NaF)_{(l)} \rightleftharpoons (AlF_3)_{(l)} + \underline{[3Na]}_{(dil)} \cdots\cdots (1)$$

The free energy ΔF^{o}_{1283} for the reaction has been calculated in Appendix B and is equivalent to 62,915 calories.

$$\log K = \frac{-62,915}{4.575\ (1283)} = 10.72$$

K for the reaction is equal to

$$\frac{[a_{Na}]^3}{a_{Al}} \times \frac{(a_{AlF_3})}{(a_{NaF})^3} = 1.91 \times 10^{-11}$$

As the solubility of sodium in molten aluminum is of the order of .01%, the activity of aluminum metal can be considered as unity. Therefore, a determination of the ratio of activities of aluminum fluoride and sodium fluoride in cryolite would provide sufficient information to solve the equilibrium equation for the activity of sodium in the system.

Activities of NaF have been calculated from the NaF-AlF_3 phase diagram. The technique used was developed by Wagner[27,28,19] for determining activities from phase diagrams having inter-metallic compounds. Activities of AlF_3 were calculated using the Gibbs-Duhem equation. The calculation methods for the determination of the activities is discussed in Appendix C and the data presented.

The equilibrium equation is solved for pertinent data over the range of NaF-AlF_3 ratios employed in commercial aluminum practise. The activities of sodium are plotted as a function of NaF-AlF_3 ratio in Figure 6. and this curve will be designated AB in subsequent sections.

1. Displacement of Theoretical Activity Line by Dilution

If both alumina and calcium fluoride are considered only as diluents in the melt the activities of NaF and AlF_3 calculated in Appendix C can be adjusted by a dilution factor and the activities of sodium calculated for melts contining these impurities. The dilution factor can be estimated on the basis of the phase diagrams of Fenerty and Hollingshead[32] which are presented in Appendix D. These diagrams show the saturation limits of alumina as a function of AlF_3 content and CaF_2 content.

2. Activity of Sodium in Contact with Alumina-Saturated Pure Cryolite

Measured sodium activity values for alumina-saturated pure cryolite, and alumina-saturated pure cryolite plus 5%, 10%, 15% and 20% AlF_3 are plotted in Figure 7. as a function of NaF-AlF_3 ratio. The data are shown in Table E-I.

The theoretical curve AB (see Figure 6) is adjusted by an average dilution factor of .88 and is shown as a dotted line in Figure 7. The dilution factor is obtained from Figure D-1 and the activity calculation is carried out in Table D-I.

A straight line has been drawn through the experimental points and appears in Figure 7. as a solid line CD. This line is used in subsequent sections as a reference line.

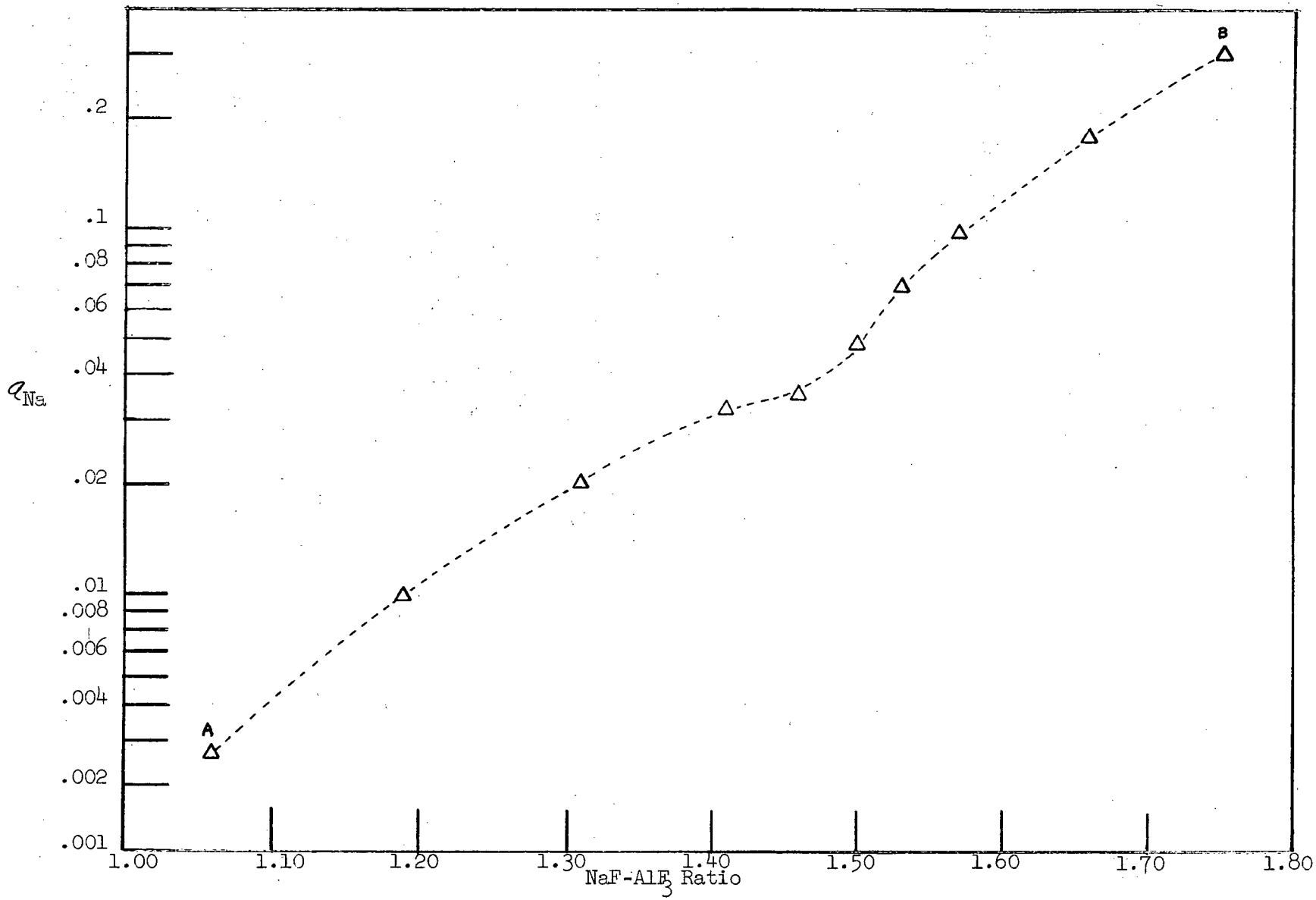

Figure 6. Plot of q_{Na} vs. NaF-AlF_3 Ratio

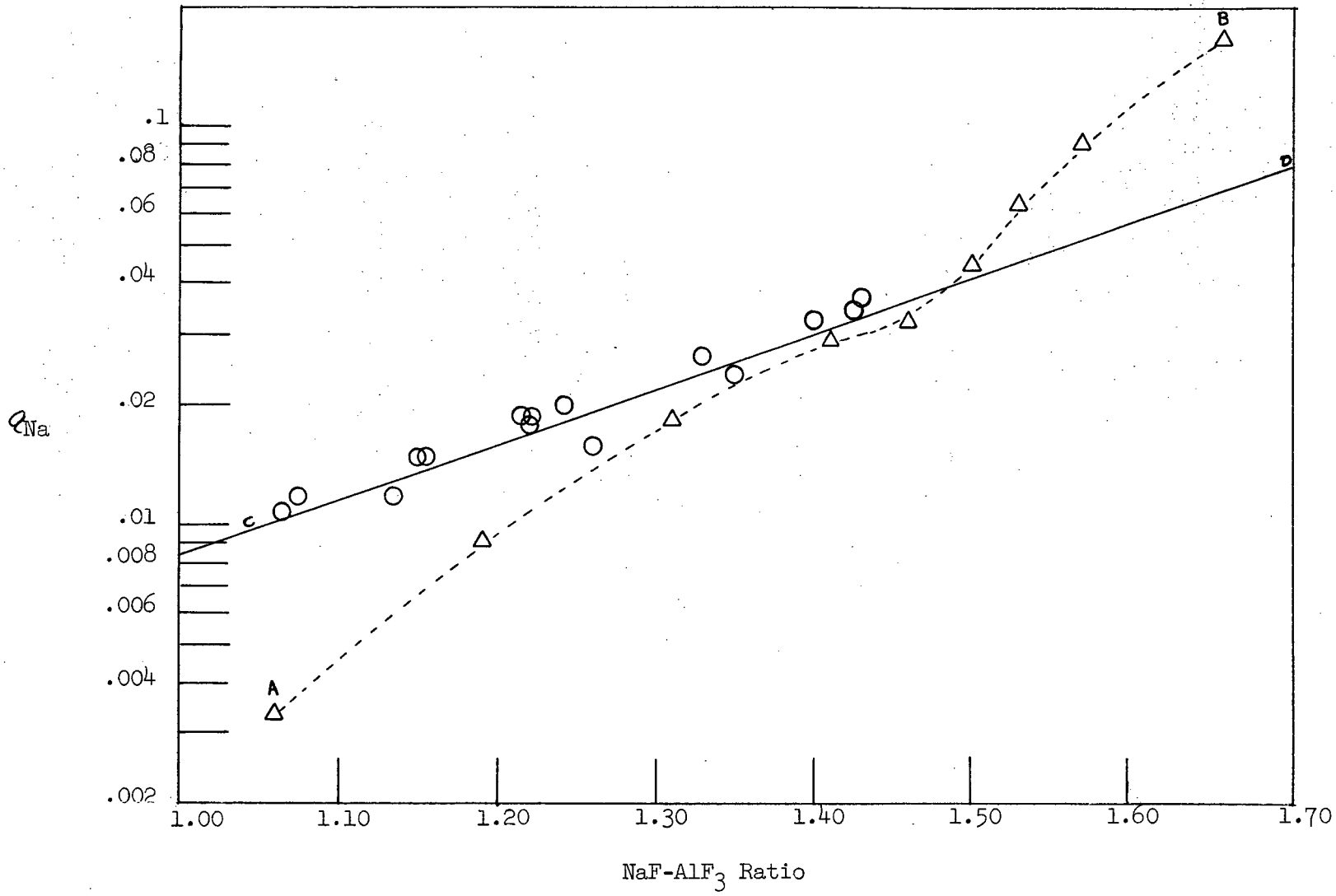

Figure 7. Plot of ϱ_{Na} vs. NaF-AlF_3 Ratio for Alumina-Saturated Pure Cryolite

3. Activity of Sodium in Contact with Commercial Reduction Cell Electrolytes

Commercial reduction cell electrolytes (alumina-saturated) of initial $NaF-AlF_3$ ratios of 1.55 and 1.39 were used in this section of the study. Analyses are shown in Table I.

Measured sodium activity values for the two commercial electrolytes and for the commercial electrolytes (ratio 1.55) plus 5% and 10% AlF_3 are plotted in Figure 8 as a function of $NaF-AlF_3$ ratio. The data are shown in Table E-II.

The theoretical curve AB (see Figure 6) is adjusted by an average dilution factor of .825 and is shown as a dotted line in Figure 8. The dilution factor is obtained by a comparison of Figures D-2 and D-3, and the activity calculation is carried out in Table D-II.

The reference line CD from Figure 7. appears as a solid line in the diagram.

4. Effect of CaF_2 Content on the Activity of Sodium in Contact with Alumina-Saturated Pure Cryolite

A batch of alumina-saturated pure cryolite was prepared with 10% AlF_3 and 7% CaF_2 as additives for this section of the study.

Measured sodium activity values for the test runs using the above batch are plotted in Figure 9 as a function of $NaF-AlF_3$ ratio. The data are shown in Table E-III.

The theoretical curve AB (see Figure 6) is adjusted by a dilution factor of .84 and is shown as a dotted line in Figure 9. The dilution factor is obtained from Figure D-3, and the activity calculation is carried out in Table D-III.

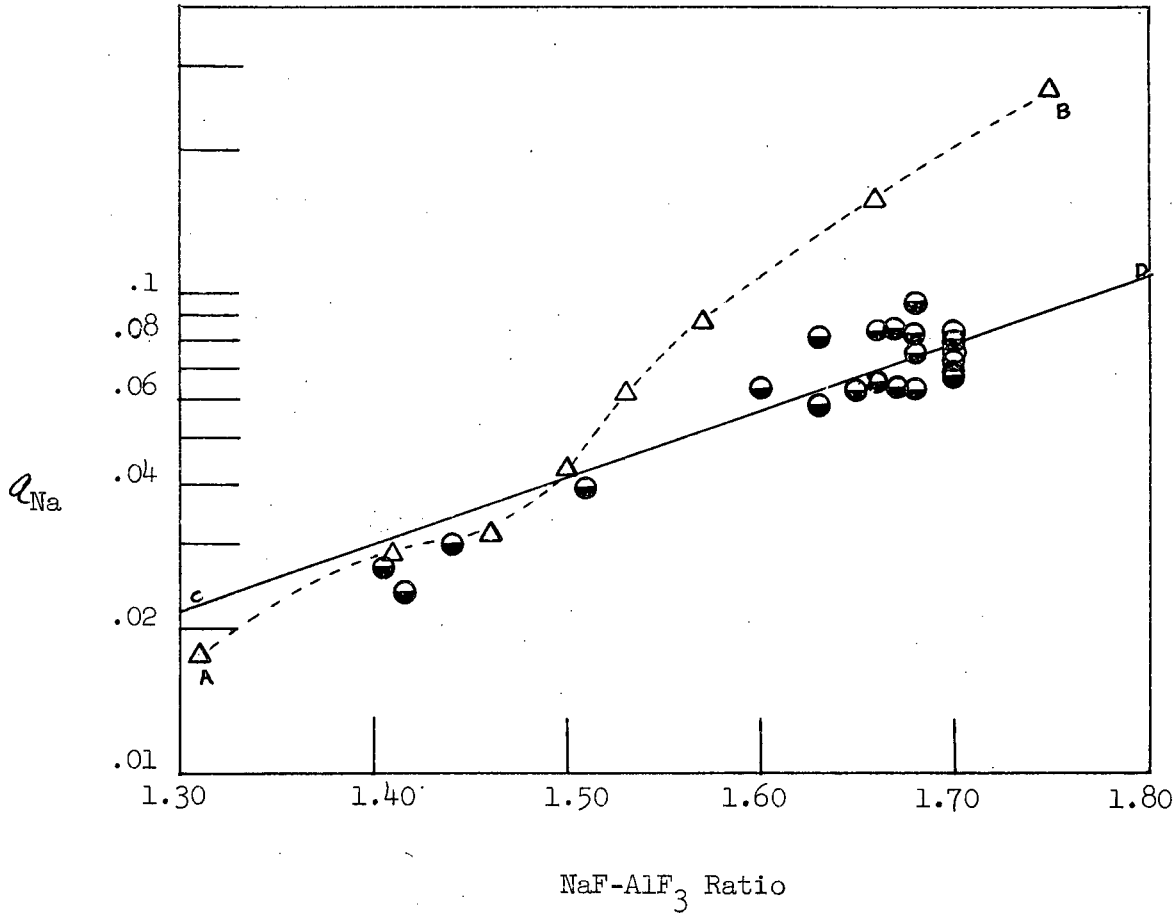

Figure 8. Plot of q_{Na} vs. NaF-AlF$_3$ Ratio for Commercial Reduction Cell Electrolytes.

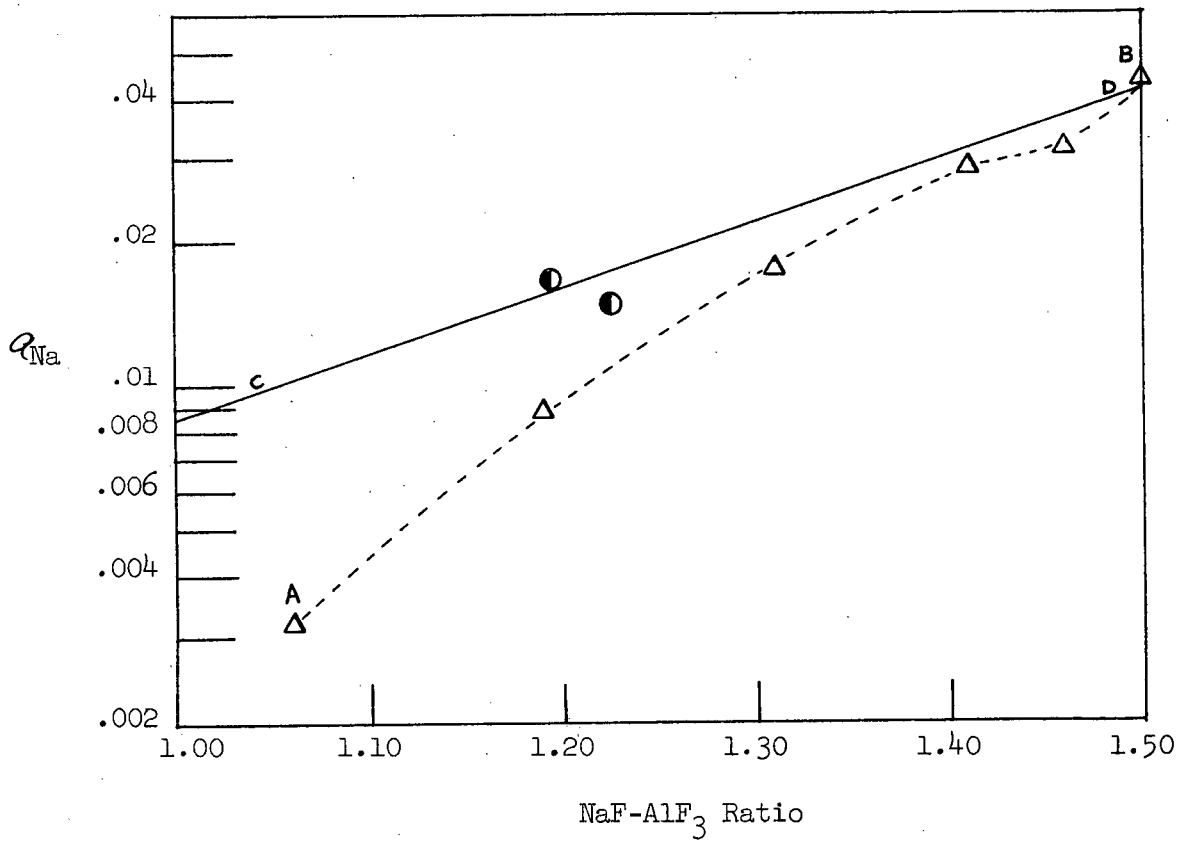

Figure 9. Plot of ϱ_{Na} vs. NaF-AlF$_3$ Ratio for Alumina-Saturated Pure Cryolite containing CaF$_2$

The reference line CD from Figure 7 appears as a solid line in the diagram.

5. Effect of CaF_2 Content on the Activity of Sodium in Contact with Commercial Reduction Cell Electrolyte

A batch of commercial reduction cell electrolyte (initial ratio 1.55) was prepared with the addition of 7% CaF_2.

Measured sodium activity values for the test runs using the above batch are plotted in Figure 10. as a function of NaF-AlF_3 ratio. The data are shown in Table E-III.

The theoretical curve AB (see Figure 6) is adjusted by a dilution factor of .78 and is shown as a dotted line in Figure 10. The dilution factor is obtained from Figure D-2, and the activity calculation is carried out in Table D-IV.

The reference line CD from Figure 7 appears as a solid line in the diagram.

6. Discussion of Dilution Factor

At this point it is interesting to note the effect that dilution has on the activity calculation. Values of activities for sodium which are adjusted for dilution affects are only slightly lower than those obtained for pure cryolite. This is due to the relationship between NaF and AlF_3 in the calcuation. The curve retains the same shape with very little displacement up to a diluent content of 22%. A comparison of the activity relationships between pure cryolite and cryolite containing 22% diluent is shown in Figure 11. As the experimental results noted in this study lie within this range of dilution it is reasonable to consider all the results as being compatible with one another. The differences in activities will not be significant and should lie within experimental error.

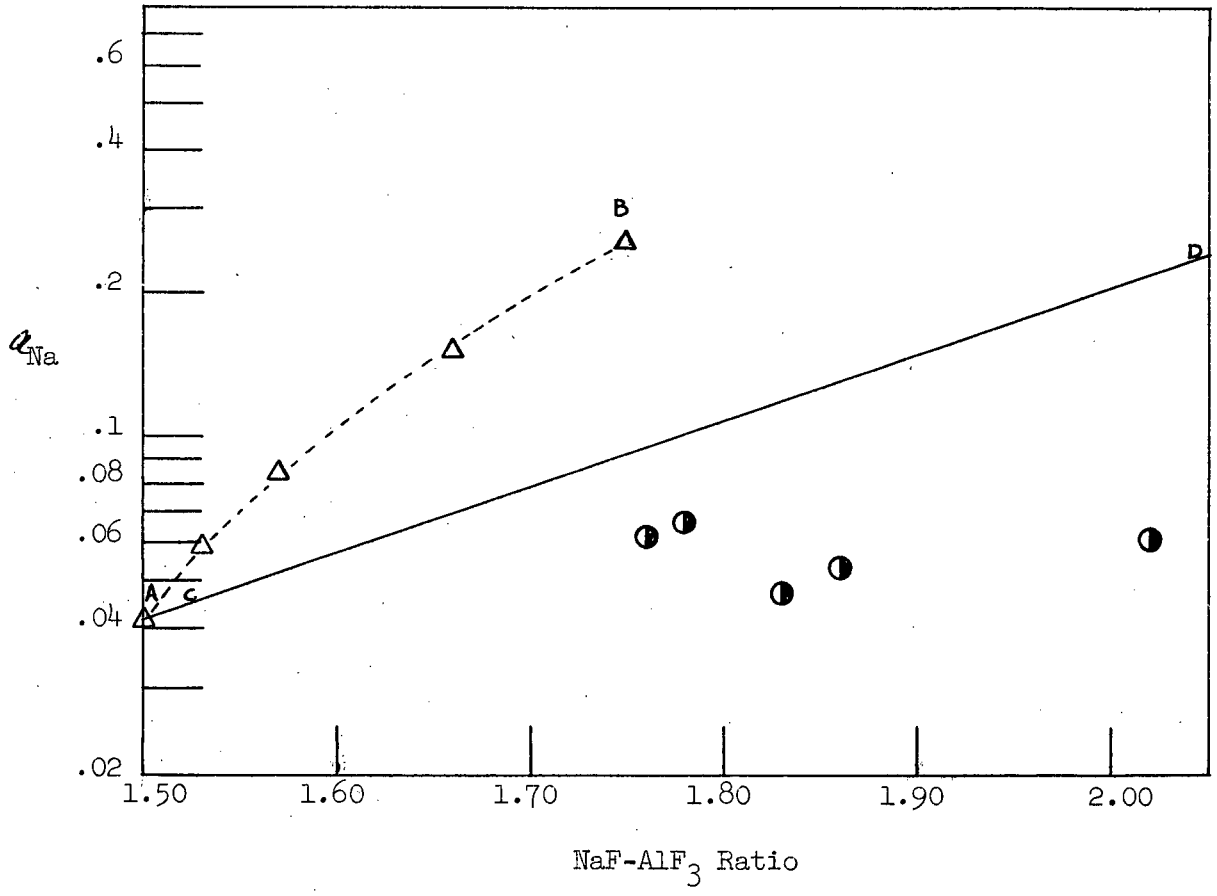

Figure 10. Plot of α_{Na} vs. NaF-AlF_3 Ratio for Commercial Reduction Cell Electrolyte containing CaF_2.

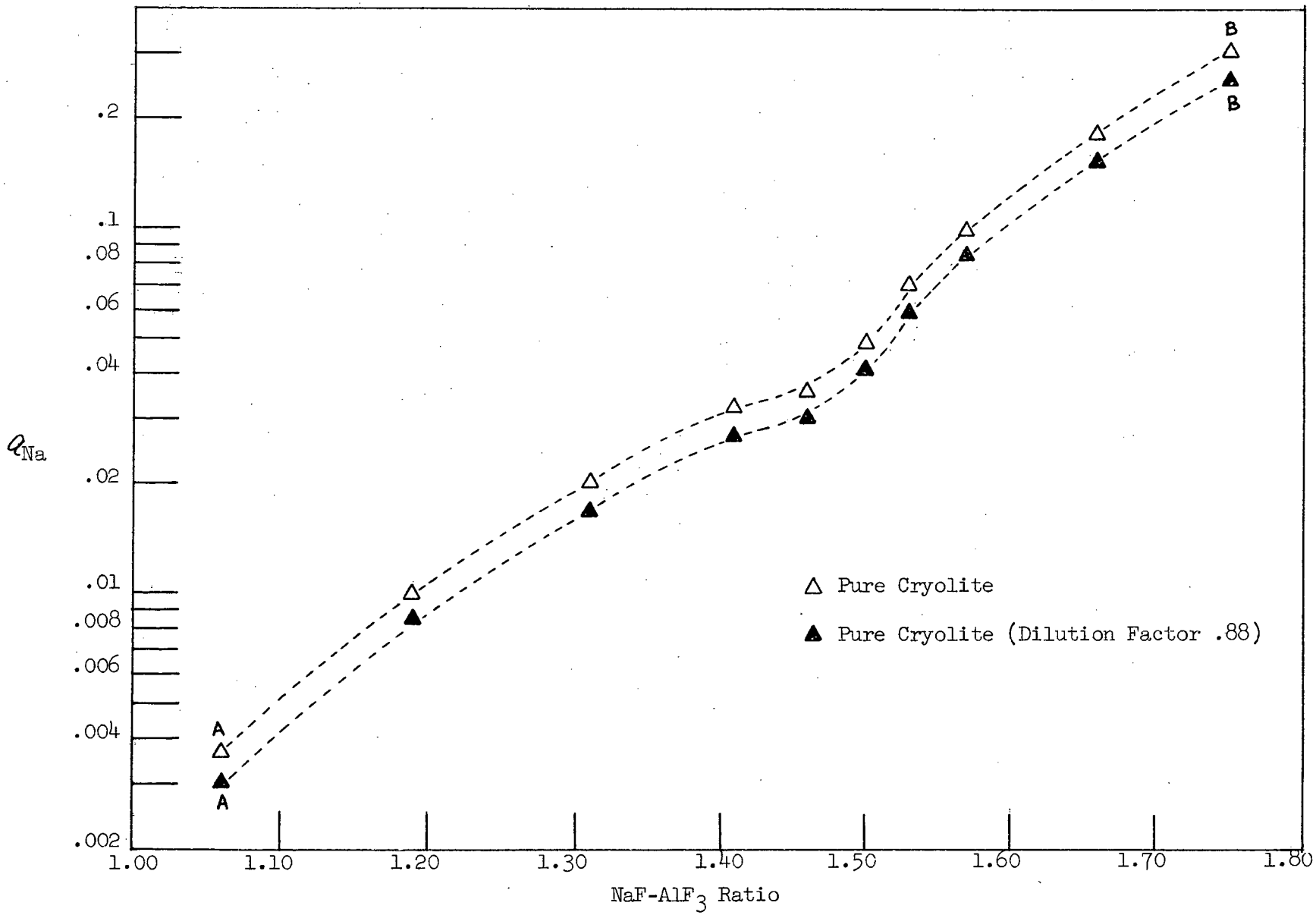

Figure 11. Comparison of a_{Na} Curves for Pure Cryolite and Cryolite containing 22% Diluent.

7. Comparison of Activity Results

The data from Figures 7, 8, 9, and 10 is combined and presented in a single plot in Figure 12. as a function of $NaF\text{-}AlF_3$ ratio. The theoretical curve from Figure 6 is superimposed on the plot as a dotted line AB.

The reference line CD from Figure 7 appears as a solid line. This line fits all of the experimental data reasonably well except for the points at high ratio which contained an excess of CaF_2 ($> 10\%$).

8. Determination of Activity Data for NaF and AlF_3

The reference line in the preceding figures has been used to analyse the experimental data and determine thermodynamic properties of NaF and AlF_3 over the experimental range. The analysis can be carried out by solving two simultaneous equations and a differential equation, assuming that one of the values on one of the $\frac{\log \gamma}{N^2}$ curves developed in Appendix C is correct (see Figures C-2,C-3). The tie point E was chosen as $N_{AlF_3} = .223$ which corresponds to an $NaF\text{-}AlF_3$ ratio of 1.75 and the corresponding activity coefficient (γ) was taken from the $\frac{\log \gamma_{NaF}}{N_{AlF_3}^2}$ curve (see Figure C-2) as the starting point for the computation. The choice of the tie point E was made because of its proximity to the tie point for the compound integration of cryolite at $N_{AlF_3} = .165$, (the eutectic between NaF and Na_3AlF_6). Furthermore, the $\frac{\log \gamma_{NaF}}{N_{AlF_3}^2}$ curve should be more accurate in this range as any error in the regular solution correction would have little effect. A computer program was written and the computation was carried out on an IBM 1620. The mathematical analysis, computer program and data appear in Appendix F.

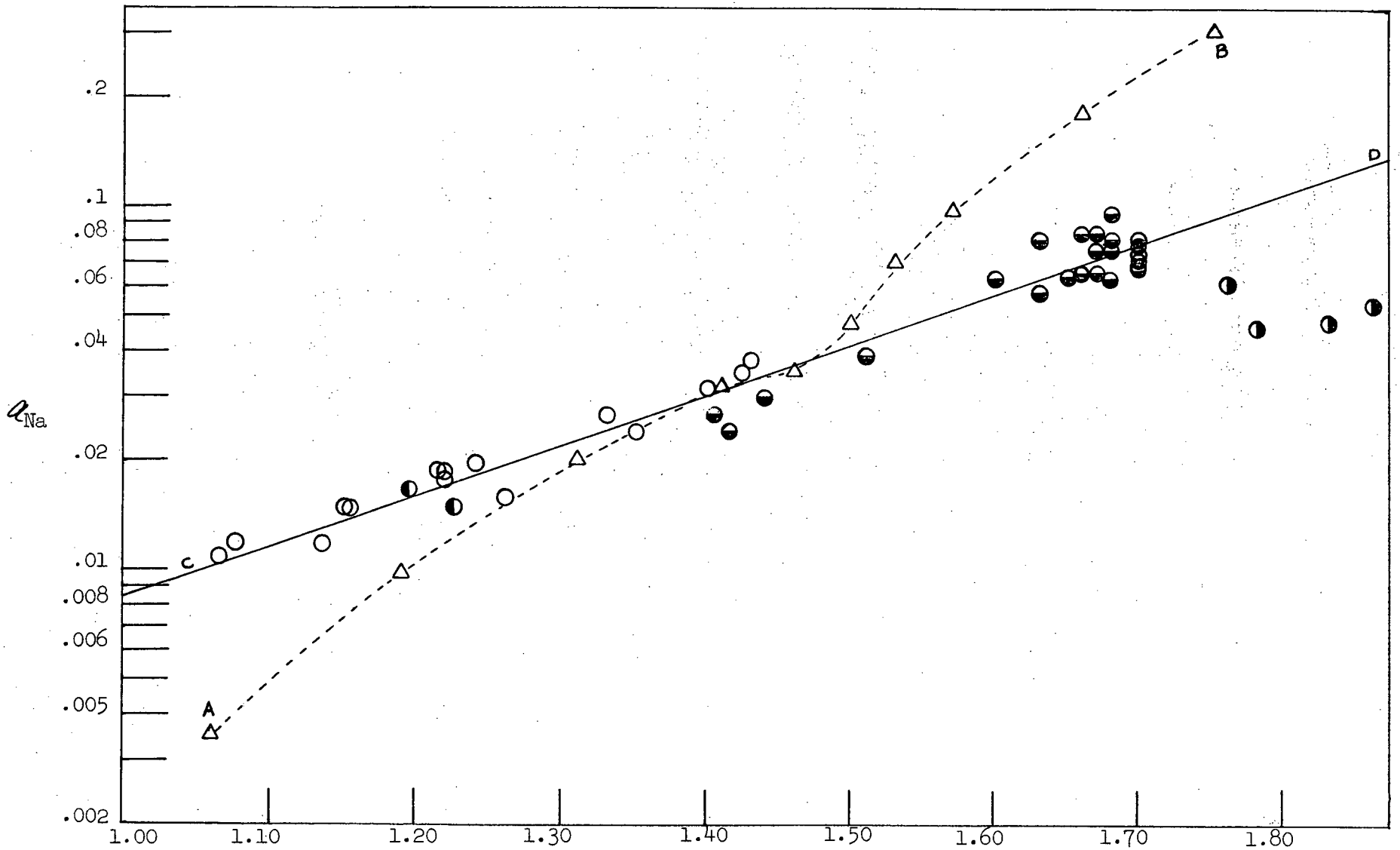

Figure 12. Composite Plot of α_{Na} vs. $NaF\text{-}AlF_3$ Ratio

$\frac{\text{Log } \gamma_{NaF}}{N_{AlF_3}^2}$ and $\frac{\log \gamma_{AlF_3}}{N_{NaF}^2}$ curves have been obtained from this data and are plotted in Figures 13, 14 and 15. An attempt to obtain heat of solution data from this calculation was not successful due the sensitivity of the numbers in this range. It would appear that the tie point E at N_{AlF_3} = .223 is slightly in error, possibly due to the shape of the liquidus curve of the cryolite compound in the NaF-AlF_3 phase diagram. The flattening of the compound peak (see Figure C-1) due to dissociation may introduce small errors in the compound integration technique for activity calcuations.

Figure 13 compares the two experimental $\frac{\log \gamma}{N^2}$ curves over the range of experimental measurements. The two theoretical curves are superimposed as dotted lines on the diagram. If the tie point E were raised slightly, both experimental curves would be shifted higher and more in line with the theoretical curves. A smoothing out of the theoretical $\frac{\log \gamma_{NaF}}{N_{AlF_3}^2}$ curve in the region of the tie point would raise the tie point and this change could be substantiated if a discrepancy occurs in the compound integration technique.

Figure 14 and 15 compare each of the experimental $\frac{\log \gamma}{N^2}$ curves with their theoretical counterparts over the full range of theoretical calculation. The general shapes of the curves compare favourably.

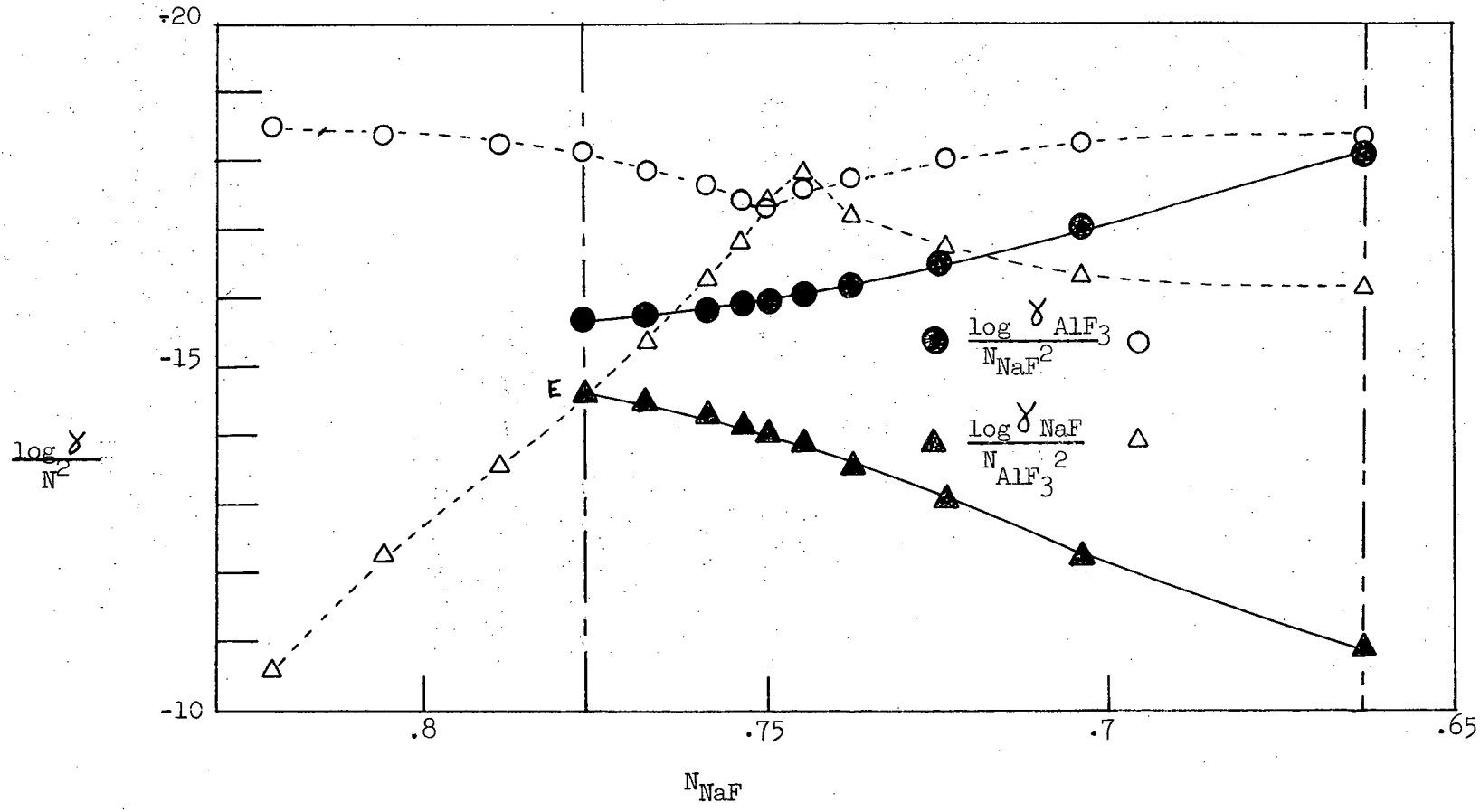

Figure 13. Experimental and Theoretical Activity Data for NaF and AlF_3

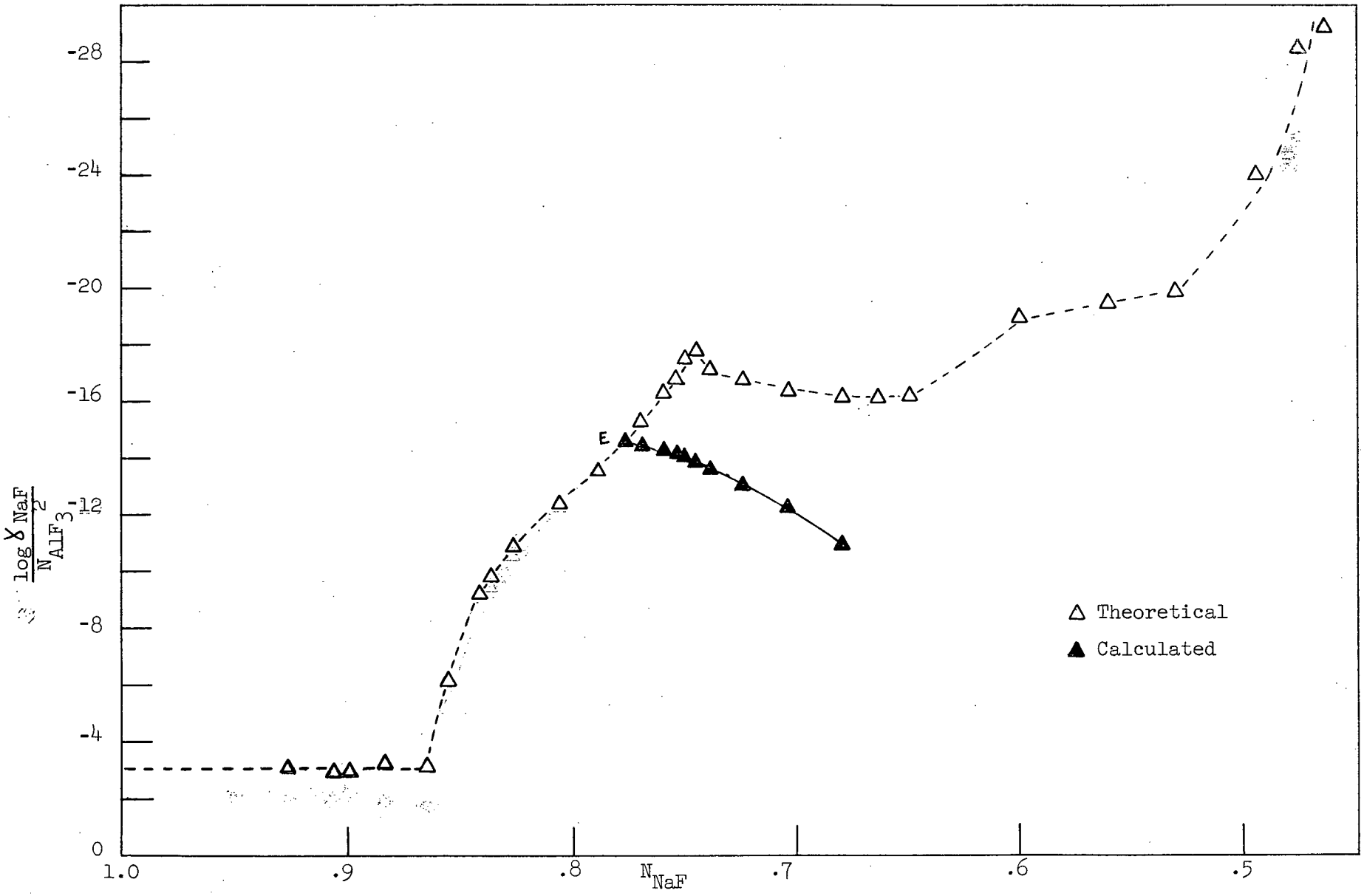

Figure 14. Activity Data for NaF

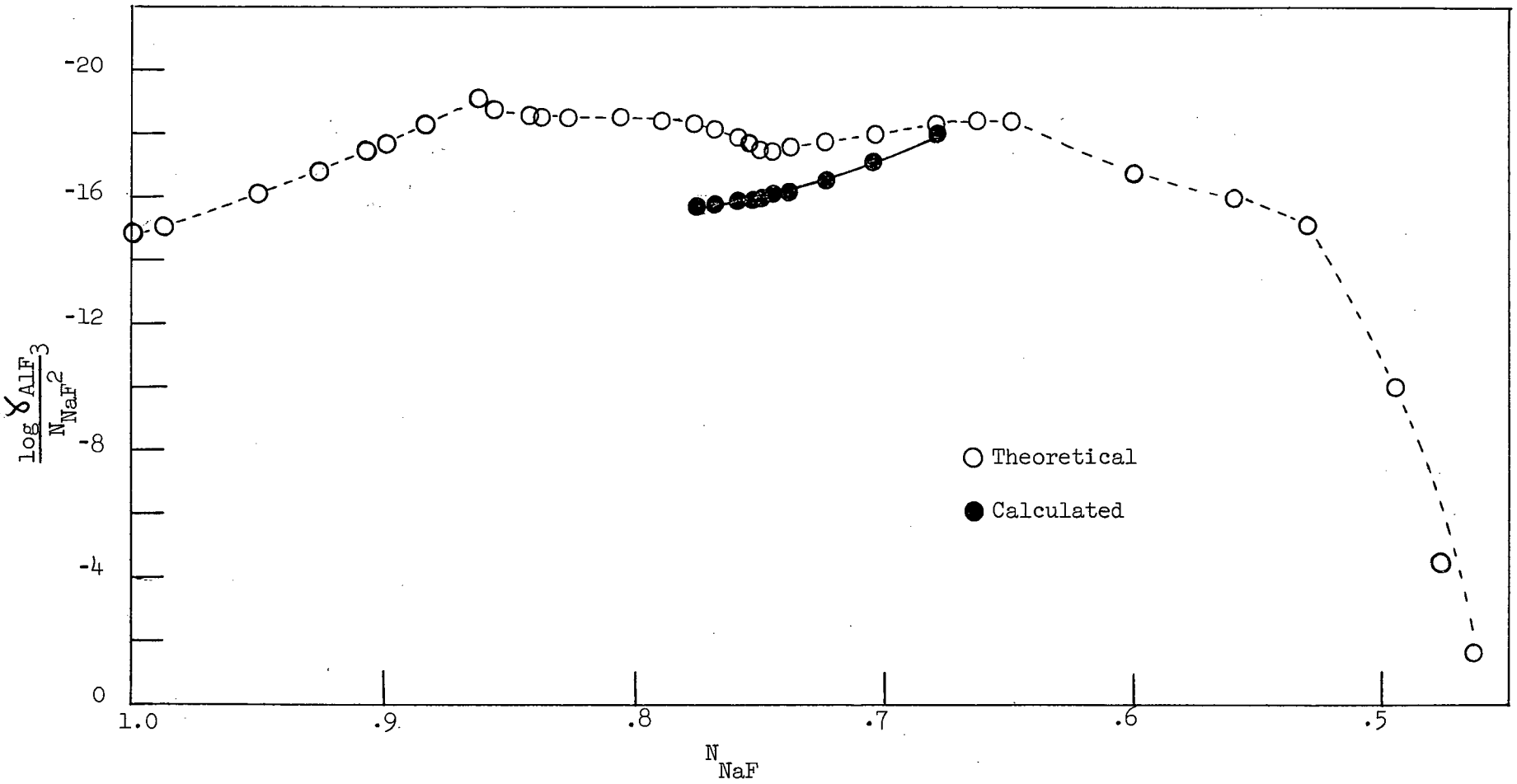

Figure 15. Activity Data for AlF_3

DISCUSSION

1. Comparison with Previous Work

The sodium concentration data of Pearson and Waddington, Jander and Hermann (see Figure 1) and Hollingshead (see Figure G-3) can be related to the activities of sodium by using the calibration curve (see Figure G-6) developed in Appendix G. The majority of these data are in reasonable agreement with the experimental line CD developed in this study, particularly at $NaF-AlF_3$ ratios common to commercial practise (see Figure 16). Activities determined from the experimental work of Feinleib and Porter[13] are also shown on this plot. The measured results were used to calculate activities using Figure A-7. Their work, which was carried out at three different temperatures, shows some divergence from the results obtained here. Sodium activities determined at 940° and 1010°C. were somewhat higher than the experimental activity line CD, whereas the values at 970°C. showed very good agreement with the results of this study. A recent paper by Stokes and Frank[35] outlines a method of determining activities of sodium by a spectroscopic measurement of sodium in the vapour phase above molten cryolite. The study was carried out with pure cryolite of $NaF-AlF_3$ ratio 1.50 over a temperature range from 700-1100°C. Their value for sodium activity at 1010°C. is plotted in Figure 16. along with a value from their thermodynamic calculations. The sodium activity calculated from thermodynamic data is in agreement with the results obtained here but their experimental value is significantly lower.

2. The Effect of CaF_2 Additions on Sodium Activity

The activity of sodium in melts containing quantities of CaF_2 tends to be lower than in pure cryolite, (see Figure 12). This can be noted between $NaF-AlF_3$ ratios of 1.35 and 1.45 where sodium activities have been determined for melts of pure cryolite and reduction cell electrolyte. At lower ratios

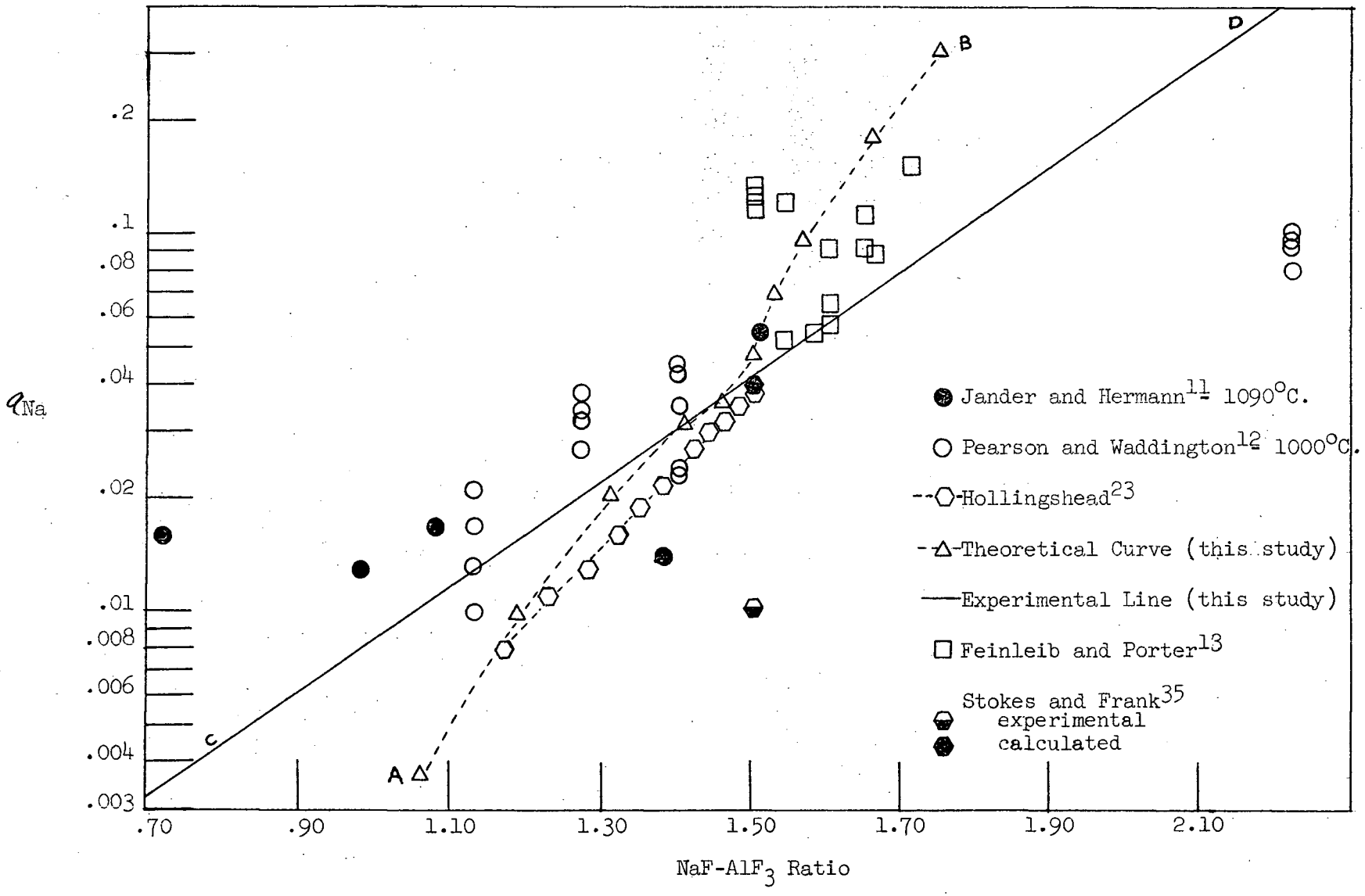

Figure 16. Comparison of Activity Data

the effect is not as noticable although for melts of pure cryolite with additions of CaF_2 the sodium activities are in the lower range of the results. A marked depression in the activities of sodium is noted at high $NaF-AlF_3$ ratios for reduction cell electrolytes containing an excess of CaF_2 (10-14%).

The depression of the sodium activities at $NaF-AlF_3$ ratios between 1.00 and 1.50 would appear to be explained by the effect of dilution. However, at higher ratios, the large depression cannot be explained by a dilution effect alone. It is possible that the large excess of fluorine ions in the melt is tending to reverse the cryolite dissociation reaction either by a direct effect on the equilibrium or by increasing the amount of dimerized sodium fluoride.

INTERPRETATION OF THE RESULTS IN TERMS OF COMMERCIAL OPERATION

An interesting sidelight to this study is the relationship between the difference of the reversible deposition potentials of aluminum and sodium at one atmosphere partial pressure as a function of $NaF\text{-}AlF_3$ ratio. The difference E_L is the extra voltage required to evolve sodium at one atmosphere pressure reversibly in conjunction with the reversible deposition potential of Al. Calculation of the extra voltage can be made by using the following expression

$$E_L = \frac{RT}{nF} \ln \frac{a_L}{a_e}$$

where a_L = the limiting activity and
a_e = the equilibrium activity.

This equation for the case of sodium at 1010°C. reduces to

$$E_L = 2.55 \times 10^{-1} \log \frac{a_L}{a_e}$$

The limiting activity a_L is equivalent to the sodium activity at one atmosphere partial pressure, that is

$$a_L = 1/P^o$$

where P^o = the vapour pressure in atmospheres of pure sodium at the temperature under consideration. This value can be calculated from the expression[24]

$$\log P_{(mm)} = \frac{-5780}{T} - 1.18 \log T + 11.50$$

P is equal to 2140 mm or 2.82 atmospheres at 1010°C. The limiting activity then becomes

$$a_L = \frac{1}{2.82} = .354$$

The equilibrium activity, a_e, is the activity of sodium at the cathode potential required to deposit aluminum reversibly.

The differences in the reversible deposition potentials, E_L, have been calculated and the data appears in Table V. and in Figure 17 as a function of $NaF\text{-}AlF_3$ ratio.

TABLE V.

Difference between Reversible Deposition Potentials of Na and Al (E_L)

Bath Ratio	Na Activity	E_L
1.00	.0085	413 mv
1.10	.0117	377 mv
1.20	.0160	343 mv
1.30	.0220	308 mv
1.40	.0305	272 mv
1.50	.0420	236 mv
1.60	.0575	202 mv
1.70	.0780	168 mv

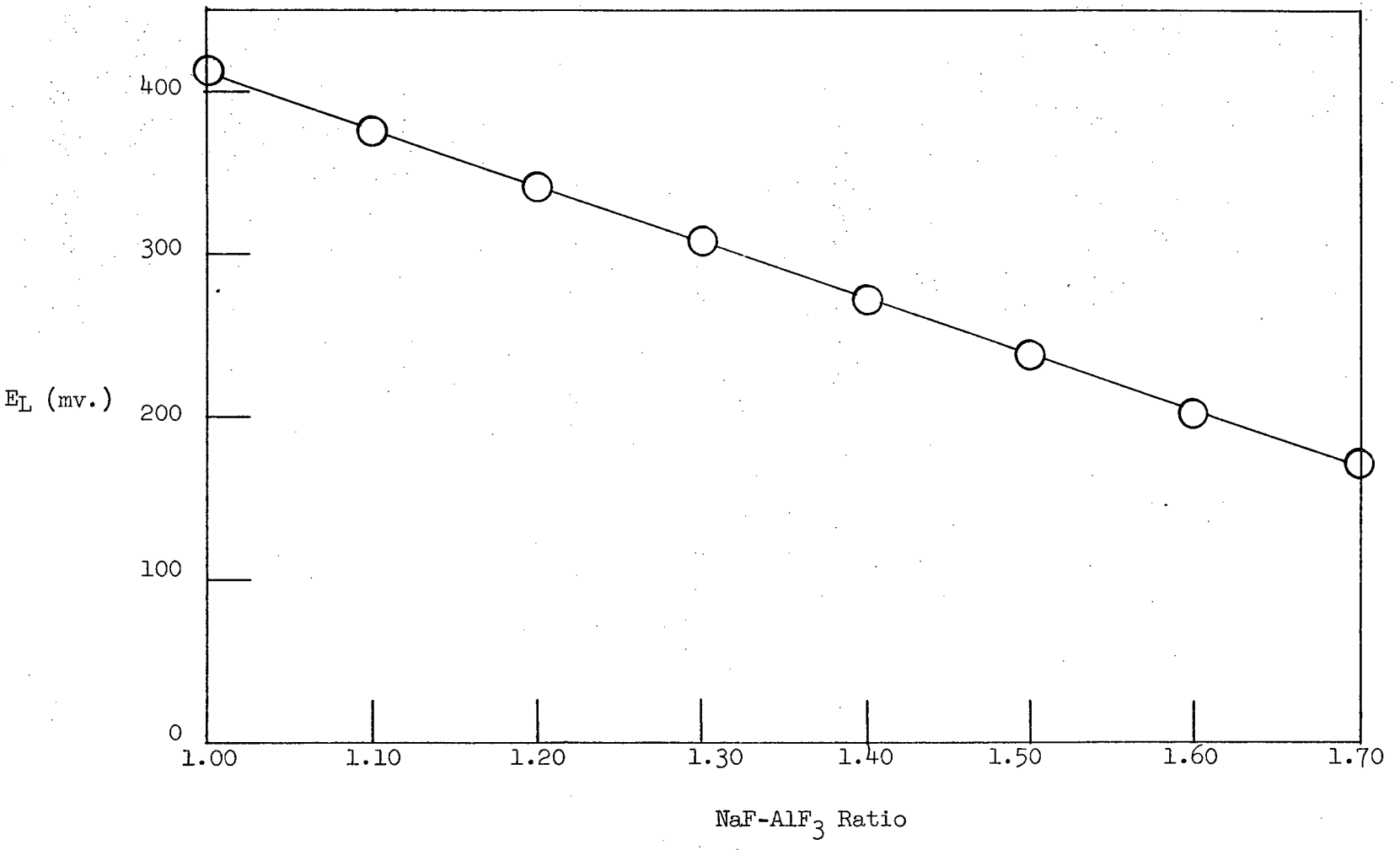

Figure 17. Difference Between Reversible Deposition Voltages of Na and Al as a function of NaF-AlF_3 Ratio

Commercial reduction cells, however, do not operate reversibly. The deposition of aluminum in an electrolytic cell is carried out as an irreversible electrode process. The cell is open to the air and the process operates under a pressure of one atmosphere. Cathodic overvoltages are set up due to kinetics of the reaction. If these overvoltages build up to the point where the limiting activity of sodium is exceeded, gaseous sodium could be produced in the melt. Providing there is no hindrance to the transport of the gaseous sodium it will be liberated to the atmosphere, thereby decreasing the efficiency of the cell.

The actual overvoltage required for the release of sodium at the cathode and its eventual liberation to the air may be somewhat more than the difference in the reversible deposition potentials. Not only may the sodium have its own overvoltage (probably very small in comparsion to that of aluminum) but sodium may exist in a gaseous form in a metastable condition in the melt due to pressure from the melt and transport phenomena. Therefore the data calculated here can only be considered as an indication of the order of overvoltage required for the simultaneous deposition and release of sodium.

From the data in Figure 17 it would appear that overvoltages of the order of .2-.4 volts would cause sodium to be deposited at the aluminum cathode of the cell. As sodium is often observed in industrial cells it seems probable that cathodic overvoltages in the cell are high enough to exceed the necessary voltage difference for co-deposition of the two metals and for the release of sodium gas. Piontelli and Montanelli[10] indicate that at normal cathode current densities commercial reduction cells are operating at a cathode overvoltage of .4-.5 volts. However in a more recent paper, Piontelli[33] indicates that these values are a maximum and that overvoltages of the order of .20 volts are more probable.

A well known characteristic of commercial reduction cells is the variation of current efficiency with $NaF-AlF_3$ ratio. As the ratio increases, current efficiency decreases. This trend can be related to the results obtained here. At high bath ratios an overvoltage of .1-.2 volts may cause the deposition and release of sodium, whereas at lower ratios a higher overvoltage is required. Even at low ratios, however, sodium deposition may be a factor in the current inefficiency of an aluminum reduction cell. During the daily operation of a cell, changes in current densities and electrolyte composition may cause localized overvoltages on the aluminum cathode which exceed the critical value for sodium deposition and release. Furthermore throughout the life of an aluminum reduction cell variations occur in the current distribution to the metal cathode. These variations may effect current densities such that overvoltages in certain areas of the cell may exceed the critical value.

CONCLUSIONS

Activities of sodium in aluminum-cryolite melts have been measured by the equilibration of the three phase system alumina-saturated cryolite, aluminum and lead. An approximate linear increase in the activity of sodium was noted on a log plot of activity as a function of $NaF-AlF_3$ weight ratio over the range pertinent to commercial reduction cell operation. Additions of CaF_2 to cryolite melts appeared to depress the activity of sodium slightly.

Activities of sodium in aluminum-cryolite melts have been estimated by a thermodynamic analysis of the $NaF-AlF_3$ phase diagram, employing Wagner's technique of compound integration for the determination of activities of NaF and the Gibbs-Duhem equation for the determination of activities of AlF_3. Substitution of the activities of NaF and AlF_3 in the K equilibrium equation for the reaction between cryolite and aluminum metal gives the sodium activities. These theoretically determined activities show a fair agreement with the experimental values except at $NaF-AlF_3$ ratios above 1.50.

The experimental results are in fair agreement with previous work carried out by Pearson and Waddington, Jander and Hermann, Feinleib and Porter, and Hollingshead.

The experimental data has been used to compute activity data for NaF and AlF_3 which shows a fair agreement with the theoretical calculations.

The difference between the reversible deposition potential of aluminum and that of sodium at one atmosphere partial pressure varies from .15-.40 volts over a range of $NaF-AlF_3$ ratio of 1.70 to 1.00; increasing with decreasing ratio. Indications are that the cathodic overvoltages in

commercial reduction cells are high enough to cause the simultaneous deposition of sodium and aluminum and that this mechanism contributes to the current inefficiency of the cell. The relationship between the differences in deposition potentials as a function of $NaF-AlF_3$ ratio developed here corresponds to observations made in commercial practise, that is, current efficiency decreases as the $NaF-AlF_3$ ratio increases.

RECOMMENDATION FOR FURTHER WORK

It could be of interest to determine activities of sodium over a range of $NaF-AlF_3$ wt. ratios of 1.00-2.00 using one basic material, alumina-saturated pure cryolite to determine if their is any break in the experimental relationship of low activity sodium as a function of $NaF-AlF_3$ ratio above ratios of 1.50.

The depressive effect of CaF_2 additions on the activities of sodium indicated here may well be another field worthy of investigation. The effect on sodium activity of additions of materials such as MgF_2, LiF, BeF_2, NaCl, $BaCl_2$ and KCl could also be of interest as these materials have all been suggested for use in the electrolytic melts.

Finally, a study of the pure system cryolite-aluminum would be of interest in order to resolve the assumptions which it is necessary to make when using saturated alumina melts. This study will depend upon the development of an inert container material.

APPENDIX A

Analysis of Pb-Na Binary System

APPENDIX A

Analysis of Pb-Na Binary System

The lead-sodium binary has been investigated thoroughly and the best representation of the data is given by Hansen[17]. The significant section involved in this work lies in the range 60-100% Pb (see Figure A-1),

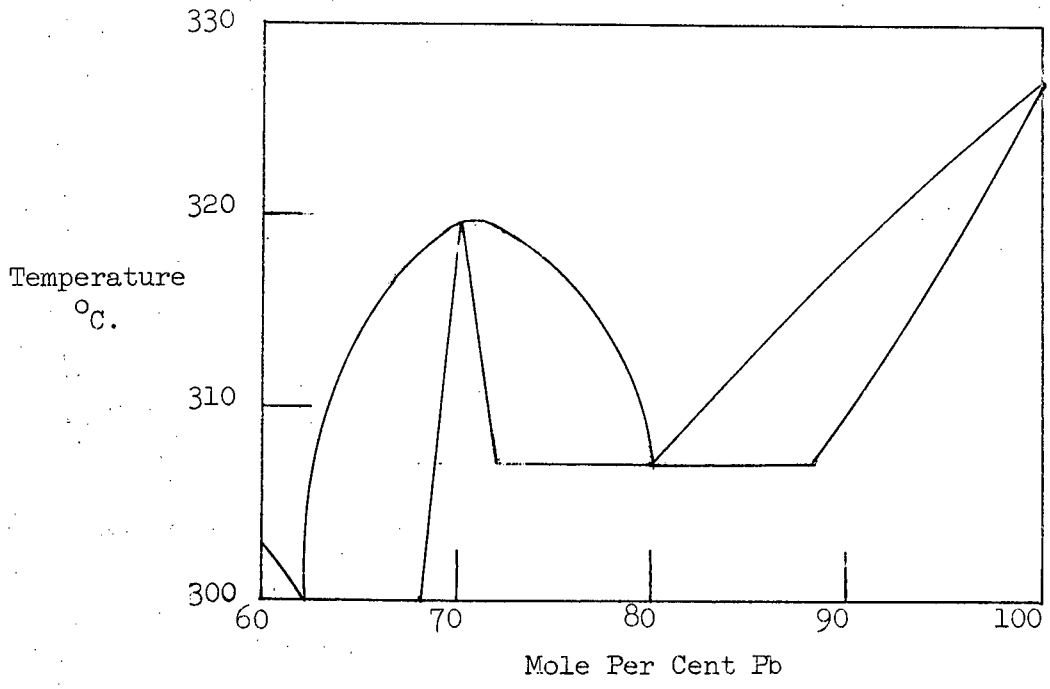

Figure A-1. Significant Section of Pb-Na Binary

which includes the compound $NaPb_3$. The presence of the compound explains some of the deviations from regularity which are found in the following analysis.

Very little published data is available on the activity of sodium in lead at high temperatures. Hauffe and Vierke[18] measured the activity at 425°C. and 475°C. by an emf technique between pure sodium and various sodium lead alloys and Feinleib and Porter[14] carried out a similar investigation up to 820°C. The activity of sodium in the alloy was obtained by the Nernst equation

$$E = \frac{RT}{nF} \ln \frac{a_{Na(Pb)}}{a_{Na(pure)}} = 1.984 \times 10^{-4} T \log a_{Na(Pb)}$$

Hauffe and Vierke noted wide departures from ideal solution behaviour in their study.

The temperature coefficient of the emf of a cell is directly related to the change in entropy in the cell reaction. This is expressed by the equation

$$\frac{dE}{dT} = \frac{\Delta S}{nF}$$

If the cell is that of a regular solution or a semi-regular solution

$$nF \frac{dE}{dT} = - D R \ln N$$

where D is a constant. The value of D is unity for a regular solution and lies between the limits of 0.95 and 1.5 for those solutions wich appear to be semi-regular[19]. An analysis of Feinleib and Porter's data, on the basis of the temperature coefficient of the emf, is presented in Table A-I and plotted in Figure A-2. This shows a wide divergence from regular or semi-regular solution behaviour over the significant range of composition. The presence of the compound $NaPb_3$ is probably the cause of the inconsistency in this region.

TABLE A-I

Temperature, EMF Data for Pb-Na Alloys

N_{Na}	ln N_{Na}	ΔE	$\Delta T(^{o}C.)$	dE/dT
.151	-1.89	.011	317	35×10^{-6}
.212	-1.55	.015	325	46×10^{-6}
.223	-1.50	.017	336	51×10^{-6}
.293	-1.23	.019	297	64×10^{-6}
.358	-1.03	.029	355	82×10^{-6}
.361	-1.02	.047	312	151×10^{-6}
.401	-0.91	.039	250	156×10^{-6}

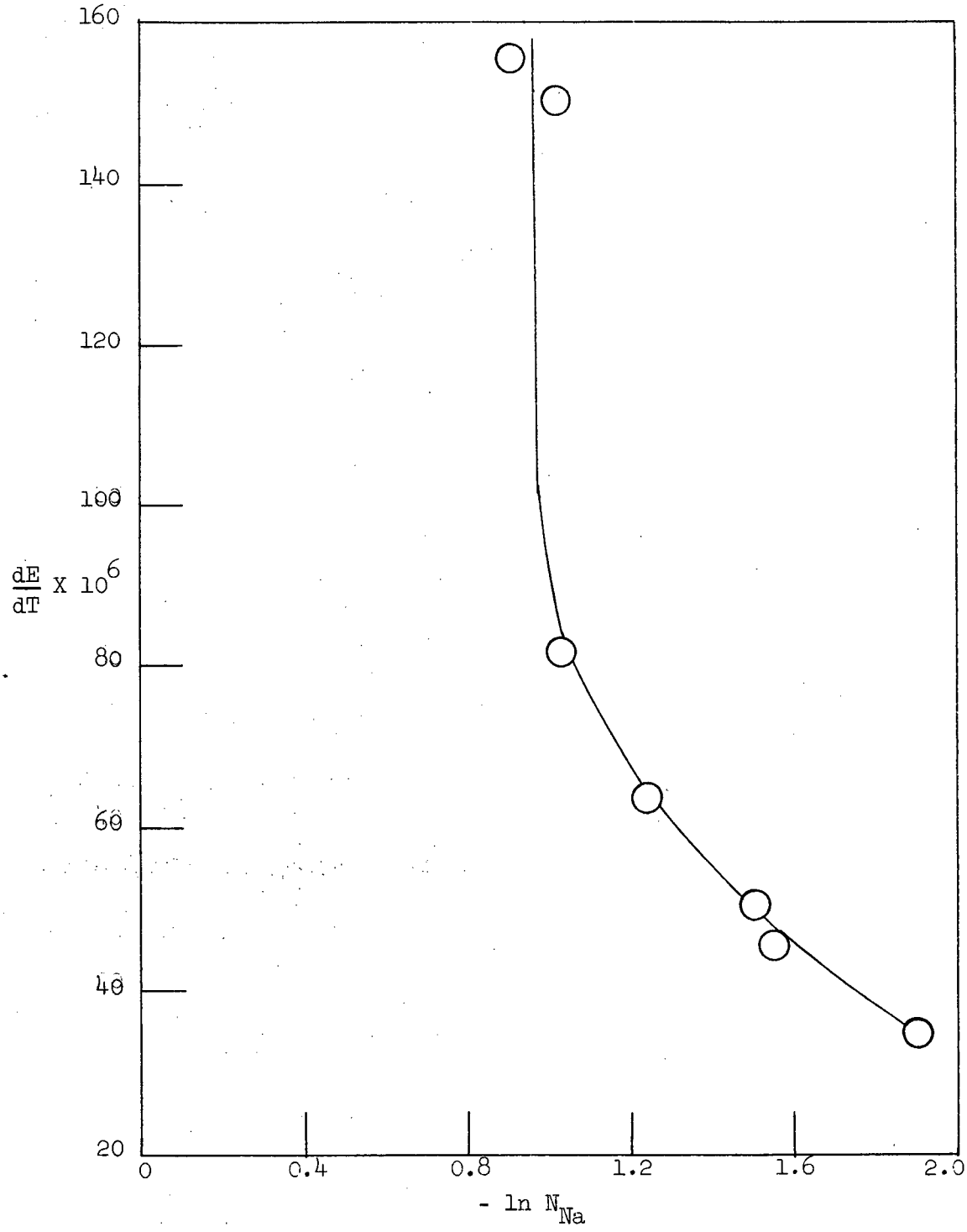

Figure A-2. Temperature Coefficient of EMF from Hauffe and Vierke's Data

Feinleib and Porter[14] extrapolated their data to 1010°C. to obtain sodium activity values which could be used in a study of the aluminum-cryolite system. They checked their extrapolated activity data using a double alloy cell at high temperatures. For this case the Nernst equation becomes

$$E = 1.984 \times 10^{-4} T \log \frac{a_1^{Na(Pb)}}{a_2^{Na(Pb)}}$$

They obtained a fair agreement between the data obtained from the double alloy cells and their extrapolated data and therefore assumed the extrapolation to be correct.

As a check on their data, a plot of log a vs. 1/T was determined. A plot of this data should give a straight line with a slope equivalent to the heat of solution. It can be seen from Figure A-3. that the data is thermodynamically inconsistent.

In order to adjust the activities to fit thermodynamic theory and extrapolate this data to higher temperatures, the two sets of data of Hauffe and Vierke and Feinleib and Porter (see Table A-II) were used to establish a rigid thermodynamic analysis. At low temperatures both sets of data were consistent and a plot of log γ_{Na} vs. $(1-N_{Na})^2$ was determined at 475°C. (see Figure A-4). Making use of Feinleib and Porter's activity data, (see Table A-III) a series of log γ vs. 1/T plots were drawn and the best possible straight lines were determined. The heats of solution ($\bar{L}$) were calculated from these lines. A plot of the heats of solution, as a function of concentration, was then developed by obtaining the best fit with this data and that of the double alloy cells (see Figure A-5). The log γ vs. 1/T plot was redrawn (see Figure A-6) using γ values at 475°C.

obtained from Figure A-4 as the base point and extrapolating to 1010°C. by the heats of solution obtained from Figure A-5. The composite data from the plots is tabulated in Table A-IV. The γ values were converted to activities and a calibration plot established (see Figure A-7).

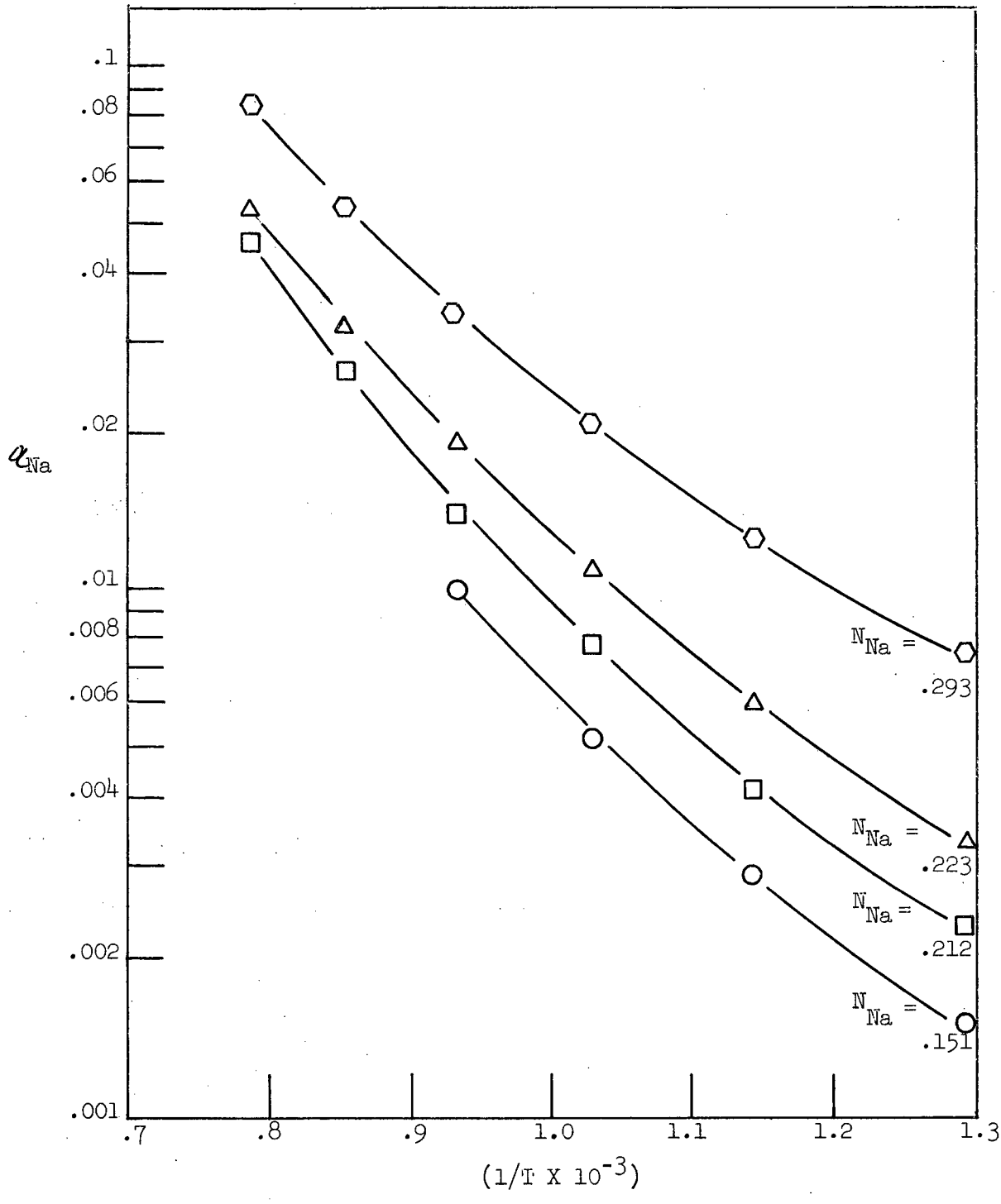

Figure A-3. Plot of Log a vs. 1/T from Feinleib and Porter's Pb-Na Activity Data

TABLE A-II

Pb-Na Activity Data at 475°C. (from Hauffe and Vierke[18] and Feinleib and Porter[14])

N_{Na}	ϱ_{Na}	γ_{Na}	log γ Na	$1-N_{Na}$	$(1-N_{Na})^2$	$\frac{\log \gamma_{Na}}{(1-N_{Na})^2}$
Data from Hauffe and Vierke						
.935	.925	.989	-.004804	.065	.004225	-1.14
.815	.710	.871	-.059982	.185	.034225	-1.75
.757	.363	.479	-.319664	.243	.059049	-5.41
.678	.215	.317	-.498941	.322	.103684	-4.81
.567	.090	.158	-.801343	.433	.187489	-4.27
.470	.038	.081	-1.091515	.530	.280900	-3.89
.392	.011	.029	-1.537602	.608	.369664	-4.16
.873	.840	.963	-.016374	.127	.016121	-1.02
.794	.515	.649	-.187755	.206	.042436	-4.42
.705	.246	.349	-.457175	.295	.087025	-5.25
.625	.135	.216	-.665546	.375	.140625	-4.73
.562	.074	.131	-.882729	.438	.191844	-4.60
.444	.020	.046	-1.337242	.556	.309136	-4.33
.336	.007	.019	-1.721246	.664	.440896	-3.90
Data from Feinleib and Porter						
.151	.00124	.00821	-2.085657	.849	.720801	-2.89
.212	.0020	.00943	-2.025488	.788	.620944	-3.26
.223	.0028	.0126	-1.899629	.777	.603729	-3.15
.293	.0065	.0222	-1.653647	.707	.499849	-3.31
.358	.010	.0279	-1.554396	.642	.412164	-3.77
.361	.0076	.0211	-1.675718	.639	.408321	-4.10
.401	.014	.0349	-1.457175	.599	.358801	-4.06

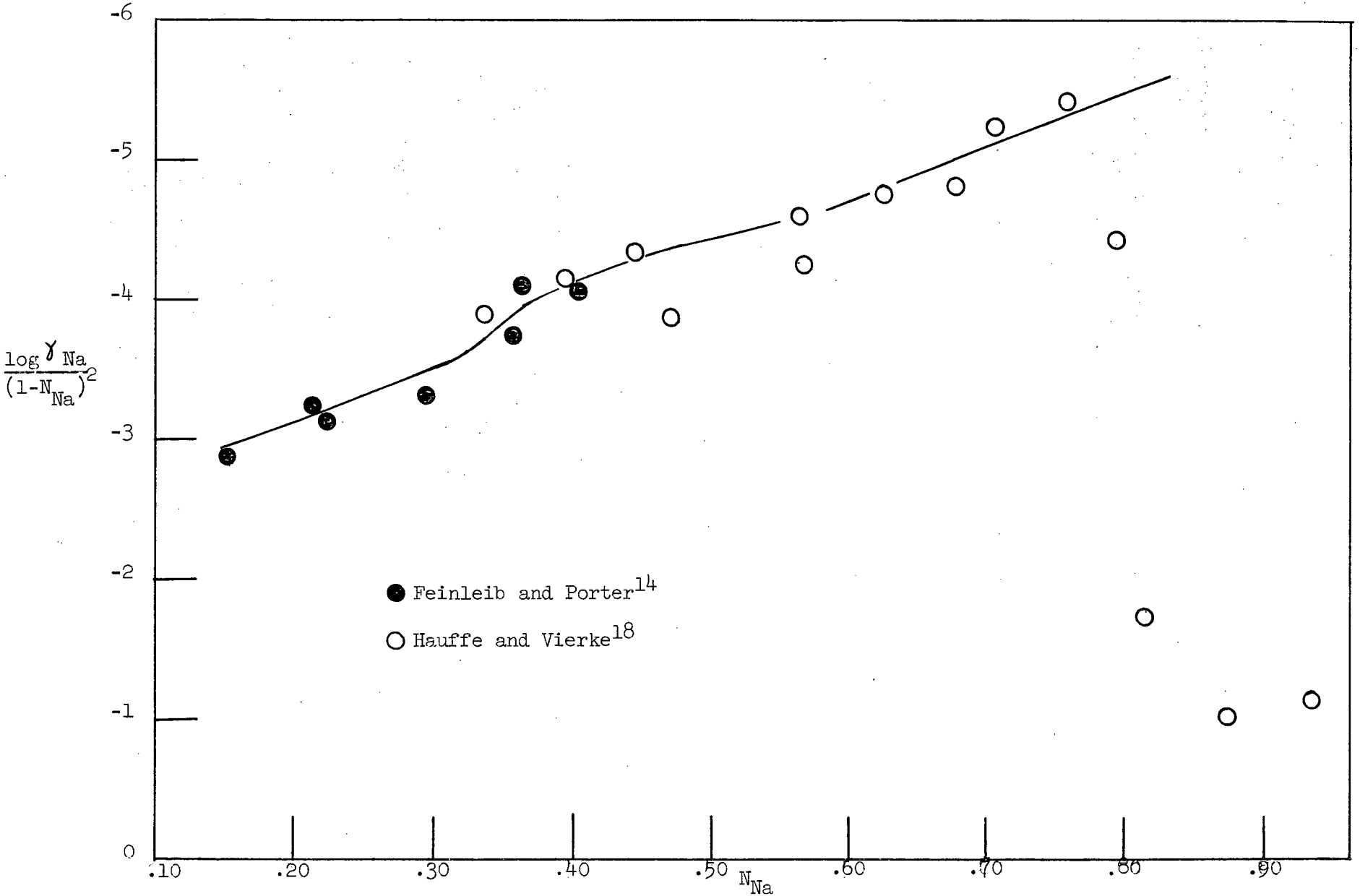

Figure A-4. Plot of $\frac{\log \gamma_{Na}}{(1-N_{Na})^2}$ vs. N_{Na} for Feinleib and Porter's and Hauffe and Vierke's Data

TABLE A-III

Pb-Na Activity Data
(from Feinleib and Porter[14])

N	α	γ	$\bar{L}$	T(°K.)	1/T (X 10^{-3})
0.151	.00142	.0094	10,398	768	1.302
	.00215	.0142		826	1.211
	.00295	.0195		873	1.145
	.00400	.0265		925	1.081
	.00585	.0387		989	1.011
	.00720	.0477		1020	.980
	.00875	.0580		1051	.952
	.01090	.0722		1085	.922
0.212	.00236	.0111	10,398	775	1.290
	.00317	.0150		825	1.212
	.00498	.0235		895	1.117
	.00638	.0301		937	1.067
	.00778	.0367		968	1.033
	.00977	.0461		1003	.997
	.0116	.0547		1031	.970
	.0142	.0670		1071	.934
	.0165	.0778		1100	.909
0.223	.00300	.0135	9,394	758	1.319
	.00415	.0186		804	1.244
	.00590	.0265		868	1.152
	.00825	.0370		923	1.083
	.0107	.0480		961	1.041
	.0139	.0623		1022	.979
	.0170	.0762		1063	.941
	.0215	.0964		1095	.913
0.293	.0088	.0300	8,714	803	1.245
	.0105	.0358		838	1.193
	.0137	.0468		891	1.122
	.0181	.0618		948	1.055
	.0231	.0788		1000	1.000
	.0292	.0997		1048	.954
	.0385	.131		1100	.909
0.358	.0095	.0265	8,288	745	1.342
	.0150	.0419		812	1.232
	.0205	.0573		866	1.155
	.0285	.0796		931	1.074
	.0362	.101		982	1.018
	.0425	.119		1021	.979
	.0500	.140		1061	.943
	.0580	.162		1099	.910

continued...

Table A-III Continued

N	α	γ	$\bar{L}$	T(°K)	$1/T$ (X 10^{-3})
0.361	.0088	.0244	9,839	773	1.294
	.0125	.0346		834	1.214
	.0185	.0513		895	1.117
	.0215	.0596		933	1.072
	.0290	.0803		973	1.028
	.0370	.103		1010	.990
	.0460	.127		1051	.952
	.0570	.158		1085	.922
0.401	.0175	.0436	8,748	783	1.277
	.0230	.0574		833	1.200
	.0310	.0773		885	1.130
	.0410	.102		936	1.068
	.0500	.125		978	1.022
	.0655	.163		1013	.987
	.0715	.178		1033	.968

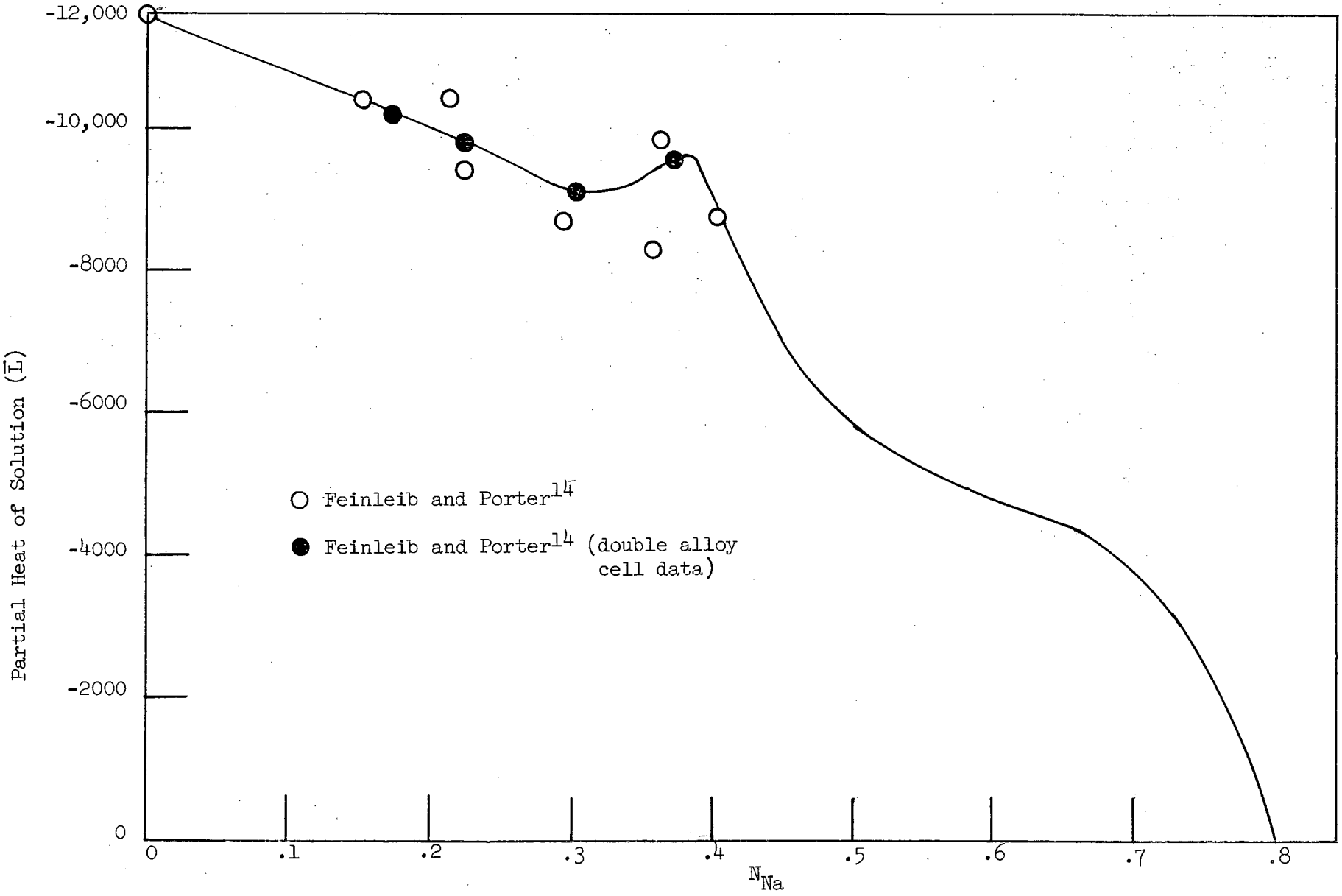

Figure A-5. Partial Heats of Solution of Pb-Na Alloy

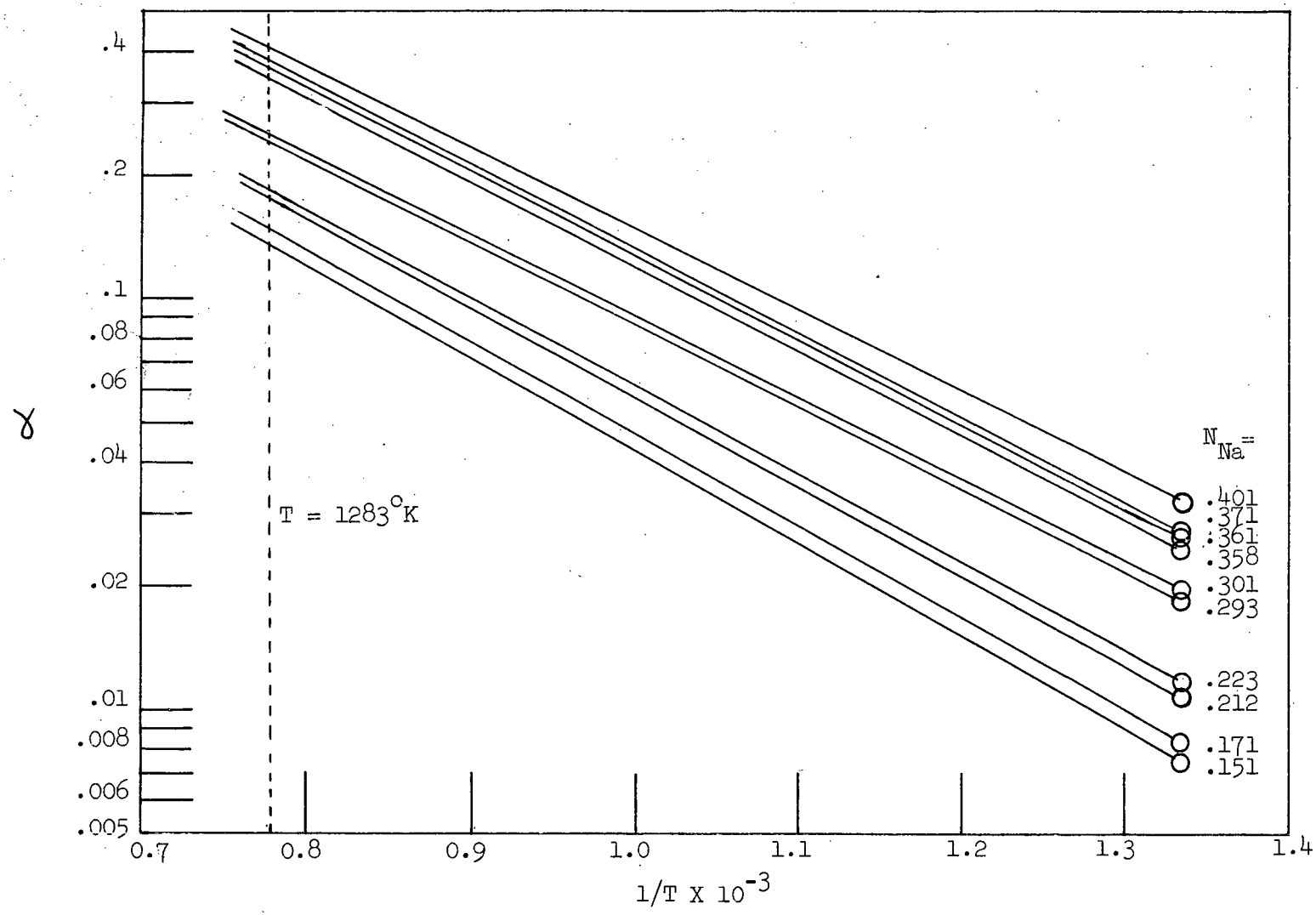

Figure A-6. Plot of log γ Na vs. 1/T for Na Data

TABLE A-IV

Composite Pb-Na Activity Data

N_{Na}	$\frac{\log \gamma_{Na}}{(1-N_{Na})^2}$	$(1-N_{Na})$	$(1-N_{Na})^2$	$\log \gamma_{Na}$	γ_{Na}	$a_{Na_{475}}$	$\bar{L}$	$1/T \times 10^{-3}$ diff.	γ_{1010}	a_{1010}
.151	-2.95	.849	.720801	-2.1264	.00748	.00113	-10.400	.400	.138	.0208
.171	-3.02	.849	.687241	-2.0755	.00840	.00143	-10,200	.449	.149	.0254
.212	-3.11	.788	.620944	-1.9622	.0109	.00231	- 9,900	.462	.173	.0367
.222	-3.20	.778	.605284	-1.9369	.0116	.00258	- 9,800	.467	.181	.0402
.223	-3.20	.777	.603729	-1.9319	.0117	.00261	- 9,800	.467	.181	.0404
.293	-3.48	.707	.499849	-1.7395	.0182	.00533	- 9,200	.497	.241	.0706
.301	-3.50	.699	.488601	-1.7101	.0195	.00587	- 9,100	.503	.250	.0753
.358	-3.90	.642	.412164	-1.607440	.0247	.00884	- 9,400	.487	.348	.125
.361	-3.92	.639	.408321	-1.600618	.0251	.00906	- 9,450	.484	.360	.130
.371	-4.00	.629	.3945641	-1.582564	.0261	.00968	- 9,550	.479	.380	.141
.401	-4.14	.599	.358801	-1.4854	.0327	.0131	- 9,000	.508	.410	.164

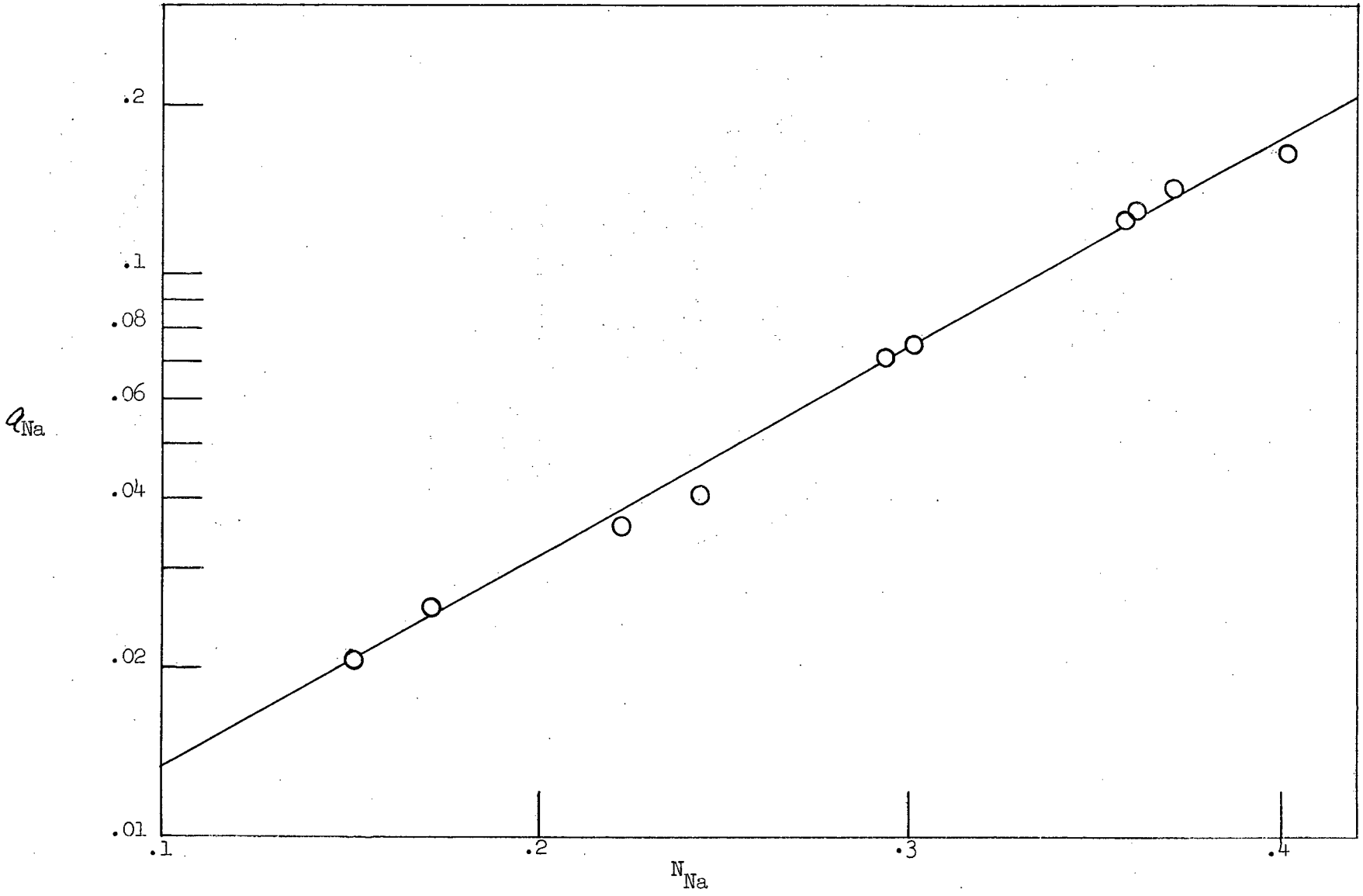

Figure A-7. Activity of Na in Na-Pb Alloys as a Function of Concentration at 1010°C.

APPENDIX B

Calculation of K Equilibrium

APPENDIX B

Calculation of K Equilibrium at 1010°C. (1283°K) from Free Energy Data[25, 34].

$$(Al)_{(l)} + (3NaF)_{(l)} \rightleftharpoons (AlF_3)_{(l)} + [3Na]\ (dil)$$

$$3Na_{(l)} + 3/2F_{2(g)} \rightleftharpoons 3NaF_{(l)} \qquad .....(1)\ \Delta F_1$$

$$Al_{(l)} + 3/2F_{2(g)} \rightleftharpoons AlF_{3(l)} \qquad .....(2)\ \Delta F_2$$

$$\Delta F_T \text{ reaction} = \Delta F_2 - \Delta F_1 = -RT \ln K$$

$$K = \frac{[a_{Na}]^3 \quad (a_{AlF_3})}{a_{Al} \quad (a_{NaF})^3}$$

1. Calculation of ΔF_1

$$3NaF_{(s)298} \rightleftharpoons 3NaF_{(l)1283} \qquad .....(3)\ \Delta F_3$$

$$3Na_{(s)298} \rightleftharpoons 3Na_{(l)1283} \qquad .....(4)\ \Delta F_4$$

$$3/2F_{2(g)298} \rightleftharpoons 3/2F_{2(g)1283} \qquad .....(5)\ \Delta F_5$$

$$\Delta F_1 = \Delta F_3 - \Delta F_4 - \Delta F_5$$

$$(a)\quad \Delta F_3 = \Delta H_{298} + \int_{298}^{1283} CpdT + \Delta H_F - T\left[\Delta S_{298} + \int_{298}^{1283} \frac{Cp}{T}\,d\,T + \Delta S_F\right]$$

$$\Delta H_{298} = -136{,}000 \text{ cal/mole}^{34}$$

$$\Delta S_{298} = 13.1 \text{ e.u.}^{34}$$

$$\Delta H_F = 8030 \text{ cal/mole}^{25}$$

$$\Delta S_F = 6.35 \text{ e.u.}^{25, 2}$$

$$\int_{298}^{1283} CpdT = 10.40\,T + 1.94 \times 10^{-3}\,T^2 + 0.33 \times 10^5\,T^{-1} - 3384^{25}$$

$$\int_{298}^{1283} \frac{Cp}{T}\,dT = 10.40 \ln T + 3.88 \times 10^{-3}\,T + \frac{0.165 \times 10^5}{T^2} - 60.61^{25}$$

$$\Delta F_3 = -491{,}292 \text{ calories}$$

$$(b)\quad \Delta F_4 = \Delta H_{298} + \int_{298}^{371} CpdT + \Delta H_{trans} + \int_{371}^{1283} CpdT - T\left[\Delta S_{298} + \int_{298}^{371} \frac{CpdT}{T} + \Delta S_{trans} + \int_{371}^{1283} \frac{Cp\,dT}{T}\right]$$

$$\Delta H_{298} = 0$$

$$\Delta S_{298} = 12.31 \text{ e.u.}^{34}$$

$$\Delta H_{trans} = 622 \text{ cal/mole}^{25}$$

$$\Delta S_{trans} = 1.68 \text{ e.u.}^{25}$$

$$\int_{298}^{371} CpdT = 4.02\,T + 4.52 \times 10^{-3}\,T^2 - 1599^{25}$$

$$\int_{371}^{1283} CpdT = 6.83\,T - 1.08 \times 10^{5}\,T^{-1} - 2243^{25}$$

$$\int_{298}^{371} \frac{CpdT}{T} = 4.02 \ln T + 9.04 \times 10^{-3}\,T - 25.59^{25}$$

$$\int_{371}^{1283} \frac{CpdT}{T} = 6.83 \ln T - .54 \times 10^{5}\,T^{-2} - 40.02^{25}$$

$$\Delta F_4 = -71{,}085 \text{ calories}$$

$$(c)\quad \Delta F_5 = \Delta H_{298} + \int_{298}^{1283} CpdT - T\left[\Delta S_{298} + \int_{298}^{1283} \frac{Cp}{T}\,dT\right]$$

$$\Delta H_{298} = 0$$

$$\Delta S_{298} = 48.58 \text{ e.u.}^{34}$$

$$\int_{298}^{1283} CpdT = 8.26\,T + 0.30 \times 10^{-3}\,T^2 + 0.84 \times 10^{5}\,T^{-1} - 2771^{25}$$

$$\int_{298}^{1283} \frac{CpdT}{T} = 8.26 \ln T + 0.60 \times 10^{-3}\,T + 0.42 \times 10^{5}\,T^{-2} - 47.71^{25}$$

$$\Delta F_5 = -104{,}412 \text{ calories}$$

$$\underline{\Delta F_1} = -491{,}292 + 71{,}085 + 104{,}412 = -315{,}795 \text{ Calories}$$

2. Calculation of ΔF_2

$$AlF_{3(s)298} \longrightarrow AlF_{3(l)1283} \quad \ldots\ldots(6)\ \Delta F_6$$

$$Al_{(s)298} \longrightarrow Al_{(l)1283} \quad \ldots\ldots(7)\ \Delta F_7$$

$$3/2F_{2(g)298} \longrightarrow 3/2F_{2(g)298} \quad \ldots\ldots(8)\ \Delta F_8 = \Delta F_5$$

$$\Delta F_2 = \Delta F_6 - \Delta F_7 - \Delta F_5$$

$$(a)\quad \Delta F_6 = \Delta H_{298} + \int_{298}^{727} CpdT + \Delta H_{trans} + \int_{727}^{1283} CpdT + \Delta H_F - T\left[\Delta S_{298} + \int_{298}^{727} \frac{Cp}{T}\,dT + \Delta S_{trans} + \int_{727}^{1283} \frac{Cp}{T}\,dT + \Delta S_F\right]$$

ΔH_{298} = -323,000 cal/mole[34]

ΔS_{298} = 23.8 e.u.[34]

ΔH_{trans} = 150 cal/mole[25]

ΔS_{trans} = .21 e.u.

ΔH_F = 6200 cal/mole (see Appendix C)

ΔS_F = 4 e.u. (see Appendix C)

$$\int_{298}^{727} CpdT = 17.27\,T + 5.48 \times 10^{-3}\,T^2 + 2.30 \times 10^{5}\,T^{-1} - 6408^{25}$$

$$\int_{727}^{1283} CpdT = 20.93\,T + 1.50 \times 10^{-3}\,T^2 - 16{,}009^{25}$$

$$\int_{298}^{727} \frac{Cp}{T}\,dT = 17.27 \ln T + 10.96 \times 10^{-3}\,T + 1.15 \times 10^{5}\,T^{-2} - 102.97^{25}$$

$$\int_{727}^{1283} \frac{Cp}{T}\,dT = 20.93 \ln T + 3.00 \times 10^{-3}\,T - 140.13^{25}$$

ΔF_6 = -372,715 calories

$$(b)\quad \Delta F_7 = \Delta H_{298} + \int_{298}^{932} CpdT + \Delta H_F + \int_{932}^{1283} CpdT - T\left[\Delta S_{298} + \int_{298}^{932} \frac{Cp}{T}\,dT + \Delta S_F + \int_{932}^{1283} \frac{Cp}{T}\,dT\right]$$

$$\Delta H_{298} = 0$$

$$\Delta S_{298} = 6.77 \text{ e.u.}^{34}$$

$$\Delta H_F = 2570 \text{ cal/mole}^{25}$$

$$\Delta S_F = 2.76 \text{ e.u.}^{25}$$

$$\int_{298}^{932} CpdT = 4.94\,T + 1.48 \times 10^{-3}\,T^2 - 1604^{25}$$

$$\int_{932}^{1283} CpdT = 7.00\,T - 6524^{25}$$

$$\int_{298}^{932} \frac{Cp}{T}\,dT = 4.94 \ln T + 2.96 \times 10^{-3}\,T - 29.03^{25}$$

$$\int_{932}^{1283} \frac{Cp}{T}\,dT = 7.00 \ln T - 47.86^{25}$$

$$\Delta F_7 = -15{,}423 \text{ calories}$$

$$\underline{\Delta F_2} = -372{,}715 + 15{,}423 + 104{,}412 = \underline{-252{,}880 \text{ Calories}}$$

$$\Delta F_{reaction} = -252{,}880 + 372{,}715$$

$$= 62{,}915 \text{ calories}$$

$$\Delta F = -RT \ln K$$

$$\log_{10} K = \frac{-62{,}915}{4.575\,(1283)} = -10.72$$

$$K = 1.91 \times 10^{-11}$$

APPENDIX C

Analysis of $NaF-AlF_3$ Binary System

APPENDIX C

Analysis of $NaF-AlF_3$ Binary System

1. Determination of the Activity of NaF from the $NaF-AlF_3$ Phase Diagram

Sodium fluoride activities were determined by the method developed by Wagner[27,28,19]. This method has been employed recently for the investigation of binary chlorides by Chu and Egan[29].

The phase diagram of Grjotheim[2] (see Figure C-1) has been used for the thermodynamic calculations. The activity of NaF can be calculated by successive integrations of the compounds in the system using the expression

$$RT \log a_{NaF} = \frac{\Delta H_f}{T_M} \left[\frac{(1-N_2)}{N_2 - X_2} \Delta T + (1-X_2) \int_{X_2}^{N_2} \frac{N_2 \Delta T}{(N_2-X_2)^2} \, dN_2 \right]$$

where ΔH_f = heat of fusion of the compound
T_M = melting point of the compound
ΔT = $T_M - T$
T = liquidus temperature
N_1, N_2 = mole fractions of AlF_3 and NaF
X_1, X_2 = mole fractions of AlF_3 and NaF corresponding to the compound.

Estimation of the heat of fusion of the intermediate compounds is a major uncertainty in this method. In previous work involving this technique the substances have been considered as ideal mixtures and in this case the heat of fusion can be determined by calculating an entropy term which is corrected for the heat of mixing. However, in the case of fused salts, which dissociate on melting, measured calorimetric heats of fusion include heats of dissociation. The contribution of this heat term to the observed value is often difficult to determine. In the study by Chu and Egan[29] on molten binary mixtures, the heat of fusion was calculated on an empirical basis. They assumed the entropy of fusion to be equivalent to the sum of the entropies of the pure components. The entropy of fusion of the intermediate compounds in the $NaF-AlF_3$ syste

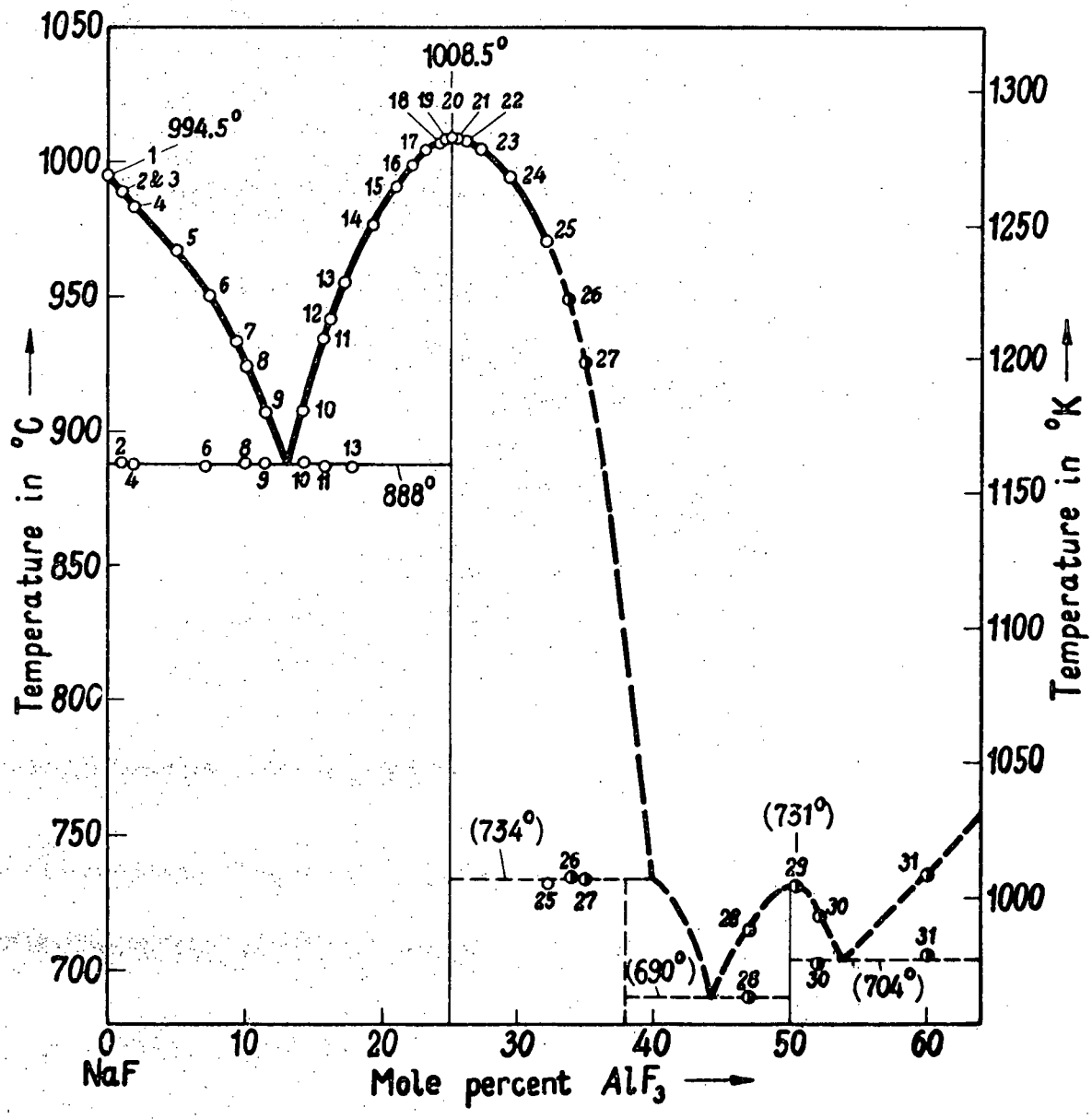

Figure C-1. $NaF-AlF_3$ Phase Diagram (Diagram from Grjotheim[2])

is chosen on an empirical basis and substantiated by the following analysis. It is suggested that a melt of Na_3AlF_6 will contain preponderately Na^+ and $AlF_6^{\equiv}$ ions as statistically independent constituents. As a broad assumption one can consider each particle as dissociating into four particles. Therefore, it is reasonable to expect that the entropy of fusion could be about the same as that of two particles of NaF which also breaks up into four particles[30].

The recent summary of the cryolite situation by Foster[3] assumes the extensive dissociation of the compound into simpler ions. The possibility that dissociation is not complete or that secondary dissociation of the $AlF_6^{\equiv}$ ion is dissociated further to AlF_4^- and F^- ions should not affect the entropy approximation greatly as these two possibilities would tend to compensate for one another. However, it can be seen that these complications make it very difficult to estimate the entropies with any degree of certainty.

The heat of fusion of pure NaF was determined from the most recent data of Kelley[25] and the entropy of fusion calculated to be 6.35 e.u.'s. Therefore the entropy of fusion for the intermediate compounds in the NaF-AlF_3 system are assumed to be 12.70 entropy units.

Relative values of log a_{NaF} have been calculated over the composition range 86.5 mole per cent to 60 mole per cent NaF as shown in Column 16 of Table C-I. These values are relative to the compound cryolite and are not absolute values. In order to obtain the correct values it is necessary to obtain a tie point with the activity of pure NaF. This is accomplished by calculating the a_{NaF} at the eutectic point 86.5 mole per cent NaF. As in general, thermodynamic calculations of this nature are carried out using γ and log γ the correction is applied in Column 19 of Table C-I.

TABLE C-I

Determination of a_{NaF} by Integration of Compound Na_3AlF_6 in $NaF-AlF_3$ Phase Diagram

1	2	3	4	5	6	7
$T^oK.$	X_2	X_1	N_{2NaF}	N_{1AlF_3}	ΔT	N_2-X_2
1007	.75	.25	.600	.400	274.6	-.150
1198	.75	.25	.649	.351	83.6	-.101
1221.5	.75	.25	.663	.337	60.1	-.087
1243.7	.75	.25	.679	.321	37.9	-.071
1267.2	.75	.25	.704	.296	14.4	-.046
1277.5	.75	.25	.724	.276	4.1	-.026
1281.0	.75	.25	.738	.262	0.6	-.012
1281.3	.75	.25	.745	.255	0.3	-.005
1281.6	.75	.25	.750	.250	0	0
1281.3	.75	.25	.754	.246	0.3	.004
1280.4	.75	.25	.759	.241	1.2	.009
1277.2	.75	.25	.768	.232	4.4	.018
1272.6	.75	.25	.777	.223	9.0	.027
1264.1	.75	.25	.789	.211	17.5	.039
1249.5	.75	.25	.806	.194	32.1	.056
1227.2	.75	.25	.827	.173	54.4	.077
1214.3	.75	.25	.837	.163	67.3	.087
1207.2	.75	.25	.842	.158	74.4	.092
1180.8	.75	.25	.856	.144	100.8	.106
1161.0	.75	.25	.865	.135	120.6	.165
1161.0	1.0	0	.865	.135	106.5	-.135
1180.5	1.0	0	.883	.117	87.0	-.117
1196.9	1.0	0	.899	.101	70.6	-.101
1206.8	1.0	0	.907	.093	60.7	-.093
1223.3	1.0	0	.926	.074	44.2	-.074
1240.0	1.0	0	.949	.051	27.5	-.051
1225.7	1.0	0	.976	.024	12.5	-.024
1261.8	1.0	0	.987	.013	5.7	-.013
1262.0	1.0	0	.988	.012	5.5	-.012
1267.5	1.0	0	1	0	0	0

TABLE C-I Continued

8	9	10	11	12	13	14
$\frac{N_1 \Delta T}{N_2 - X_2}$	$X_1 \Delta T$	$(N_2 - X_2)^2$	$\frac{X_1 \Delta T}{(N_2 - X_2)^2}$	$\int_{X_2}^{N_2} \frac{X_1 \Delta T}{(N_2 - X_2)^2} dN$	8 + 12	X 12.70
-732.27	68.65	.0225	3051	-311.90	-1044.17	-13,261.0
-290.53	20.90	.0102	2049	-186.95	- 477.48	- 6,064.0
-232.80	15.03	.00757	1986	-158.74	- 391.54	- 4,972.6
-171.35	9.48	.00504	1881	-127.78	- 299.13	- 3,799.0
- 92.66	3.60	.00212	1698	- 82.78	- 175.44	- 2,228.1
- 43.52	1.03	.000676	1524	- 50.28	- 93.80	- 1,191.3
- 13.10	.15	.000144	1042	- 31.38	- 44.48	- 564.9
- 15.30	.075	.000025	3000	- 17.38	- 32.68	- 415.0
0	0	0	0	0	0	0
18.45	.075	.00016	4688	17.10	35.55	451.5
32.13	.30	.000081	3704	36.85	68.98	876.1
56.71	1.10	.000324	3395	68.62	125.33	1591.7
74.33	2.25	.000729	3086	97.87	172.20	2186.9
94.68	4.38	.00152	2882	133.57	228.25	2898.8
111.20	8.03	.00314	2557	179.47	290.67	3691.5
122.22	13.60	.00593	2293	230.08	352.30	4474.2
126.09	16.83	.00757	2223	252.58	378.67	4809.1
127.77	18.60	.00846	2199	263.63	391.40	4970.8
136.94	25.20	.0112	2250	294.78	431.72	5482.8
141.57	30.15	.0132	2284	315.17	456.74	5800.6
						X 6.35
-106.5	-	-	-	-	-106.5	-676
- 87.0	-	-	-	-	- 87.0	-553
- 70.6	-	-	-	-	- 70.6	-448
- 60.7	-	-	-	-	- 60.7	-385
- 44.2	-	-	-	-	- 44.2	-281
- 27.5	-	-	-	-	- 27.5	-175
- 12.5	-	-	-	-	- 12.5	- 79.4
- 5.7	-	-	-	-	- 5.7	- 36.2
- 5.5	-	-	-	-	- 5.5	- 34.9
0	-	-	-	-	0	0

TABLE C-I Continued

15	16	17	18	19	20
RT	log a_{NaF}	log N_{NaF}	log γ_{NaF}	log γ_{NaF} @ T's add -1.219	log γ_{NaF} @ 1283
4607	-2.878	-.222	-2.656	-3.875	-3.042
5481	-1.106	-.188	- .918	-2.137	-1.996
5588	- .890	-.178	- .712	-1.931	-1.839
5690	- .668	-.168	- .500	-1.719	-1.669
5797	- .384	-.152	- .232	-1.451	-1.434
5845	- .204	-.140	- .064	-1.283	-1.278
5861	- .096	-.132	.036	-1.183	-1.182
5862	- .071	-.128	.057	-1.162	-1.161
5863	0	-.125	.125	-1.094	-1.093
5862	.077	-.123	.200	-1.019	-1.018
5858	.150	-.120	.270	- .949	- .947
5843	.272	-.115	.387	- .832	- .827
5822	.376	-.110	.486	- .733	- .726
5783	.501	-.103	.604	- .615	- .606
5717	.646	-.094	.740	- .479	- .467
5614	.797	-.082	.879	- .340	- .325
5555	.866	-.077	.943	- .276	- .261
5523	.900	-.075	.975	- .244	- .230
5402	1.015	-.067	1.082	- .137	- .126
5312	1.092	-.063	1.155	- .064	- .058
5312	- .127	-.063	- .064	-	- .058
5401	- .102	-.054	- .048	-	- .044
5476	- .0818	-.0462	- .0356	-	- .033
5521	- .0697	-.0424	- .0273	-	- .026
5597	- .0502	-.0333	- .0169	-	- .016
5673	- .0309	-.0227	- .0082	-	- .008
5745	- .0138	-.0105	- .0033	-	- .003
5773	- .00627	-.00568	- .00059	-	- .001
5774	- .00604	-.00524	- .00080	-	- .001
5799	0	0	0	-	0

The two other calculations are carried out over the peritectic compound $Na_5Al_3F_{14}$ (see Table C-II) and the compound $NaAlF_4$ (see Table C-III) to extend the data across the diagram. These are tied in respectively to the corrected values over the cryolite compound range, and the eutectic at 56 mole per cent NaF. All the values are corrected to 1283°K assuming regular solution behaviour. This assmumption can be made as the significant data for this work near the cryolite peak is fairly close to the experimental temperature.

2. Determination of the Activity of AlF_3

Once the thermodynamic data for one of the constituents of a binary diagram is known, it is possible to obtain the data for the other by applying the Gibbs-Duhem equation[26,19]. The expression used for this case is

$$\log \gamma_{AlF_3} = \frac{-N_{NaF} \times N_{AlF_3}}{(N_{AlF_3})^2} \log \gamma_{NaF} + \int_{N_{NaF}=.463}^{N_{NaF}=1} \frac{\log \text{ NaF}}{(N_{AlF_3})^2} \, dN_{NaF}$$

The first term is calculated for the N_{NaF} values obtained from Tables C-I, C-II, and C-III. The data is shown in detail in Table C-IV. The second term is evaluated by plotting the $\frac{\log \gamma \text{ NaF}}{(N_{AlF_3})^2}$ term as a function of NaF concentration and performing a graphical integration. The $\frac{\log \gamma \text{ NaF}}{(N_{AlF_3})^2}$ vs. N_{NaF} plot is shown in Figure C-2. The sum of the two terms gives a relative log γ AlF_3 value, but a correction must be applied at the tie point of 46.3 mole per cent NaF. The tie point is established by obtaining a consistent set of data in respect to the metastable standard state of pure molten AlF_3. Assuming that AlF_3 has a melting point of approximately 1550°K. which is slightly above the actual sublimation point, and using an entropy of fusion of 4 entropy units, a value for the heat of fusion of 6200 calories is obtained. Using this data log γ AlF_3

TABLE C-II

Determination of φ_{NaF} by Integration of Compound $Na_5Al_3F_{14}$ in NaF-AlF_3 Phase Diagram

1	2	3	4	5	6	7	8	9
T^oK	X_2	X_1	N_{2NaF}	N_{1AlF_3}	ΔT	N_2-X_2	$\frac{N_1 \Delta T}{(N_2 - X_2)}$	$(N_2-X_2)^2$
1013	.625	.375	.625	.375	0	0	0	0
1010.5	.625	.375	.6125	.3875	2.5	-.0125	-77.50	.000156
1007	.625	.375	.600	.400	6	-.025	-96.00	.000625
963	.625	.375	.560	.440	50	-.065	-338.46	.00423

10	11	12	13	14	15	16	17	18
$\frac{X_1 \Delta T}{(N_2 - X_2)^2}$	$\int_{X_2}^{N_2} \frac{X_1 \Delta T}{(N_2 - X_2)^2}$	8 + 11	X 12.70	RT	$\log \varphi_{NaF}$	$\log N_{NaF}$	$\log \gamma_{NaF}$	$\log \gamma_{NaF}$ @ T's add -3.425
0	0	0	0	4635	0	-.204	-.204	0
6010	-87.56	-165.56	-2102.61	4623	-.455	-.213	-.242	0
3600	-147.62	-243.62	-3093.97	4607	-.672	-.222	-.450	-3.875
4433	-308.26	-646.72	-8213.34	4406	-1.864	-.252	-1.612	-5.037

TABLE C-III

Determination of α_{NaF} by Integration of Compound $NaAlF_4$ in NaF-AlF_3 Phase Diagram

1	2	3	4	5	6	7	8	9
T°K	X_2	X_1	N_{2NaF}	N_{1AlF_3}	ΔT	N_2-X_2	$\frac{N_1 \Delta T}{(N_2- X_2)}$	$(N_2- X_2)^2$
977	.494	.506	.463	.537	27	-.031	-467.71	.000961
993	.494	.506	.479	.521	11	-.015	-382.07	.000225
1004	.494	.506	.494	.506	0	0	0	0
988	.494	.506	.530	.470	16	.036	208.89	.00130
963	.494	.506	.560	.440	14	.066	273.33	.00436

10	11	12	13	14	15	16	17	18
$\frac{X_1 \Delta T}{(N_2- X_2)^2} \int_{X_2}^{N_2} \frac{X_1 \Delta T}{(N_2- X_2)^2}$		8 + 11	X 12.70	RT	log α_{NaF}	log N_{NaF}	log γ NaF	log γ NaF @ T's add -8.158
14,216	-682.70	-1150.41	-14,610.2	4470	-3.269	-.334	-2.935	-11.093
24,738	-371.07	- 753.14	- 9,564.9	4543	-2.105	-.320	-1.785	- 9.943
0	0	0	0	0	0	-.307	.307	- 7.851
6,228	557.39	766.28	- 9,731.8	4520	+2.153	-.276	2.429	- 5.729
4,758	722.18	995.51	12,642.3	4406	2.869	-.252	3.121	- 5.037

TABLE C-IV

Determination of ϱ_{AlF_3} by Gibbs-Duhem Integration

1	2	3	4	5	6
N_{2NaF}	N_1^2	$\frac{N_1 \times N_2}{N_1^2}$	$\log \gamma_{NaF}$ 1283	$\frac{N_1 \times N_2}{N_1^2 \log \gamma_{NaF}}$	$\frac{\log \gamma_{NaF}}{N_1^2}$
.463	.288	.865	-8.447	7.307	-29.33
.479	.271	.923	-7.695	7.103	-28.40
.414	.256	.977	-6.143	6.002	-24.00
.530	.221	1.127	-4.410	4.970	-19.95
.560	.194	1.1268	-3.782	4.796	-19.49
.600	.160	1.500	-3.042	4.563	-19.01
.649	.123	1.854	-1.996	3.701	-16.23
.663	.114	1.956	-1.839	3.597	-16.13
.679	.103	2.117	-1.665	3.525	-16.17
.704	.0876	2.374	-1.434	3.404	-16.37
.724	.0762	2.625	-1.279	3.357	-16.78
.738	.0686	2.813	-1.181	3.322	-17.22
.745	.0650	2.923	-1.160	3.391	-17.85
.750	.0625	3.008	-1.093	3.288	-17.49
.754	.0605	3.074	-1.018	3.129	-16.83
.759	.0581	3.150	- .947	2.983	-16.30
.768	.0538	3.309	- .827	2.737	-15.37
.777	.0497	3.481	- .726	2.527	-14.61
.789	.0445	3.753	- .606	2.274	-13.62
.806	.0376	4.149	- .467	1.938	-12.42
.827	.0299	4.783	- .325	1.555	-10.86
.837	.0266	5.113	- .261	1.335	- 9.81
.842	.0250	5.320	- .230	1.224	- 9.20
.856	.0207	5.942	- .126	.749	- 6.09
.865	.0182	6.429	- .058	.373	- 3.19
.886	.0137	7.518	- .044	.331	- 3.21
.899	.0102	8.902	- .033	.294	- 3.24
.907	.00865	9.757	- .026	.254	- 3.01
.926	.00548	12.500	- .016	.200	- 2.92
.949	.00260	18.615	- .008	.149	- 3.08
.987	.00017	75.294	- .001	.075	- 5.88
1	0	0	0	0	0

TABLE C-IV Continued

7	8	9	10	11
$\int_{1}^{N_2} \frac{\log \gamma_{NaF}}{N_1^2} dN_2$	$\int_{.463}^{N_2} \frac{\log \gamma}{N_2^2} dN_2$	5 + 8	$\log \gamma_{AlF_3}$ (1283) add -7.644	$\frac{\log \gamma_{AlF_3}}{N_2^2}$
0	0	7.307	- .337	- 1.58
-.432	-.432	6.642	-1.002	- 4.38
-.365	-.797	5.205	-2.439	-10.00
-.791	-1.588	3.382	-4.262	-15.17
-.592	-2.180	2.616	-5.028	-16.01
-.770	-2.950	1.613	-6.031	-16.75
-.863	-3.813	- .112	-7.756	-18.42
-.227	-4.040	- .443	-8.087	-18.38
-.258	-4.298	- .773	-8.417	-18.26
-.407	-4.705	-1.301	-8.945	-18.03
-.331	-5.036	-1.679	-9.323	-17.79
-.238	-5.274	-1.952	-9.596	-17.61
-.123	-5.397	-2.006	-9.650	-17.39
-.088	-5.485	-2.197	-9.841	-17.48
-.069	-5.554	-2.425	-10.069	-17.70
-.083	-5.637	-2.654	-10.298	-17.88
-.143	-5.780	-3.043	-10.687	-18.11
-.135	-5.915	-3.388	-11.032	-18.26
-.169	-6.084	-3.817	-11.461	-18.40
-.220	-6.304	-4.387	-12.031	-18.51
-.240	-6.544	-5.028	-12.672	-18.53
-.100	-6.644	-5.355	-12.999	-18.54
-.046	-6.690	-5.530	-13.174	-18.58
-.098	-6.788	-6.146	-13.790	-18.81
-.031	-6.819	-6.613	-14.257	-19.06
-.033	-6.852	-6.656	-14.300	-18.33
-.033	-6.885	-6.680	-14.324	-17.73
-.017	-6.902	-6.736	-14.380	-17.47
-.038	-6.940	-6.802	-14.446	-16.84
-.050	-6.990	-6.878	-14.522	-16.12
-.155	-7.145	-7.070	-14.714	15.11
-.076	-7.221	-7.221	-14.865	14.87

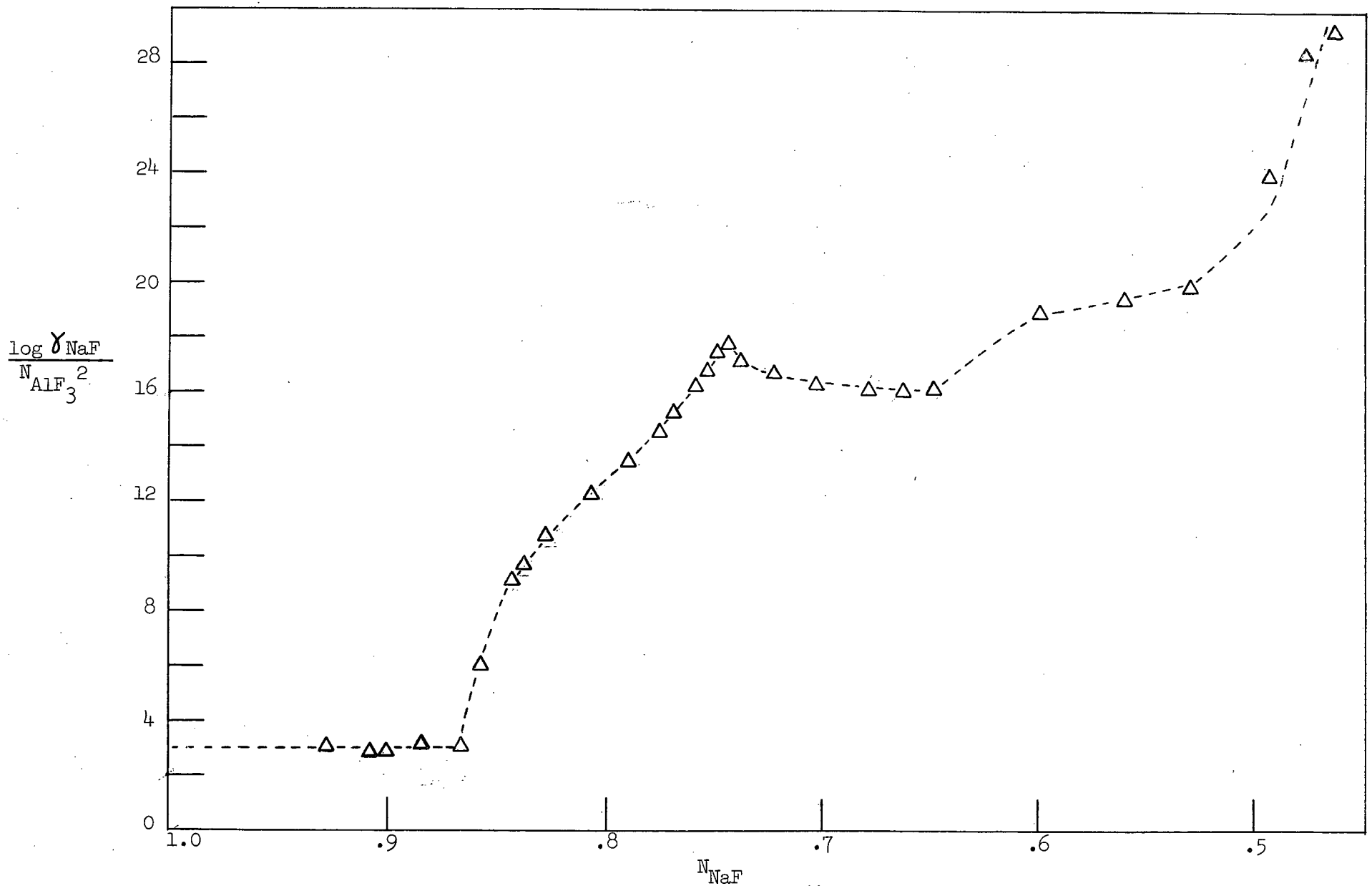

Figure C-2. Plot of $\frac{\log \gamma_{NaF}}{N_{AlF_3}^2}$ vs. N_{NaF}

at 46.3 mole per cent AlF_3 has a value of -.191 which when adjusted by the regular solution correction becomes -.337. The $\log \gamma_{AlF_3}$ values in Column 10 of Table C-IV can then be corrected by adding -7.644. A plot of $\frac{\log \gamma_{AlF_3}}{N_{NaF}^2}$ vs. N_{NaF} is shown in Figure C-3. The shape and location of this curve is consistent with the previous assumptions.

3. Determination of Activity of Sodium in Aluminum

Numerical values for $\log \gamma_{NaF}$ and $\log \gamma_{AlF_3}$ are now available from Tables C-I, C-II, C-III and C-IV. Activity data for sodium in molten aluminum is calculated for a range of NaF-AlF_3 ratios in Tables C-V and C-VI, using the equilibrium equation. The curve is plotted in Figure 6. This curve represents the activity of sodium metal dissolved in pure aluminum in equilibrium with pure fused cryolite electrolyte of a given ratio at 1010°C.

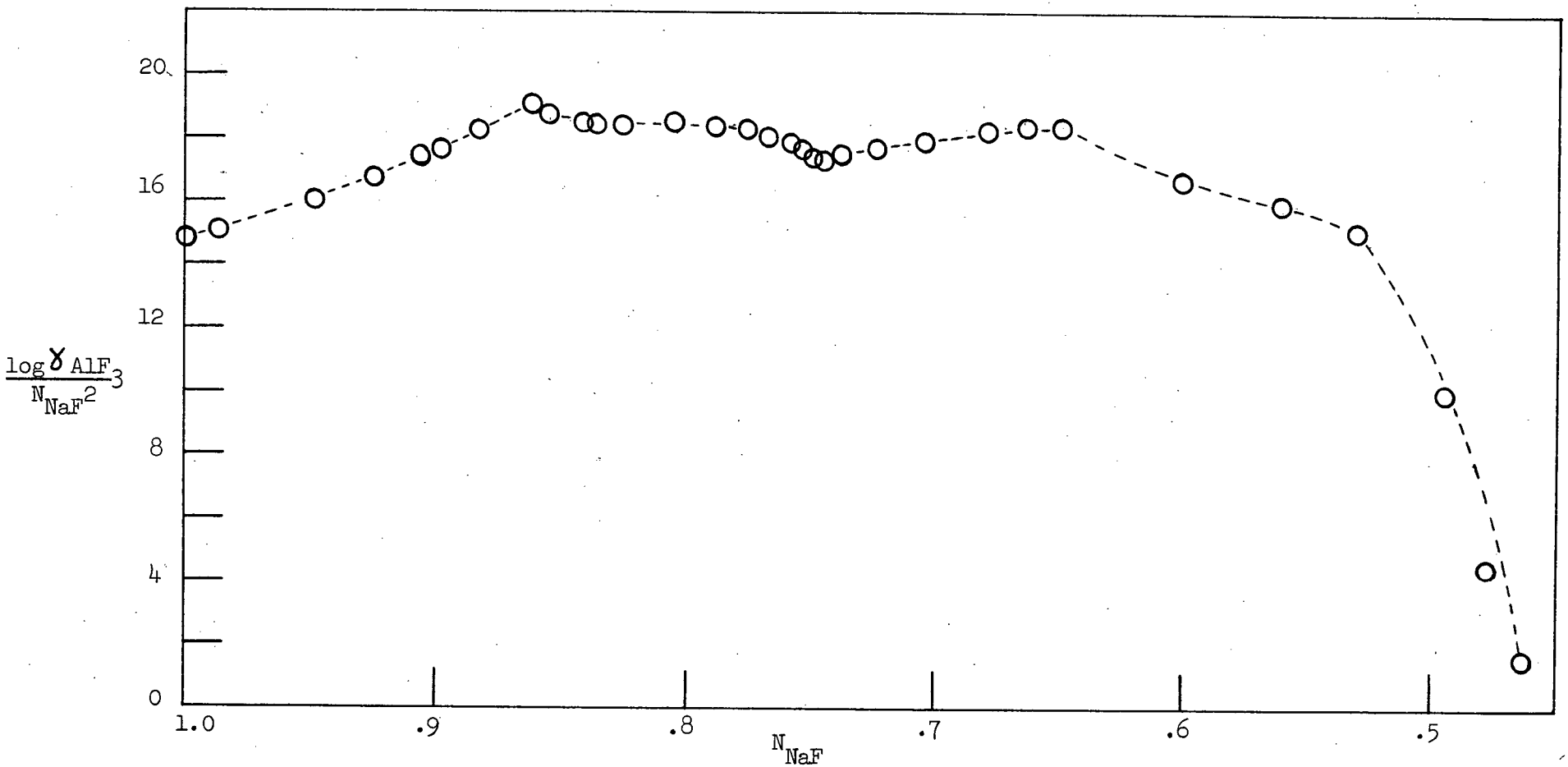

Figure C-3. Plot of $\frac{\log \gamma AlF_3}{N_{NaF}^2}$ vs. N_{NaF}

TABLE C-V

Activity Data for NaF and AlF_3 from Phase Diagram

N_{NaF}	N_{AlF_3}	Bath Ratio	$\log \gamma_{NaF}$	γ_{NaF}	ϱ_{NaF}	$\log \gamma_{AlF_3}$	γ_{AlF_3}	ϱ_{AlF_3}
.697	.321	1.06	-1.665	2.16×10^{-2}	1.47×10^{-2}	-8.417	3.83×10^{-9}	1.23×10^{-9}
.704	.296	1.19	-1.434	3.68×10^{-2}	2.59×10^{-2}	-8.945	1.14×10^{-9}	3.37×10^{-10}
.724	.276	1.31	-1.279	5.26×10^{-2}	3.81×10^{-2}	-9.323	4.75×10^{-10}	1.31×10^{-10}
.738	.262	1.41	-1.181	6.59×10^{-2}	4.86×10^{-2}	-9.596	2.54×10^{-10}	6.65×10^{-11}
.745	.255	1.46	-1.160	6.92×10^{-2}	5.16×10^{-2}	-9.650	2.24×10^{-10}	5.71×10^{-11}
.750	.250	1.50	-1.093	8.07×10^{-2}	6.05×10^{-2}	-9.841	1.44×10^{-10}	3.60×10^{-11}
.754	.246	1.53	-1.018	9.59×10^{-2}	7.23×10^{-2}	-10.069	8.53×10^{-11}	2.10×10^{-11}
.759	.241	1.57	- .947	1.13×10^{-1}	8.58×10^{-2}	-10.298	5.04×10^{-11}	1.22×10^{-11}
.768	.232	1.66	- .827	1.49×10^{-1}	1.14×10^{-1}	-10.687	2.06×10^{-11}	4.78×10^{-12}
.777	.223	1.75	- .726	1.88×10^{-1}	1.46×10^{-1}	-11.032	9.29×10^{-12}	2.07×10^{-12}

TABLE C-VI

Activities of Sodium from Phase Diagram

Bath Ratio	a_{AlF_3}	a_{NaF}	$(a_{NaF})^3$	$K\ (a_{NaF})^3$ 1.91×10^{-11}	$\frac{K\ (a_{NaF})^3}{a_{AlF_3}}$	a_{Na}
1.75	2.07×10^{-2}	1.46×10^{-1}	3.11×10^{-3}	5.94×10^{-14}	2.87×10^{-2}	.306
1.66	4.78×10^{-2}	1.14×10^{-1}	1.48×10^{-3}	2.83×10^{-14}	5.92×10^{-3}	.181
1.57	1.22×10^{-11}	8.58×10^{-2}	6.32×10^{-4}	1.21×10^{-14}	9.92×10^{-4}	.0997
1.53	2.10×10^{-11}	7.23×10^{-2}	3.78×10^{-4}	7.22×10^{-15}	3.44×10^{-4}	.0701
1.50	3.60×10^{-11}	6.05×10^{-2}	2.21×10^{-4}	4.22×10^{-15}	1.17×10^{-4}	.0489
1.46	5.71×10^{-11}	5.16×10^{-2}	1.37×10^{-4}	2.62×10^{-15}	4.59×10^{-5}	.0358
1.41	6.65×10^{-11}	4.86×10^{-2}	1.15×10^{-4}	2.20×10^{-15}	3.31×10^{-5}	.0321
1.31	1.31×10^{-10}	3.81×10^{-2}	5.53×10^{-5}	1.06×10^{-15}	8.09×10^{-6}	.0201
1.19	3.37×10^{-10}	2.59×10^{-2}	1.74×10^{-5}	3.32×10^{-16}	9.85×10^{-7}	.00995
1.06	1.23×10^{-9}	1.47×10^{-2}	3.18×10^{-6}	6.07×10^{-17}	4.94×10^{-8}	.00367

APPENDIX D

Dilution Calculations

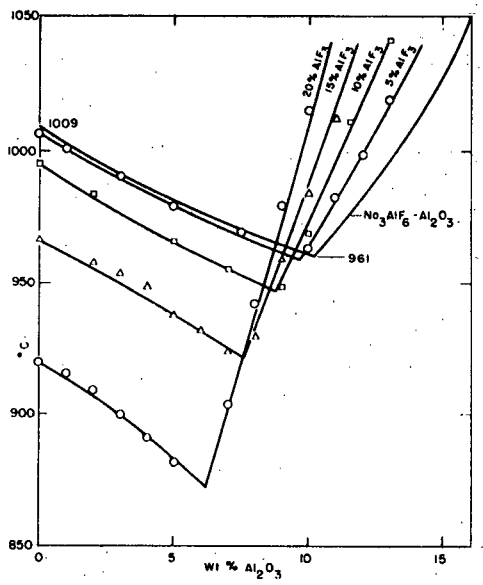

Figure D-1. Liquidus Diagrams for Cryolite-Alumina with 5, 10, 15 and 20% Aluminum Fluoride

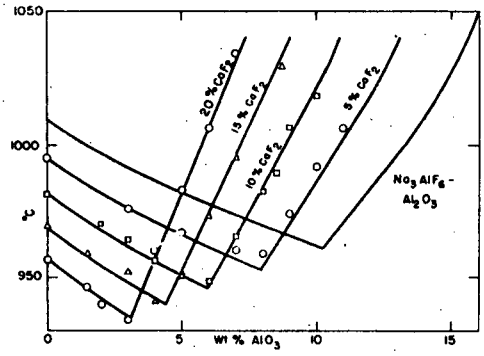

Figure D-2. Liquidus Diagrams for Cryolite-Alumina with 5, 10, 15 and 20% Calcium Fluoride

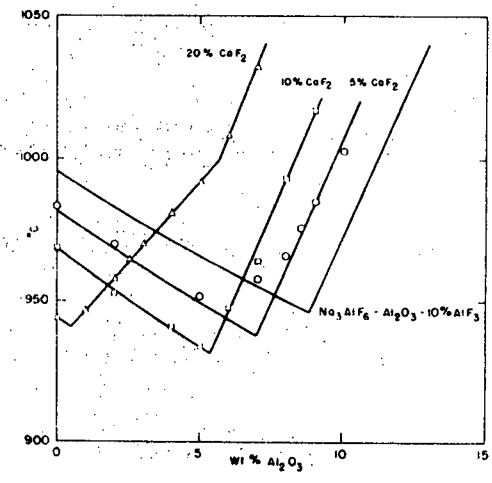

Figure D-3. Liquidus Diagrams for Cryolite-Alumina-10% Aluminum Fluoride with 5, 10 and 20% Calcium Fluroide

(Diagrams from Fenerty and Hollingshead[32])

TABLE D-I

Sodium Activities for Cryolite (Dilution Factor .88)

Bath Ratio	a_{AlF_3} 100%	a_{NaF} 100%	a_{AlF_3} 88%	a_{NaF} 88%	$(a_{NaF})^3$	$K.(a_{NaF})^3$	$K.\frac{(a_{NaF})^3}{a_{AlF_3}}$	a_{Na}
1.75	2.07×10^{-12}	1.45×10^{-1}	1.82×10^{-12}	1.28×10^{-1}	2.10×10^{-3}	4.10×10^{-14}	2.20×10^{-2}	.280
1.66	4.78×10^{-12}	1.14×10^{-1}	4.20×10^{-12}	1.00×10^{-1}	1.00×10^{-3}	1.91×10^{-14}	4.55×10^{-3}	.166
1.57	1.22×10^{-11}	8.58×10^{-2}	1.07×10^{-11}	7.55×10^{-2}	4.30×10^{-4}	8.21×10^{-15}	7.68×10^{-4}	.0916
1.53	2.10×10^{-11}	7.23×10^{-2}	1.85×10^{-11}	6.36×10^{-2}	2.58×10^{-4}	4.93×10^{-15}	2.66×10^{-4}	.0644
1.50	3.60×10^{-11}	6.05×10^{-2}	3.17×10^{-11}	5.32×10^{-2}	1.51×10^{-4}	2.88×10^{-15}	9.09×10^{-5}	.0450
1.46	5.71×10^{-11}	5.14×10^{-2}	5.03×10^{-11}	4.52×10^{-2}	9.24×10^{-5}	1.77×10^{-15}	3.52×10^{-5}	.0328
1.41	6.65×10^{-11}	4.86×10^{-2}	5.85×10^{-11}	4.28×10^{-2}	7.84×10^{-5}	1.50×10^{-15}	2.56×10^{-5}	.0295
1.31	1.31×10^{-10}	3.82×10^{-2}	1.15×10^{-10}	3.36×10^{-2}	3.79×10^{-5}	7.24×10^{-16}	6.29×10^{-6}	.0184
1.19	3.37×10^{-10}	2.59×10^{-2}	2.96×10^{-10}	2.28×10^{-2}	1.19×10^{-5}	2.27×10^{-16}	7.66×10^{-7}	.00915
1.06	1.23×10^{-9}	1.46×10^{-2}	1.08×10^{-9}	1.29×10^{-2}	2.15×10^{-6}	4.11×10^{-17}	3.80×10^{-8}	.00336

TABLE D-II

Sodium Activities for Cryolite (Dilution Factor .825)

Bath Ratio	a_{AlF_3} 100%	a_{NaF} 100%	a_{AlF_3} 82.5%	a_{NaF} 82.5%	$(a_{NaF})^3$	$K.(\frac{a_{NaF}}{1.91 \times 10^{-11}})^3$	$K.(\frac{a_{NaF}}{a_{AlF_3}})^3$	a_{Na}
1.75	2.07×10^{-12}	1.45×10^{-1}	1.71×10^{-12}	1.20×10^{-1}	1.73×10^{-3}	3.30×10^{-14}	1.93×10^{-2}	.268
1.66	4.78×10^{-12}	1.14×10^{-1}	4.06×10^{-12}	9.41×10^{-2}	8.33×10^{-4}	1.59×10^{-14}	3.91×10^{-3}	.158
1.57	1.22×10^{-11}	8.58×10^{-2}	1.01×10^{-11}	7.08×10^{-2}	3.55×10^{-4}	6.78×10^{-15}	6.71×10^{-4}	.0875
1.53	2.10×10^{-11}	7.23×10^{-2}	1.73×10^{-11}	5.97×10^{-2}	2.13×10^{-4}	4.07×10^{-15}	2.35×10^{-4}	.0616
1.50	3.60×10^{-11}	6.05×10^{-2}	2.97×10^{-11}	4.99×10^{-2}	1.24×10^{-4}	2.37×10^{-15}	7.98×10^{-5}	.0430
1.46	5.71×10^{-11}	5.14×10^{-2}	4.71×10^{-11}	4.24×10^{-2}	7.62×10^{-5}	1.46×10^{-15}	3.10×10^{-5}	.0314
1.41	6.65×10^{-11}	4.86×10^{-2}	5.49×10^{-11}	4.01×10^{-2}	6.45×10^{-5}	1.23×10^{-15}	2.24×10^{-5}	.0282
1.31	1.31×10^{-10}	3.82×10^{-2}	1.08×10^{-10}	3.15×10^{-2}	3.13×10^{-5}	5.98×10^{-16}	5.54×10^{-6}	.0177

TABLE D-III

Sodium Activities for Cryolite (Dilution Factor .84)

Bath Ratio	a_{AlF_3} 100%	a_{NaF} 100%	a_{AlF_3} 84%	a_{NaF} 84%	$(a_{NaF})^3$	$K.(a_{NaF})^3$ 1.91×10^{-11}	$\frac{K.(a_{NaF})^3}{a_{AlF_3}}$	a_{Na}
1.75	2.07×10^{-12}	1.45×10^{-1}	1.74×10^{-12}	1.22×10^{-1}	1.82×10^{-3}	3.48×10^{-14}	2.00×10^{-2}	.272
1.66	4.78×10^{-12}	1.14×10^{-1}	4.01×10^{-12}	9.58×10^{-2}	7.79×10^{-4}	1.68×10^{-14}	4.19×10^{-3}	.161
1.57	1.22×10^{-11}	8.58×10^{-2}	1.03×10^{-11}	7.21×10^{-2}	3.75×10^{-4}	7.16×10^{-15}	6.95×10^{-4}	.0885
1.53	2.10×10^{-11}	7.23×10^{-2}	1.77×10^{-11}	6.07×10^{-2}	2.24×10^{-4}	4.28×10^{-15}	2.42×10^{-4}	.0623
1.50	3.60×10^{-11}	6.05×10^{-2}	3.02×10^{-11}	5.08×10^{-2}	1.31×10^{-4}	2.50×10^{-15}	8.27×10^{-5}	.0435
1.46	5.71×10^{-11}	5.14×10^{-2}	4.80×10^{-11}	4.32×10^{-2}	8.06×10^{-5}	1.54×10^{-15}	3.28×10^{-5}	.0318
1.41	6.65×10^{-11}	4.86×10^{-2}	5.58×10^{-11}	4.08×10^{-2}	6.79×10^{-5}	1.30×10^{-15}	2.33×10^{-5}	.0286
1.31	1.31×10^{-10}	3.82×10^{-2}	1.10×10^{-10}	3.21×10^{-2}	3.31×10^{-5}	6.32×10^{-16}	5.75×10^{-6}	.0179
1.19	3.37×10^{-10}	2.59×10^{-2}	2.83×10^{-10}	2.18×10^{-2}	1.04×10^{-5}	1.99×10^{-16}	7.04×10^{-7}	.0089
1.06	1.23×10^{-9}	1.46×10^{-2}	1.93×10^{-9}	1.23×10^{-2}	1.86×10^{-6}	3.55×10^{-17}	3.45×10^{-8}	.00326

TABLE D-IV

Sodium Activities for Cryolite (Dilution Factor .78)

Bath Ratio	ϱ_{AlF_3} 100%	ϱ_{NaF} 100%	ϱ_{AlF_3} 78%	ϱ_{NaF} 78%	$(\varrho_{NaF})^3$	$K.(\varrho_{NaF})^3$ 1.91×10^{-11}	$\frac{K.(\varrho_{NaF})^3}{\varrho_{AlF_3}}$	ϱ_{Na}
1.75	2.07×10^{-12}	1.45×10^{-1}	1.62×10^{-12}	1.13×10^{-1}	1.44×10^{-3}	2.75×10^{-14}	1.70×10^{-2}	.257
1.66	4.78×10^{-12}	1.14×10^{-1}	3.72×10^{-12}	8.89×10^{-2}	7.03×10^{-4}	1.34×10^{-14}	3.60×10^{-3}	.153
1.57	1.22×10^{-11}	8.58×10^{-2}	9.52×10^{-12}	6.69×10^{-2}	2.99×10^{-4}	5.71×10^{-15}	6.00×10^{-4}	.0844
1.53	2.10×10^{-11}	7.23×10^{-2}	1.64×10^{-11}	5.64×10^{-2}	1.79×10^{-4}	3.42×10^{-15}	2.08×10^{-4}	.0592
1.50	3.60×10^{-11}	6.05×10^{-2}	2.81×10^{-11}	4.72×10^{-2}	1.05×10^{-4}	2.01×10^{-15}	7.16×19^{-5}	.0415
1.46	5.71×10^{-11}	5.14×10^{-2}	4.45×10^{-11}	4.01×10^{-2}	6.45×10^{-5}	1.23×10^{-15}	2.76×10^{-5}	.0302
1.41	6.65×10^{-11}	4.86×10^{-2}	5.19×10^{-11}	3.79×10^{-2}	5.44×10^{-5}	1.04×10^{-15}	2.00×10^{-5}	.0271
1.31	1.31×10^{-10}	3.82×10^{-2}	1.02×10^{-10}	2.98×10^{-2}	2.65×10^{-5}	5.06×10^{-16}	4.96×10^{-6}	.0170
1.19	3.37×10^{-10}	2.59×10^{-2}	2.63×10^{-10}	2.10×10^{-2}	9.30×10^{-6}	1.78×10^{-16}	6.76×10^{-7}	.00875
1.06	1.23×10^{-9}	1.46×10^{-2}	9.60×10^{-10}	1.14×10^{-2}	1.48×10^{-6}	2.83×10^{-17}	2.95×10^{-8}	.00308

APPENDIX E

Experimental Results

TABLE E-I

Sodium Activities (Alumina-Saturated Pure Cryolite)

Run No.	Initial Composition	Bath Ratio	Wt. % Na	Mole % Na	a_{Na}
44	Pure	1.44 1.41	2.90	21.2	.035
45	Pure	1.43	3.10	22.4	.038
57	Pure	1.43 1.37	2.80	20.6	.033
47	5% AlF_3	1.36 1.34	2.20	16.8	.024
58	5% AlF_3	1.34 1.32	2.40	18.1	.027
50	10% AlF_3	1.25 1.18	1.80	14.2	.019
51	10% AlF_3	1.24 1.24	1.90	14.8	.020
59	10% AlF_3	1.25 1.27	1.50	12.1	.016
60	10% AlF_3	1.24 1.20	1.70	13.5	.018
61	10% AlF_3	1.26 1.18	1.80	14.2	.019
48	15% AlF_3	1.17 1.13	1.40	11.3	.015
49	15% AlF_3	1.19 1.12	1.40	11.3	.015
52	20% AlF_3	1.18 1.09	1.00	8.3	.012
53	20% AlF_3	1.14 0.99	0.90	7.6	.011
54	20% AlF_3	1.08	1.00	8.3	.012

TABLE E-II

Sodium Activities (Alumina-Saturated Reduction Cell Electrolyte)

Run No.	Initial Composition	Bath Ratio	Wt. % Na	Mole % Na	a_{Na}
13	1.55	1.68	4.78	31.2	.082
14	1.55	1.68	4.58	30.2	.076
15	1.55	1.68	4.58	30.2	.076
16	1.55	1.70	4.38	29.2	.069
17	1.55	1.66	4.28	28.6	.066
18	1.55	1.67	4.90	31.6	.085
19	1.55	1.66	4.88	31.6	.085
20	1.55	1.68	5.20	33.0	.096
21	1.39	1.60	4.18	28.2	.064
22	1.39	1.63	4.00	27.2	.058
23	1.39	1.67	4.30	28.8	.067
24	1.39	1.65	4.20	28.2	.064
31	1.55 + 5% AlF_3	1.70	4.40	29.25	.070
32	1.55 + 5% AlF_3	1.70	4.70	30.8	.079
33	1.55 + 5% AlF_3	1.70	4.50	29.8	.073
34	1.55 + 5% AlF_3	1.70	4.60	30.3	.076
35	1.55 + 5% AlF_3	1.70	4.80	31.2	.082
36	1.55 + 10% AlF_3	1.67	4.90	31.6	.085
37	1.55 + 10% AlF_3	1.67	4.30	28.8	.067
38	1.55 + 10% AlF_3	1.68	4.20	28.2	.064
39	1.55 + 10% AlF_3	1.63	4.80	31.2	.082
40	1.55 + 10% AlF_3	1.51	3.10	22.4	.039
41	1.55 + 10% AlF_3	1.42 1.41	2.20	16.8	.024
42	1.55 + 10% AlF_3	1.44 1.37	2.40	18.1	.027
43	1.55 + 10% AlF_3	1.45 1.43	2.60	19.4	.030

TABLE E-III

Sodium Activities (Pure Cryolite and Reduction Cell Electrolyte with 7% CaF_2 Addition)

Run No.	Initial Composition	$NaF-AlF_3$ Ratio	Wt. % Na	Mole % Na	a_{Na}
26	1.55 + 7% CaF_2	1.76	4.10	27.8	.062
27	1.55 + 7% CaF_2	1.86	3.58	25.0	.048
28	1.55 + 7% CaF_2	2.02	4.13	28.0	.062
29	1.55 + 7% CaF_2	1.86	3.84	26.4	.054
30	1.55 + 7% CaF_2	1.78	4.30	28.8	.067
55	Pure + 10% AlF_3 + 7% CaF_2	1.26 1.13	1.60	12.8	.017
56	Pure + 10% AlF_3 + 7% CaF_2	1.25 1.20	1.40	11.3	.015

APPENDIX F

Mathematical Analysis and Computer Data

APPENDIX F

Mathematical Analysis and Computer Data

Symbols

$Y_{(I)}$ = ln $\gamma_{NaF_{1283}}$

YC = log $\gamma_{NaF_{1283}}$

$A_{(I)}$ = ln $\gamma_{AlF_{3_{1283}}}$

AC = log $\gamma_{AlF_{3_{1283}}}$

ANA = $\varrho_{Na_{1283}}$

$N_{(I)}$ = N_{AlF_3}

C = K = 1.91×10^{-11} (equilibrium constant)

$X_{(I)}$ = log γ_{NaF_T}

$T_{(I)}$ = $T^{\circ}K$

R = gas constant (4.575)

$EL_{(I)}$ = heat of solution

1. Chemical equilibrium equation

$$ANA = \frac{(1-N)\ e^{Y}}{\sqrt[3]{\frac{N\ e^{A}}{C}}}$$

$$\frac{e^{3Y}}{e^{A}} = \frac{N}{C}\left(\frac{ANA}{1-N}\right)^{3}$$

$$3Y-A = \ln\left[\frac{N}{C}\left(\frac{ANA}{1-N}\right)^{3}\right] = Z$$

$$3Y-A = Z \qquad .....(1)$$

2. Gibbs-Duhem equation

$$A_{(I)} = -\frac{[1-N]}{N}\ Y - \int_{N=.223}^{N=N} \frac{Y}{N^2}\ dN + B \qquad .....(2)$$

for I = 1, N = .223 Y = -1.672

for I ≠ 1, Substitute 2 into 1

$$3Y + \frac{Y}{N}(1-N) + \int_{N=.223}^{N=N} \frac{Y}{N^2}\ dN - B = Z$$

$$Y\left(2 + \frac{1}{N}\right) = -\int_{N=.223}^{N=N} \frac{Y}{N^2}\ dN + B + Z$$

Differentiating with respect to N

$$\left(2 + \frac{1}{N}\right) Y' - \frac{Y}{N^2} = -\frac{Y}{N^2} + Z'$$

$$Y'_{N} = \frac{N}{2N+1}\ Z'$$

$$Y_{N} = \int_{.223}^{N} \frac{N}{2N+1}\ Z'\ dN + \text{constant}$$

where the constant equals the value of $Y_{.223} = -1.672$

$$\therefore \quad Y_N = -1.672 + \int_{.223}^{N} \frac{N}{2N+1} Z' \, dN = -1.672 + \left[\frac{NZ}{2N+1}\right]_{.223}^{N} - \int_{.223}^{N} Z \left(\frac{1}{2N+1}\right)^2 dN$$

$$YC = Y/2.3026$$

$$AC = A/2.3026$$

$$EL = \frac{(YC-X)\,R}{\frac{1}{I283} - \frac{1}{T}}$$

```
     PRINTED ON JUL. 11/1962          FOR     P. E. AYLEN

FORTRAN 1A  COMPILE


 8300 C      W. DETTWILER FOR P. AYLEN
 8300 C
 8300        READ 2, N, C, R
 8348 2      FORMAT(I3,3X,E12.2,F12.0)
 8394        PRINT 3
 8418 3      FORMAT(7X1HZ11X1HY11X1HA11X1HL/)
 8584        DO 4 I=1,N
 8596        READ 5, EN, ANA, X, T
 8656 5      FORMAT(F12.0,F12.0,F12.0,F12.0)
 8694        Z= LOG((EN/C)*(ANA/(1.0-EN)) **3 )
 8814        YN = Z*1.0/((2.0*EN+1.0)**2)
 8922        IF (I-1) 6,7,6
 8990 7      Y = -1.672
 9026        GO TO 8
 9034 6      Y = Y + (ENP-EN)*(YN+YO)/2.0 +EN*Z/(2.0*EN+1.0)-ENP*S/(2.0*ENP+1.)
 9370 8      YO = YN
 9394        S = Z
 9418        ENP = EN
 9442        A = 3.0*Y - Z
 9490        AC = A/2.3026
 9526        YC = Y/2.3026
 9562        EL = ((YC - X)*R)/(1.0/1283.0 - 1.0/T)
 9718 4      PRINT 10,Z,YC,AC,EL
 9814 10     FORMAT(F12.5,F12.5,F12.5,F12.5)
 9852        SKIP TO 1
 9864        END
```

Figure F-1. Computer Program

TABLE F-I

Activity Data for NaF and AlF_3

Computer Data				Computer Results			Calculated Thermodynamic Values	
N	ANA	X	T	Z	YC	AC	$\frac{YC}{N_{AlF_3}^2}$	$\frac{AC}{N_{NaF}^2}$
.223	.094	- .733	1272.6	16.84431	-.72613	-9.49375	14.61	15.72
.232	.070	- .832	1277.2	16.03443	-.78113	-9.30703	14.52	15.78
.241	.053	- .949	1280.4	15.27324	-.83422	-9.13570	14.35	15.86
.246	.0465	-1.019	1281.3	14.92108	-.85926	-9.05789	14.20	15.92
.250	.042	-1.094	1281.6	14.64782	-.87893	-8.99824	14.06	15.98
.255	.037	-1.162	1281.3	14.30744	-.90374	-8.92482	13.91	16.08
.262	.032	-1.183	1281.0	13.92729	-.93187	-8.84413	13.59	16.23
.276	.023	-1.283	1277.5	13.04608	-.99882	-8.66228	13.11	16.53
.296	.0158	-1.451	1267.2	12.07363	-1.07569	-8.47057	12.28	17.08
.321	.012	-1.719	1243.7	11.43787	-1.12841	-8.35263	10.95	18.12

APPENDIX G

Analysis of Na-Al Binary System

APPENDIX G

Analysis of Na-Al Binary System

A review of the literature[20] shows very little published data on the Na-Al system. Originally it was thought that there was no mutual solubility in the liquid state. However, re-investigation of the Al-rich alloys by Fink, Willey and Stumpf[21] and Ransley and Neufeld[22] established the existence of a true monotectic. Fink et al. established the hypo-monotectic liquidus by both direct and differential thermal analysis and set the monotectic point at .18 weight per cent sodium and at a temperature 1.2°K. below the melting point of pure aluminum. They also found that the solubility of liquid sodium decreased with increasing temperature.

Ransley and Neufeld accepted Fink et al.'s thermal data for the hypo-monotectic liquidus and concentrated their interest on the solid solubility limits and the liquid miscibility boundary. They established the monotectic at 0.14 weight per cent sodium and observed a more orthodox increase of solubility with increasing temperature. The solid solubility of sodium in aluminum was reported by both teams of researchers to be $<.003$ weight per cent at the monotectic temperature. A composite of the two phase diagrams appears as Figure G-1.

An attempt was made to calculate thermodynamic data from the composite phase diagrams. Several inconsistencies became apparent during this treatment. Ransley and Neufeld's data (see Table G-I) on the solubility of liquid sodium was plotted to obtain a graph of log N Vs. 1/T (see Figure G-2). This plot established the monotectic point at .0017 mole per cent sodium (.145 weight per cent). The slope of the line gives a value for the partial heat of solution of 9230 calories.

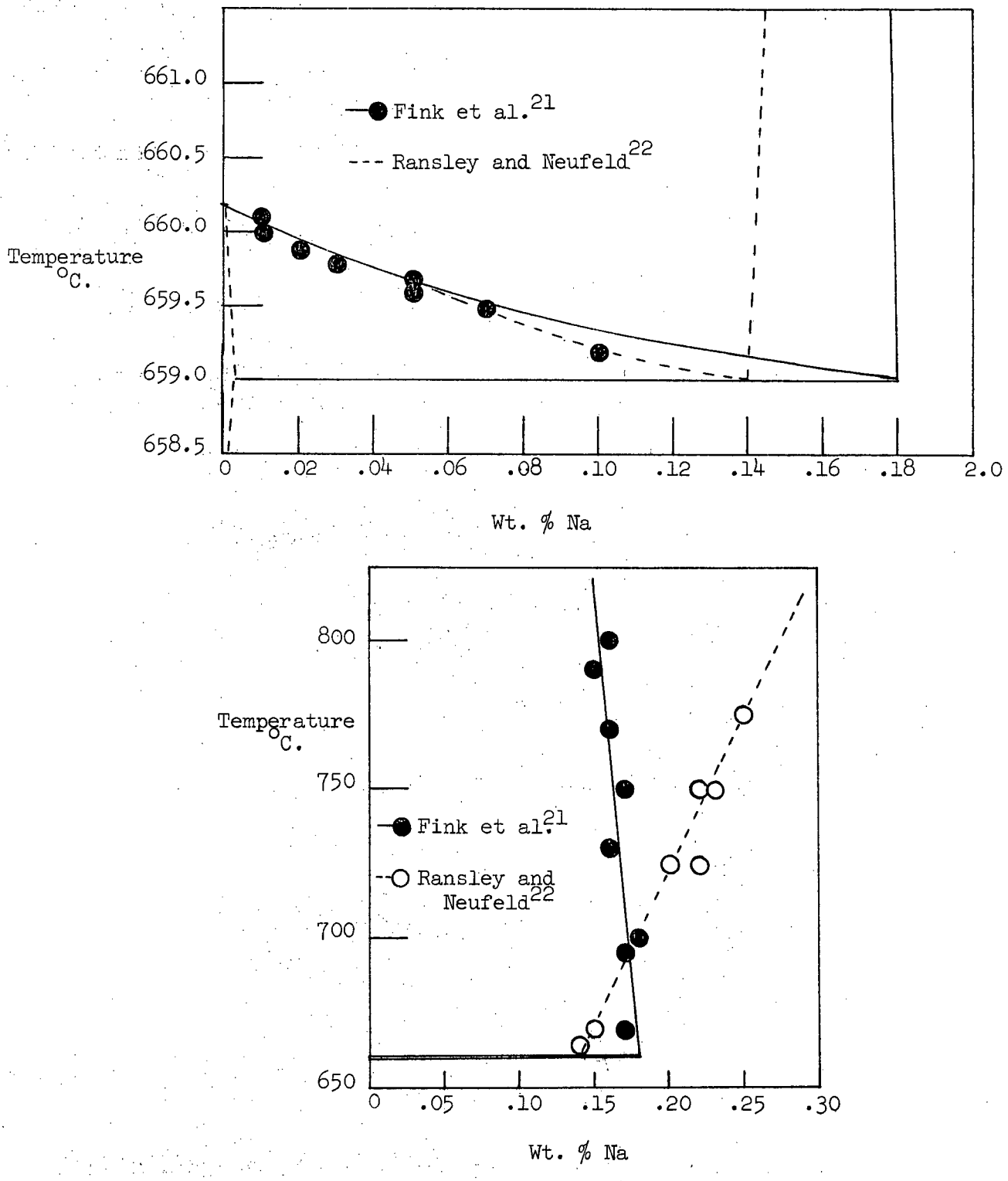

Figure G-1. Na-Al Phase Diagrams from Data of Fink et al. and Ransley and Neufeld.

TABLE G-I

Partial Heat of Solution Data for Na-Al Binary

Na Content wt. %	N_{Na}	$T^{o}K$	1/T
0.14	.001643	938	1.066×10^{-3}
0.15	.001761	943	1.060×10^{-3}
0.15	.001761	943	1.060×10^{-3}
0.18	.002112	973	1.028×10^{-3}
0.22	.002582	998	1.002×10^{-3}
0.20	.002347	998	1.002×10^{-3}
0.23	.002699	1023	$.9775 \times 10^{-3}$
0.22	.992582	1023	$.9775 \times 10^{-3}$
0.25	.002934	1048	$.9542 \times 10^{-3}$
0.15	.001761	958	1.044×10^{-3}
0.19	.002230	988	1.012×10^{-3}

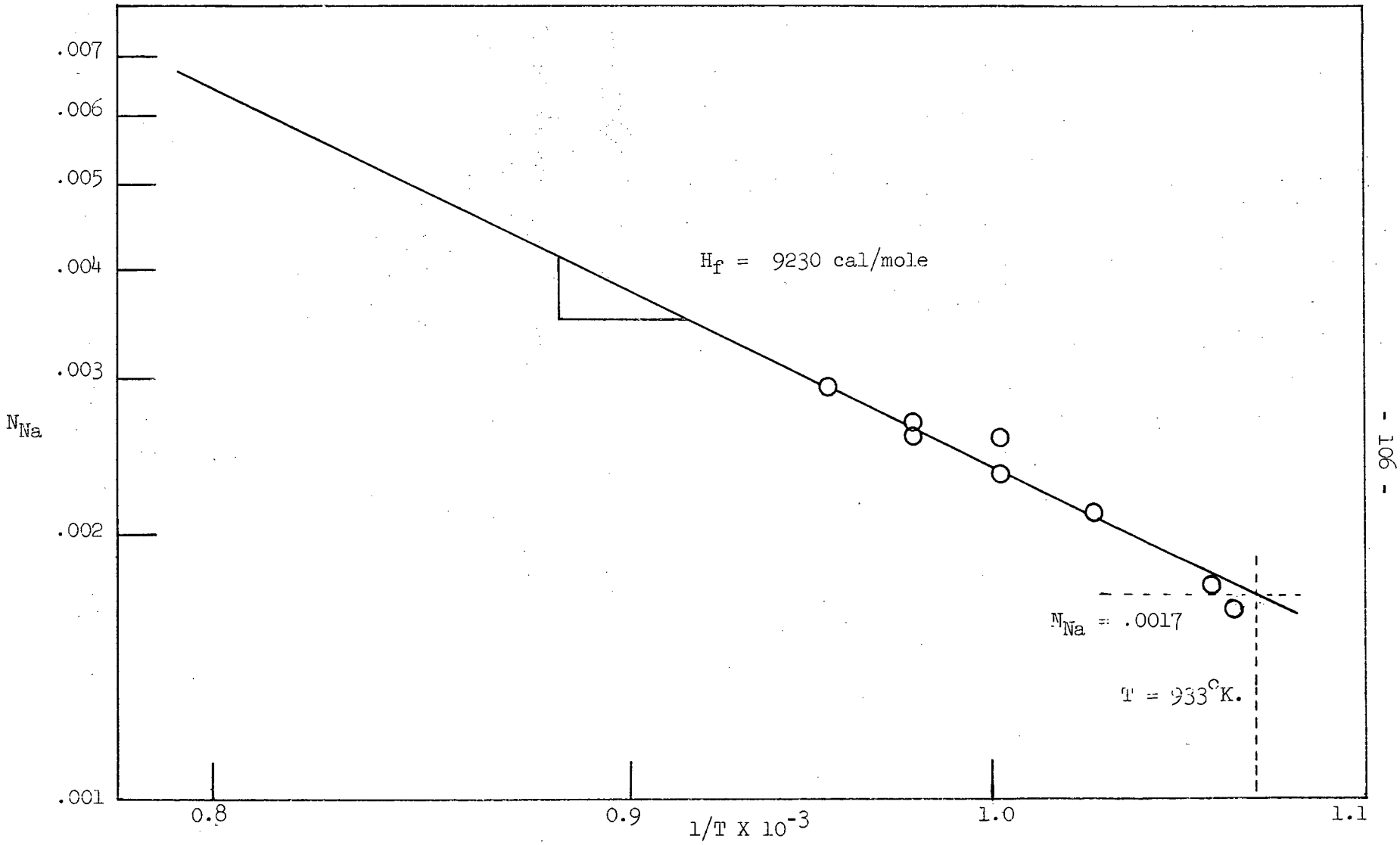

Figure G-2. Plot of Log N vs. 1/T for Ransley and Neufeld's Data

Examination of the hypo-monotectic liquidus established by Fink et al. showed further discrepancies. Therefore, it was necessary to reconstruct a phase diagram which was consistent with thermodynamics but compatible with the limited experimental data. Data supplied by Hollingshead[23] (see Table G-II) on the concentration of sodium in aluminum at different $NaF-AlF_3$ bath ratios was used to obtain γ_{Na} values in the low concentration region. A plot of the data is shown in Figure G-3. The γ_{Na} values were obtained by utilizing the plot developed from Appendix C (see Figure 9.) adjusted for CaF_2 and Al_2O_3 content. Using this data, it was possible to establish a hypo-monotectic liquidus for the Na-Al binary (see Figure G-4). It was necessary to alter the temperature differential between the melting point of aluminum and the monotectic temperature to .8°K from 1.2°K. to provide thermodynamic consistency. This change should be well within the expected experimental error of the original researchers.

The activities of aluminum are calculated from the relationship[24]

$$\log a_{T_{Al}} = \frac{(T_o - T_{N_{Al}})\ \Delta H_f}{4.575\ T_{N_{Al}}\ T_o} + \log N'$$

where T_o = 933.0°K.

$T_{N_{Al}}$ = m.p. at N_{Al} (from phase diagram, Figure G-4)

H_f = 2570 calories[25]

N' = solid solubility of Na in Al = $<$.003%

As the solid solubility of sodium in aluminum is negligible, it can be disregarded in this calculation. The relationship then reduced to

$$\log a_{T_{Al}} = \frac{(T_o - T_{N_{Al}})\ \Delta S_f}{4.575\ T_{N_{Al}}}$$

where $\Delta S_f = \frac{2570}{933.0} = 2.7575$ e.u.

TABLE G-II

Sodium Content of Aluminum from Reduction Cells as a Function of NaF/AlF_3 Ratio (from Hollingshead[23])

NaF/AlF_3 by wt.	Na ppm	CaF_2 %	Temperature °C.
1.16	18	8.9	939
1.22	30	8.7	964
1.23	33	9.0	944
1.25	40	8.5	946
1.27	42	8.8	957
1.28	30	-	978
1.30	40	-	969
1.30	40	-	975
1.32	53	9.1	960
1.33	50	-	957
1.37	85	8.1	970
1.38	70	-	960
1.38	75	8.0	982
1.39	70	8.3	960
1.39	70	8.3	972
1.41	80	8.4	947
1.43	105	9.0	982
1.44	90	8.4	967
1.47	160	8.2	971

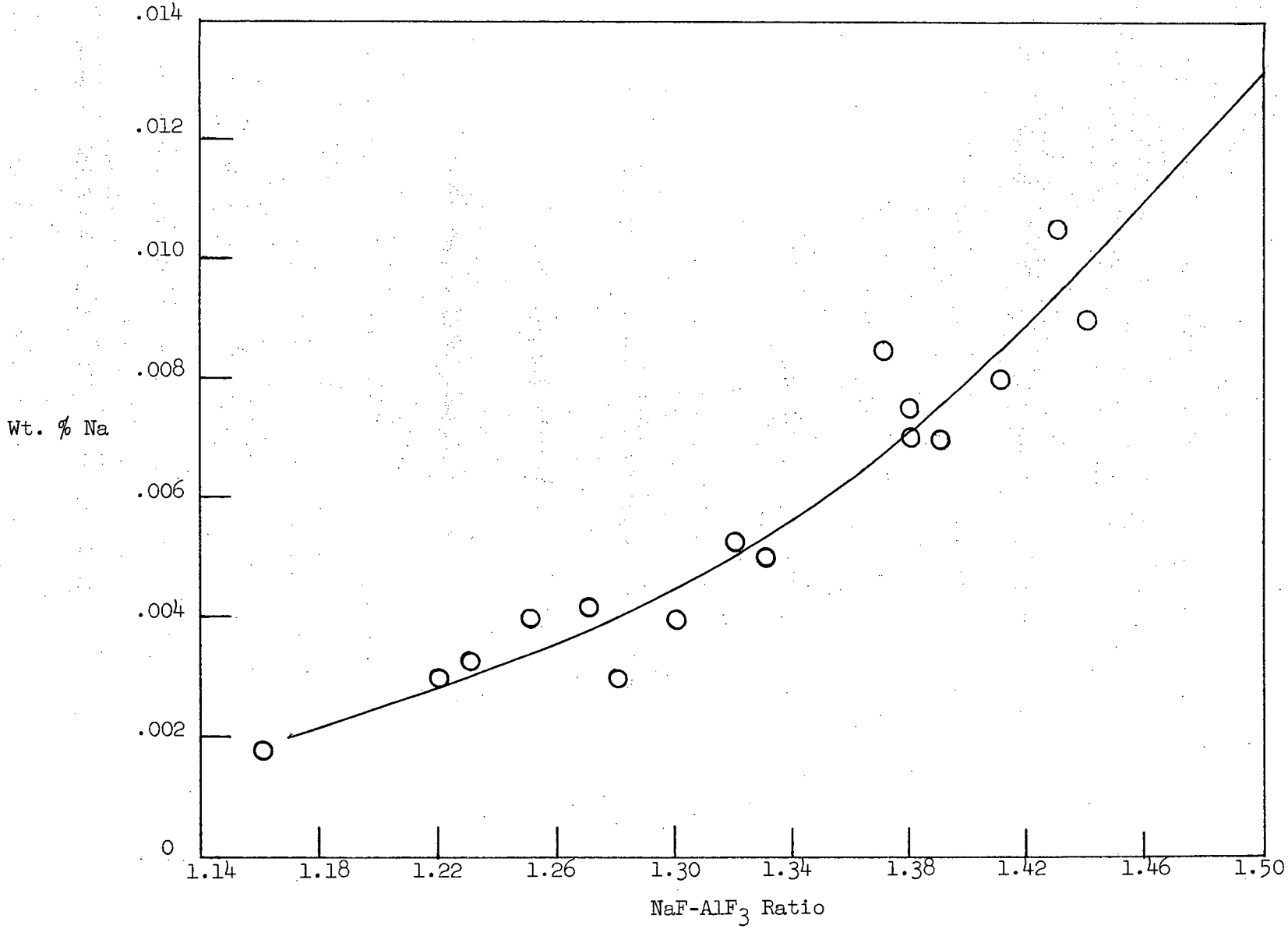

Figure G-3. Sodium Content of Aluminum from Reduction Cells as a Function of $NaF-AlF_3$ Ratio (from Hollingshead[23])

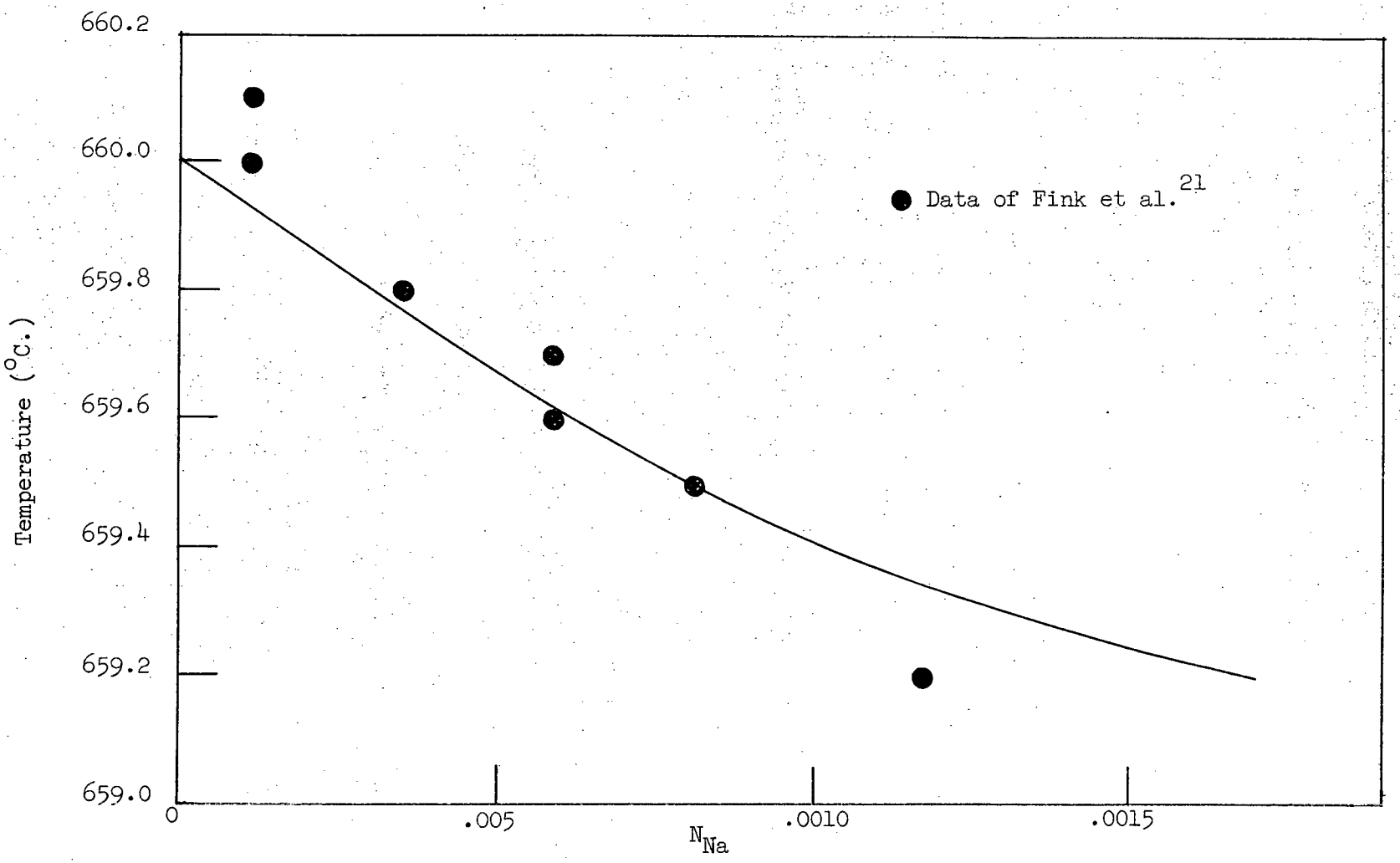

Figure G-4. Revised Na-Al Binary

The activities of sodium can then be calculated using the Gibbs-Duhem integration technique[26,19] (see Table G-III). The tie point in the integration is the monotectic point where the activity of sodium is unity, since the alloy is in equilibrium with pure sodium gas at this point. The value of γ_{Na} at the monotectic is 588 and Column 13 of Table G-III has to be corrected by a constant factor.

The values of γ_{Na} can then be determined at 1283°K. assuming that the solution is non-ideal using the relationship[19]

$$\frac{d \ln a}{d T} = \frac{d \ln \gamma}{d T} = \frac{\bar{L}}{RT^2}$$

this reduces to

$$\ln \frac{\gamma_2}{\gamma_1} = - \frac{\bar{L} \left(\frac{1}{T_2} - \frac{1}{T_1} \right)}{R}$$

where γ_2, γ_1 = the activity coefficients at T_2 and T_1

$\bar{L}$ = heat of solution (9230 calories)

R = the gas constant.

The ratio of $\frac{\gamma_2}{\gamma_1}$ is 3.79 for the above case. The activities of sodium calculated by this method (Table G-III) are plotted against concentration in Figure G-5, and as a function of weight per cent sodium in Figure G-6.

TABLE G-III

Determination of Sodium Activity from Revised Na-Al Binary

1	2	3	4	5	6	7	8	9
T	N_{Na}	N_{Al}	q_{Al}	γ_{Al}	$\log \gamma_{Al}$	N^2_{Na}	$\frac{-N_{Na}N_{Al}}{N_{Na}^2}$	$\frac{-N_{Na}N_{Al}}{N_{Na}^2} \log \gamma_{Al}$
933.00	0	1	1	1	0	-	-	-
932.988	.000020	.999980	.999980	1.0000000	0	4×10^{-10}	4.9999×10^{4}	-
932.976	.000040	.999960	.999963	1.000003	.0000013	1.6×10^{-9}	2.4999×10^{4}	-.032499
932.963	.000060	.999940	.999947	1.000007	.0000030	3.6×10^{-9}	1.666567×10^{4}	-.049897
932.951	.000080	.999920	.999923	1.000003	.0000013	6.4×10^{-9}	1.2499×10^{4}	-.016249
932.939	.000100	.999900	.999907	1.000007	.0000030	1×10^{-8}	9.999×10^{3}	-.029997
932.927	.000120	.999880	.999891	1.000011	.0000048	1.44×10^{-8}	8.332333×10^{3}	-.039995
932.915	.000140	.999860	.999871	1.000011	.0000048	1.96×10^{-8}	7.141857×10^{3}	-.034281
932.903	.000160	.999840	.999855	1.000015	.0000065	2.56×10^{-8}	6.249×10^{3}	-.040619
932.86	.000235	.999765	.999791	1.000026	.0000113	5.523×10^{-8}	4.2539×10^{3}	-.048069
932.78	.000353	.999647	.999671	1.000024	.0000104	1.246×10^{-7}	2.83207×10^{3}	-.029454
932.64	.000587	.999413	.999466	1.000053	.0000230	3.446×10^{-7}	1.70242×10^{3}	-.039156
932.50	.000823	.999177	.999255	1.000078	.0000339	6.773×10^{-7}	1.21412×10^{3}	-.04159
932.35	.001174	.998826	.999034	1.000208	.0000903	1.378×10^{-6}	8.50959×10^{2}	-.076842
932.24	.001550	.998450	.998867	1.000418	.0001814	2.4025×10^{-6}	6.441612×10^{2}	-.116851
932.20	.001700	.998300	.998807	1.000508	.0002205	2.89×10^{-6}	5.87235×10^{2}	-.129485
	.002000	.998000	.998807	1.000809	.0003511	4×10^{-6}	4.99×10^{2}	-.175199

TABLE G-III Continued

10	11	12	13	14	15	16	17	18
$\frac{\log \gamma_{Al}}{N_{Na}^2}$	$\int \frac{\log \gamma_{Al}}{N_{Na}^2} dN_{Al}$ 9 + 11		$\log \gamma_{Na}$ add 2.874397	$\gamma_{Na_{932}}$	N_{Na}	$\gamma_{Na_{1283}}$ $\bar{L}$ = 9230	a_{Na}	% Na
812.5	.197149	.164650	3.039047	1094	.00004	289	.0116	.0034
833.3	.180691	.130694	3.005091	1012	.00006	268	.0161	.0051
203.1	.170327	.154078	3.028475	1068	.00008	282	.0226	.0068
300.0	.165296	.135299	3.009696	1023	.00010	270	.0270	.0085
333.3	.158963	.118968	2.993365	985	.00012	260	.0306	.0102
244.9	.153181	.118900	2.993297	985	.00014	260	.0364	.0119
253.9	.148193	.107574	2.981971	959	.00016	253	.0408	.0136
204.6	.130999	.082930	2.957327	906	.000235	239	.0562	.02
83.5	.114001	.084547	2.958944	910	.000353	240	.0847	.03
66.7	.096428	.057272	2.931669	835	.000587	220	.129	.05
50.1	.082646	.041487	2.915884	824	.000823	218	.179	.07
65.5	.062358	-.014484	2.859913	724	.001174	191	.224	.10
75.5	.035850	-.081001	2.793396	622	.001550	164	.254	.14
76.3	.024465	-.105020	2.769377	588	.001700	155	.264	.17

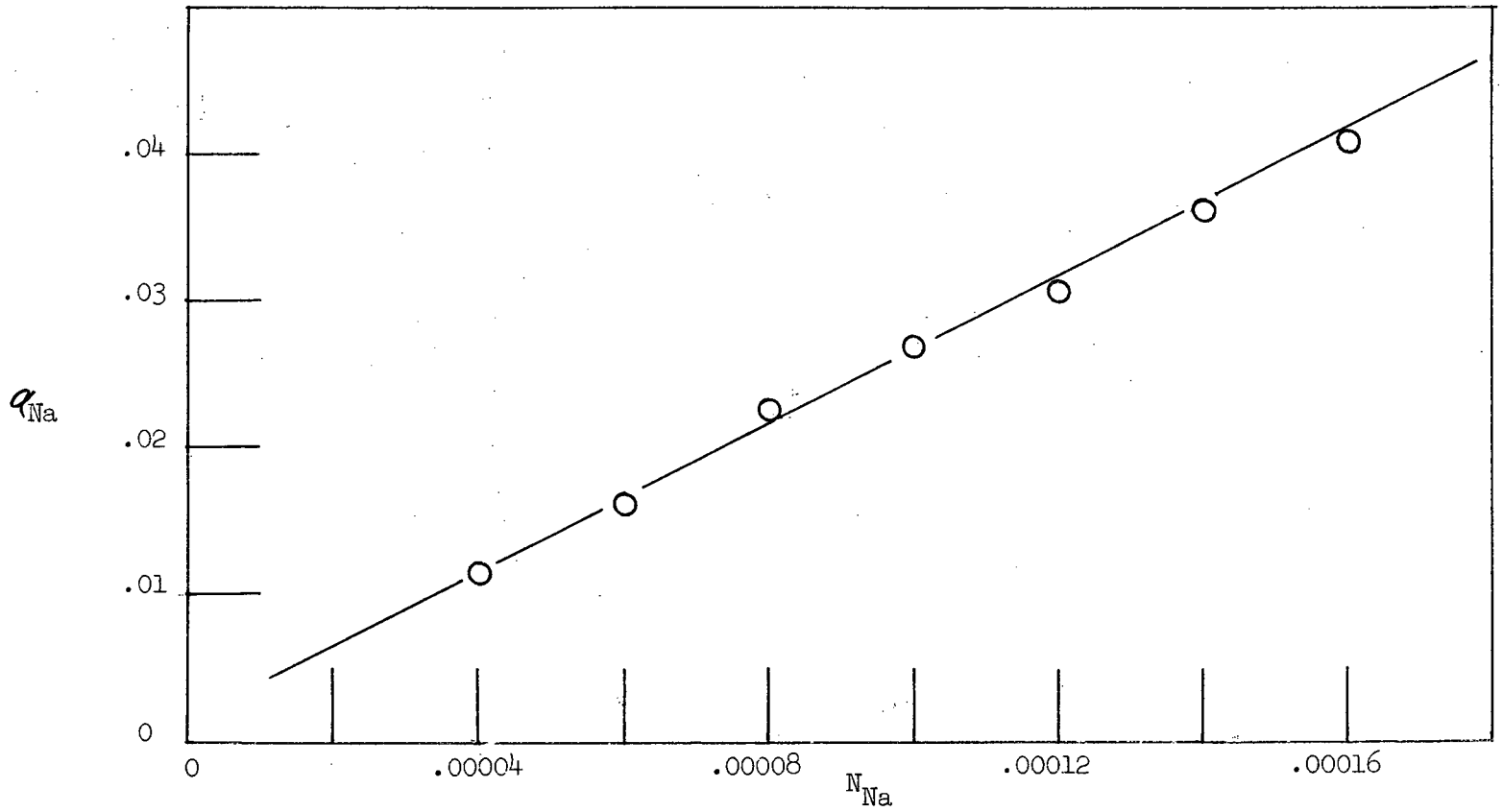

Figure G-5. Activity of Sodium as a Function of Concentration in Al Metal.

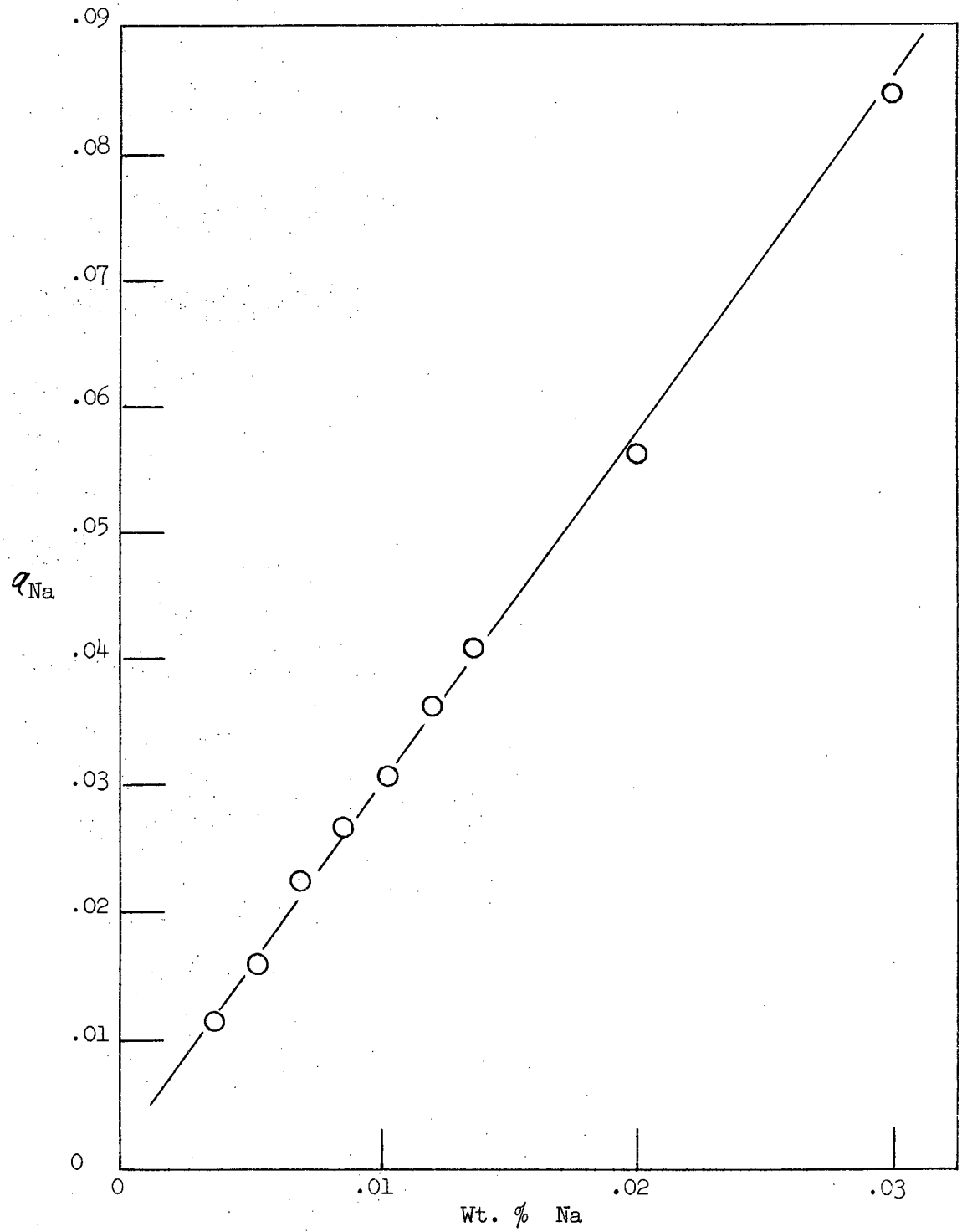

Figure G-6. Activity of Sodium as a Function of Weight Per Cent Na in Al Metal.

BIBLIOGRAPHY

1. Pearson, T. G., "The Chemical Background of the Aluminum Industry", Royal Institute Chemical Lectures, Monographs and Reports, No. 3 (1955).

2. Grjotheim, K., "Contribution to the Theory of Aluminum Electrolysis", Norke Videnskabers Selskabs Skrifter, No. 5 (1956).

3. Foster, L. M., Annals of the N. Y. Academy of Sciences, Vol. 79, Art. 11, p. 919.

4. Bonnier, E., Bull. Soc. Chim., France 1950, D 131.

5. Drossbach, P., "Electrochemistry of Fused Salts", p. 119-128, Springer, Berlin (1938).

6. Fréjacques, M. M., Bull. Soc. Franc. Elec. 9, 684 (1949).

7. Gadeau, R., ibid, 74, 540 (1947).

8. Grunert, E., Z. Elektrochem, 48, 393 (1942).

9. Grjotheim, K., Alluminio, 22, 6 679 (1953).

10. Piontelli, R., and Montanelli, G. ibid 22, 6 672 (1953).

11. Jander, W., and Hermann, H., Z. fur anorg. allgem. Chem. 239, 65 (1938).

12. Pearson, T. G., and Waddington, J., Discussions of the Faraday Society 1, 307 (1947).

13. Feinleib, M.and Porter, B., J. Electrochem. Soc. 103 No. 4, 232 (1956).

14. Feinleib, M. and Porter, B., ibid, No. 5, 300 (1956).

15. Frank, W. B. and Foster, L. M., "Constitution of Cryolite and $NaF-AlF_3$ Melts", Intern. Symp. on the Physical Chem. Process Metallurgy", Pittsburgh, Pa. 1959.

16. Foster, L. M., and Frank, W. B., J. Electrochem. Soc. Vol. 107, No. 12 997 (1960).

17. Hansen, M., "Constitution of Binary Alloys", McGraw-Hill, 997 (1958).

18. Hauffe, K., and Vierke, A. L., Z. Elektrochem, 53, 151 (1949).

19. Chipman, J., Discussions of the Faraday Society 4, 23, (1948).

20. Hansen, M., "Constitution of Binary Alloys", McGraw-Hill, 117 (1958)

Bibliography Continued

21. Fink, W. L., Willey, L. A., and Stumpf, H. C., Trans. of A.I.M.E., 175, 364-71 (1948).

22. Ransley, C. E., and Neufeld, H., J. Inst. Metals 78, 25-48 (1950-51)

23. Hollingshead, E. A., personal communication.

24. Kubaschewski O. and Evans., E. L. "Metallurgical Thermochemistry", (1958).

25. Kelley, K. K., Contribution to the Data on Theoretical Metallurgy, Bulletin 584, Bureau of Mines, (1960).

26. Darken, L. and Gurry, R., "Physical Chemistry of Metals", McGraw-Hill, Chpt. 10 (1953).

27. Wagner, C. "Thermodynamics of Alloys", Addison-Wesley Press, Cambridge Mass. (1952).

28. Wagner, C. Acta Metallurgica, 6, 309-19, May (1958).

29. Chu, B. and Egan, J., Annals of N. Y. Academy of Sciences, Vol. 79, Art. 11, 908 (1960).

30. Wagner, C., private communication.

31. Grube, G., and Hantelmann, B., "The Reactions of Al and Na with Melts of the System NaF-AlF_3 and NaF-AlF_3-Al_2O_3", Institut. für Physikalische Chemie der Metalle am Kaiser Wilhelm - Institut für Metallforschung, February 1945.

32. Fenerty, A., and Hollingshead, E. A., J. of Electrochem. Soc. Vol. 107, No. 12, 993.

33. Piontelli, R., "Atti simposia elettrolisi sali fusi produzione metalli speciali in Italia", Milano, 5-7 Maggio 1960.

34. Glassner, Alvin, "The Thermochemical Properties of the Oxides, Fluorides, and Chlorides to 2500°K., U. S. Atomic Energy Commission Publication, ANL - 5750.

35. Stokes, J. J, Jr. and Frank, W. B., "Spectrosocpic Investigation of the Occurrence of Sodium in the Fumes Above Molten Cryolite", A.I.M.E. International Aluminum Symposium, N. Y. February, 1962.